ISSN : 2717 - 5022

JOURNAL ON GEOINFORMATICS

Nepal

Number: 22 Jestha 2080 (May/June, 2023)

Annual Publication of Survey Department, Government of Nepal

Director General, Janak Raj Joshi participated in 9th GLTN Partner's meeting and country learning program from 2-4 May 2023 in Kenya.

Deputy Director General Susheel Dangol addressing at Twelfth session of the United Nations Committee of Experts on Global Geospatial Information Management (UN-GGIM) held on 3-5 August 2022 UN headquarter, New York.

Deputy Director General Karuna K.C. participated in "Workshop on building spatial data infrastructure" organized in South Korea from 31st October to 4th November 2022.

Team involved from Survey Office Lalitpur in UAV surveying for cadastral mapping as a pilot program of Survey Department.

Team from Survey Department and Ministry of Land Management, Cooperatives and Poverty Alleviation lead by Secretary of the Ministry participated in exposure visit to Ordnance Survey, United Kingdom to learn about the LiDAR survey and other surveying and mapping activities of UK.

Journal on Geoinformatics
Nepal

Number : 22

Jestha 2080 BS
May/June 2023 AD

Annual publication of Survey Department, Government of Nepal

The content and the ideas of the articles are solely of authors.

Published by:
Government of Nepal
Ministry of Land Management,
Cooperatives & Poverty Alleviation
Survey Department
Min Bhawan, Kathmandu
Nepal

No. of copies : 500

© *Copyright reserved by Survey Department*

FOREWORDS

Survey Department Nepal, besides regular responsibilities, has been contributing in knowledge and information sharing in the field of surveying and mapping through its annual publication and has come up with the 22nd issue of "Journal on Geoinformatics, Nepal". I would like to congratulate Editorial Board and express my gratitude to all the contributor for giving this journal to its shape.

Survey Department's contribution to national development is significant. Through accurate surveying, mapping, and geospatial information services, it supports land administration, infrastructure development, urban planning, natural resource management, disaster management, and various sectors of the economy. The department's work is instrumental in fostering economic growth, ensuring sustainable development, and improving the overall well-being of citizens.

In recent time, Survey Department has initiated adopting modern technology in surveying and mapping sector to make its services effective, efficient, transparent and reliable. Modern technology has revolutionized the way we understand and interact with our physical environment. With the introduction of high-precision instruments such as GPS (Global Positioning System), LiDAR (Light Detection and Ranging), and remote sensing, surveyors can capture highly detailed and precise data about the Earth's surface. These advancements in technology have not only enhanced the accuracy and efficiency of surveying and mapping processes but also opened up new possibilities and improved decision-making, and minimizes the cost of project.

One among the many remarkable initiatives, that the Survey Department has started, is online based Cadastral service system termed as Nepal Land Information System (NeLIS) and "MeroKitta". Citizens can receive the basic cadastral service such as map print, field book print and plot register print without visiting the office. Parcel subdivision and map updating can be carried out online. Currently this service is available in 53 offices but the Department is planning to rollout the system in all district level offices in near future. Similarly, the Department has envisioned to establish a network of Continuously Operating Reference Station

(CORS) throughout the country and strengthen the Geodetic control Network. It is expected to improve the quality of surveying and mapping services through operationalizing CORS in the days to come.

I would like to express my sincere appreciation to the fellow colleagues, the members of Advisory Council and the Editorial Board for their invaluable contribution in this issue. The team deserves special thanks for their tireless efforts in bringing this issue in the stipulated time. More importantly, I extend sincere gratitude to all the authors for their resourceful professional contribution. I further request all concerned professionals for their kind support and professional contribution in the upcoming issues too.

Thank you, and enjoy Reading !!!

Janak Raj Joshi, Director General
Janakraj.joshi@nepal.gov.np

EDITORIAL

Survey Department, the national mapping agency of Government of Nepal is conducting many different activities in the field of Surveying and Mapping. Besides the technical activities in this field, department is also contributing in academic sector of this field by publishing journal on different research and findings about geoinformatics through "Journal of Geoinformatics, Nepal", the annual publication of the department. Editorial board is happy to share the 22nd issues of this journal. The journal has been a platform for sharing information on geoinformation and its wide range of application for the researchers and professionals working in this field from wide range of community including government, non-government, international organization as well as universities. Editorial board believes that this has also supported in professional development through knowledge sharing in the field of surveying, mapping and geospatial technologies.

Driving from the first issue since 2002 till this 22nd issues, the journal has covered from the history of the surveying and mapping to the latest technologies in this field. The editorial board like to thank sincerely to all those authors who contributed in making the successful publication of the issues and also to the Advisory Council and the editorial for making this happen. This issue is also the continuous product of the previous efforts. This issue also as in previous one, includes interesting and worth reading papers related to geospatial technologies and its applications and findings.

I am also thankful to Survey Department for providing me the responsibility of the Editor-in-Chief for this 22nd issue of the journal. With the continuous guidance and critical comments from the advisory board have been able to bring this issue of the journal for readers. On behalf of all the members of the Editorial Board, I would like to express sincere thanks to all contributing authors, paper reviewers, members of Advisory Council and all other persons who have contributed for the publication of 22nd issue of the journal.

At last, on the behalf of Editorial Board, let me humbly request all of you to contribute your valuable articles, research papers, review papers for the upcoming issue of this journal.

Karuna K. C.,
Editor-in Chief,
Jestha, 2080 (May 2023)

Advisory Council

Janak Raj Joshi
Chairperson

Karuna K.C.
Member

Sushil Narsingh Rajbhandari
Member

Amir Prasad Neupane
Member

Susheel Dangol
Member

Editorial Board

Karuna K.C.
Editor-in-Chief

Bikash Kumar Karna
Member

Tanka Prasad Dahal
Member

Damodar Dhakal
Member

Journal on
GEOINFORMATICS
Nepal

Jestha 2080, May 2023
Number 22

Product Price

Maps
Page 10

Control Points
Page 10

Price of Aerial Photograph
Page 37

Land Use Digital Data Layers
Page 37

Price of Printed Maps
Page 37

Digital Orthophoto Image Data
Page 37

Digital Topogrphical Data
Page 37

Obituary
Page 38

List of Paper Reviewer

Janak Raj Joshi
Karuna K.C.
Susheel Dangol
Tanak Dahal
Hari Sharan Nepal
Ram Kumar Sapkota
Sudip Shrestha
Ajeet Kunwar
Suraj Bahadur K.C.

Cover Concept

Application of UAV for cadastral survey

Features

Articles

Contents

Contents

Contents

Application of Geo-informatics for Soil Erosion Mapping

Susheel Dangol[1] & Umesh Kumar Mandal[2]
Susheel.dangol@nepal.gov.np, umesh_jee@hotmail.com
[1]Survey Department, [2]Central Department of Geography (TU)

KEYWORDS

Geo-informatics, Universal Soil Loss Equation (USLE), Soil erosion, Modeling,

ABSTRACT

Soil erosion is a most severe environmental problem in hilly area. The study is carried out on Upper Bagmati River basin, North of Kathmandu valley having an area of 61 Sq.km. (approx). Universal Soil Loss Equation (USLE) model, with Geographic Information System (GIS) has been used to quantify the soil loss. Erosion modelling requires huge amount of information and data, usually coming from different sources and available in different formats and scales and for management of these data, GIS was used, which helped considerably in organizing the spatial data representing the effects of each factor affecting soil erosion. Five essential parameters of USLE Rainfall erosivity factor (R), Soil erodibility Factor (K), Slope length and steepness (LS) factor, Cropping management factor (C) and Support practice factor (P) have been used to estimate soil loss amount in the study area. All of these layers have been prepared in Arc GIS using various data sources and data preparation methods. DEM was prepared from the contour data with the interval of 20m which was used to generate LS factor. The monthly rainfall data (2010) of 17 rain gauge stations within the catchment area have been used to predict the R factor. K, C and P factors in basin area are adopted from the literature. The spatial distribution map of soil loss of the basin has been generated and classified into six categories depending on the calculated soil erosion amount. The annual predicted soil loss ranges between 0 and 292.878 t/ha/y. Low soil loss (mean 9.7 t/ha/y) have been recorded under forested areas. The high rate (mean 40.4 t/ha/y) of soil erosion was found in the cultivation area.

1. BACKGROUND

Land degradation is a global issue, which is manifested in various processes (Shrestha, *et al.* 2004). Soil erosion by water is a complex process that involves the interrelationship of many factors some of which influence the capacity of rainfall and runoff to detach and transport soil material, while others influence the ability of soil to resist the forces of the erosive agents. Water erosion is by far the most serious land degradation type with a global estimate of about 11 million km^2 (Oldeman, 1994).

Soil erosion is a major part of land degradation that affects the physical and chemical properties of soils and resulting in on-site nutrient loss and off-site sedimentation of water resources (Brhane and Mekonen, 2009). It is natural phenomenon which occurs due to forces from rain water, surface runoff, wind,

gravity, etc., exerting on surface soil and result in detachment and transport of soil from that area (Liengcharernsit *et al.*2007).

Soil erosion occurs when water that cannot infiltrate into the soil becomes surface runoff and transports soil down slope. A soil becomes unable to absorb water when the rainfall intensity exceeds the surface infiltration capacity, when the rain falls onto a saturated surface because of antecedent wet conditions, or when the underlying water table is at the surface. Once runoff is initiated, forms of erosion are likely to occur, that show variety in space and time: sheet hill slope erosion, parallel linear erosion, and gully erosion.

Soil erosion rate varies depending on many factors including rainfall intensity and duration, area slope, covered vegetation, soil type, wind velocity, surface runoff rate, etc. Soil erosion has resulted in loss in surface soil which normally has high nutrients. It also causes environmental problems in downstream area and receiving water body.

Over forty years of research by the U.S. Department of Agriculture has helped to identify the major factors of soil erosion and to establish their functional interrelationships (*http://www.usask.ca, retrieved on 4th Feb, 2008*). From over 40 years of research comprising more than 250,000 runoff events at 48 research stations in 26 states, the Universal Soil Loss Equation (USLE) has been developed (Wischmeier and Meyer, 1973). The USLE is the result of more than 20 years of study and development by scientists of the USDA (USDA, 1980). This equation is used extensively for sediment prediction and erosion control planning for agricultural soils and disturbed sites and has been widely accepted and utilized in most countries. USLE is a simple technique for predicting the most likely average annual soil loss in specific situations. Each factor in the equation can be predicted from easily available meteorological and soils data.

Given the limited capacity of the manual method, there is a growing need to systematically map soil erosion, using GIS and related technologies for speed and accuracy (Mongkolsawat *et al.,* 1994). The integrated approach of Remote Sensing (RS) and GIS gives quick as well as more advanced response. This technique has also been used for landslide susceptibility mapping using slope, aspect, relief, flow accumulation, soil depth, soil type, land use and distance to road in GIS environment (Dahal*, et. al,* 2008). Similarly, combination of GIS and RS has been used by Lee and Pradhan (2007) to map land slide hazard.

Four main factors are generally considered: soil, topography, land use and climate (Wischmeier and Smith 1978). However, the equation cannot predict soil loss which is solely due to snowmelt, thaw and wind (Wischmeier and Smith 1965). The USLE predicts the long term average annual rate of erosion on a field slope based on rainfall pattern, soil type, topography, crop system and management practices. However, it has been observed that the USLE/Revised USLE over-predicts low annual average erosion and under-predicts high average erosion (Risse *et al.,* 1993)

2. METHODOLOGY

GIS can be equated to both computer database and database system for producing maps and significant increase of the technology is seen globally. The technology provides operational tools for making policy, planning for management and decision making (Karim, 1995). USLE was used in GIS environment to analyze annual soil loss for upper bagmati watershed.

2.1. Study Area

The Bagmati River and its major tributaries *Nagmati Khola, Syalmati Khola* and *Thulo Khola* originate from the Northern fringe of

Kathmandu valley the hydrological boundary of the Bagmati river considering Gaurighat as outlet is selected for this case study which can be called as Upper Bagmati river basin area. The total area of the study watershed is 65.43 km^2 (Figure 1).

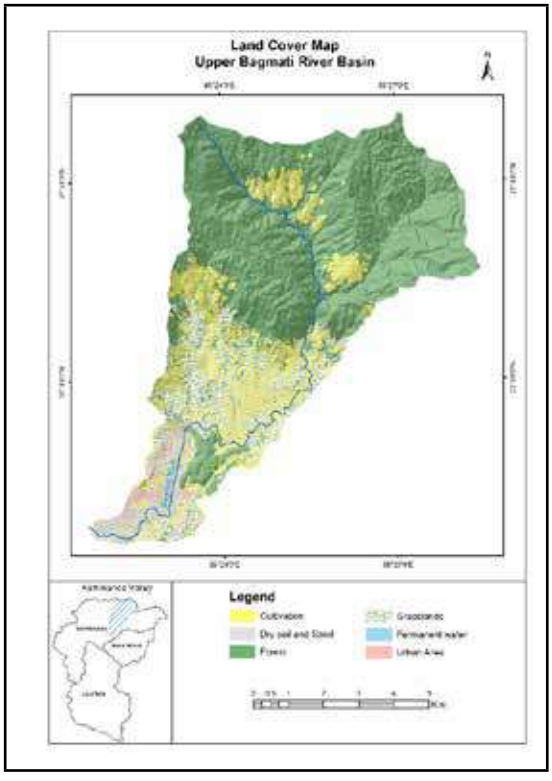

Figure 1: Study area.

The area is chosen for the study with the reason that the north facing mountains of the Kathmandu receives high rainfall than other facing mountains (Pokharel & Hallett, 2015) and hence can be assumed that there must be higher soil erosion.

2.2. Data collection

Secondary data for Upper Bagmati watershed which includes rainfall, digital topographical database, land cover data were collected from Department of Hydrology and Meteorology (DHM), Survey Department (DoS), National Land Use Project, Ministry of Agriculture and Co-operatives. Crop pattern and conservation practice were taken from the literature.

2.3. Soil erosion estimation

Annual soil loss in the form of runoff from different land forms and land uses of the watershed was estimated using USLE (*Wischmeier and Smith, 1978*).

$$A = R * K * L * S * C * P$$

Where;

A = estimated soil loss (t ha^{-1} yr^{-1}), R = Rainfall Erosivity factor, K = Soil erodibility factor, L = Slope length factor, S = Slope gradient factor, C = Land cover factor, P = Management practice factor.

All the processing was done in raster data format. Integrated Land and Water Information System (ILWIS, 3.4) was used for all the processing.

2.3.1. Rainfall factor (R)

The R-factor is defined as the measurement of the kinetic energy of a specific rain event or an average year's rainfall (Wischmeier and Smith, 1978). In this study, to determine the value of the R-factor, the average of annual historic rainfall event of 17 stations were collected from Department of Hydrology and Meteorology within the watershed. The rainfall distribution is not homogeneous all over the study area. For this reason, an interpolation of annual precipitation data was applied to have a more representative rainfall distribution. Once the interpolation is performed a map representing annual rainfall in the region is obtained. This map was the input source (P_a) for the R calculation using the Renard and Freimud (1994) equations for Pa < 850 mm:

$$\text{R factor} = 0.04830\ P_a\ 1.610 \ldots\ldots\ldots \quad (i)$$

Where Pa is mean annual precipitation.

Monthly precipitation data can give reasonable estimates of R-values for many regions throughout the world (Renard and Freimud, 1994). For this study also, monthly rainfall data of 17 stations were used for this. Regression analysis in Microsoft Excel was

done to get the relation between elevation and mean annual rainfall. The equation derived for the relation is

$$P_a = 0.1122\ Z - 24.185 \ldots\ldots\ldots\ldots\ldots\ldots (ii)$$

Where P_a is mean annual rainfall and Z is elevation.

The map of this P_a value was prepared on the basis of DEM and on the base of this map, R-factor map was prepared with the equation i.

2.3.2. Soil erodibility factor

The soil erodibility reflects the fact that various soils erode at different rates due to different physical characteristics such as texture, organic matter, structure, and bulk density and hence is defined as the rate of soil loss per unit of R-factor on a unit plot (Reinard *et al.,* 1997). This is the susceptibility of the soil or surface material to erosion, transportability of the sediment and the amount and rate of runoff given a particular rainfall input (Sheikh, *et. al.,* 2011). Table 1 presents the soil erodibility factor (K) based on the soil texture class by Shrestha (1997). A land system map prepared by Land Resource Mapping Project (LRMP) of the study area was used to define the soil texture and on the basis of the K value from the table and the soil texture, erodibility of the study area was determined.

Table 1: Soil erodibility value for different soil texture.

S.N.	Soil Texture	K - value
1	Gravely Loam, Hill	0.45
2	Loam, Hill	0.5
3	Gravely Sandy Loam, Mountain	0.43
4	Loam	0.4
5	Loamy sand, plain	0.3
6	Loam, plain	0.41
7	Sandy loam, plain	0.35

2.3.3. Slope gradient (LS) factor

LS is the topographic factor expressed as the expected ratio of soil loss per unit area from a field slope to that from a unit lot under otherwise identical conditions. The rate of soil erosion by flowing water is a function of slope length (L) and gradient (S). For the practical purpose, these two topographic characters are combined into a single topographic factor (LS). However, in this research both the factors are estimated separately. Since the input requirement is DEM, slope length and slope gradient factor is calculated as follows (*Wischmeier and Smith, 1978*).

$$L = (\lambda/22.13)^m \ldots\ldots\ldots\ldots\ldots\ldots (iii)$$

Where L is slope length factor, λ is field slope length and 'm' is the constant defined according to the slope gradient which range from 0.2 to 0.5 (Table 2).

Table 2: Constant (m) value according to slope gradient.

S.No.	Slope Gradient	Value of m
1	< 1%	0.2
2	1% - 3%	0.3
3	3% - 4.5%	0.4
4	> 4.5%	0.5

Source: Wischmeier and Smith, (1978).

Map of 'm' was created using the slope map prepared in percent. Similarly, for the slope gradient, following relation was used as defined by Wischmeier and Smith (1978) cited by Jain *et. al.* (2001).

$$S = (0.43+0.3s+0.043s^2)/6.613 \ldots..(iv)$$

Where 'S' is slope gradient factor and 's' is slope in percentage.

The combined LS factor was calculated by multiplying the L and S factor from the created maps. The factor of slope length (L) and slope gradient (S) are combined in a single topographic erodibility factor (LS).

2.3.4. Crop management (C) factor

The Crop management factor (C) is the ratio of soil loss from land with specific vegetation to the corresponding soil loss from continuous fallow (Wischmeier and Smith, 1978). It is a crucial factor to the erosion since it is a readily

managed condition to reduce erosion (Bera, 2017). C factor reflects the reduction in soil erosion that will result from growing a crop as compared with leaving the land fallow. The amount of reduction depends upon the type of crop grown, the cropping system, tillage practices, crop yield, and residue management. The C factor was calculated from literature review, since there was no local data available regarding this factor. Based on the land cover data of the study area, C value was assigned to the ones existing in the study area (Table 3). C value ranges from 1 to approximately 0, where higher value indicate no cover effect and lower value means very strong cover effect resulting in no erosion (Erencin, 2000).

2.3.5. Protection measure (P) factor

The P-factor gives the ratio between the soil loss expected for a certain soil conservation practice to that with up-and down-slope ploughing (Wischmeier and Smith, 1978). Specific cultivation practices affect erosion by modifying the flow pattern and direction of runoff and by reducing the amount of runoff (Renard and Foster, 1983). The tillage and cultivation of agricultural soils on sloping land needs to be supported by practices that will slow the velocity of runoff water. This will reduce its erosive power and the amount of soil it is capable of transporting. The most commonly used erosion control practices are; contour tillage, strip cropping on the contour, and terrace systems. P value for the study area was also determined on the basis of literature review. Based on the land cover data of the study area, P value was assigned to the ones existing in the study area (Table 3).

Table 3: Value of C factor P factor according to land cover.

S.N.	Land Cover	C Factor	P Factor
	Open scrub	0.1	0.8
	Degraded forest	0.03	0.8
	Dense forest	0.004	0.8
	Mixed forest	0.05	0.8
	Cultivation	0.3	0.6
	Fallow	0.5	0.7
	Water	0	0
	Urban	0	0

Source: Jain et. al., (2001).

3. Result and discussion

The soil erosion potential (A) has been computed by multiplying the developed raster data from each factor (A= R K L S C P) of USLE analysis. The final 'A' factor map displays the annual soil loss potential of the Upper Bagmati river basin is shown in figure 2.

3.1. Results

From the study it shows that the study area has high slope gradient. So, the erosion loss is obtained with high rate. Predicted annual mean soil loss of Upper Bagmati River basin ranged from 0 to 292.878 ton/ha/yr.

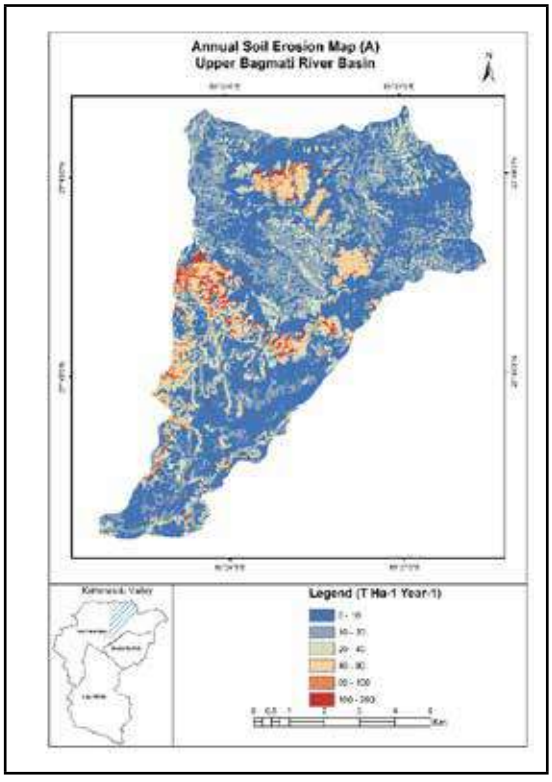

Figure 2: Soil erosion map.

Results shows that the study area has high slope so the erosion loss is obtained with

high rate in compared to other research. Bera (2017) classified predicted annual soil loss into six erosion intensity classes to assess erosion potential severity. In this study also, same class has been adopted but the class value has been considered accordingly to the result (Table 4). Negligible soil erosion was found at the lower steep area and the high soil loss was found in steep areas. According to erosion risk classes, it is observed that 44.76 % area is under negligible class whereas only 1.4 % area is under extremely high class (Table 5).

Table 4: Soil erosion intensity type.

S.N.	Soil loss class (t/ha/yr)	Erosion Intensity type
1	0 - 10	Very less erosion
2	10 - 20	Less erosion
3	20 - 40	Moderate erosion
4	40 - 80	Moderately high erosion
5	80 - 100	High erosion
6	> 100	Extremely high erosion

Table 5: Area according to soil erosion intensity type.

S.N.	Erosion Intensity type	Area (Km^2)	Area (%)
1	Very less erosion	27.39	44.76
2	Less erosion	18.42	30.09
3	Moderate erosion	8.63	14.09
4	Moderately high erosion	4.62	7.55
5	High erosion	1.29	2.10
6	Extremely high erosion	0.86	1.40

The analysis was also done for the erosion on the basis of land cover class. It is seen from the study that, cultivation has mean value of soil erosion with 40.40, dry soil and sand with 21.63, forest with 9.7, grassland with 15.48 and 0 for water and urban area (Table 6). Erosion at forest land might be because of the steepness of the area. The erosion at cultivation is very high in comparison to other. The reason must be less crop management practice and most of the cultivation area is also at high slope gradient. In comparison to this, erosion of dry soil and sand is less reason for which may be low lying land of this land cover category.

Table 6: Soil erosion probability according to land cover.

S. N.	Land Cover	Max	Mean
1	Cultivation	292.88	40.40
2	Dry soil and sand	265.63	21.63
3	Forest	261.16	9.7
4	Grassland	292.88	15.48
5	Urban area	250.4	2.34

This result is in line with the result of Jain *et. al* (2001) which showed that forested areas show less soil loss compared to other unprotected areas. Similar type of result was also found by Sheikh *et. al.* (2011), the study area was Himalayan watershed where average soil loss was highest (26 tons ha-1 year-1) in agriculture area and lowest soil loss rate was found in forest area (0.99 tons ha-1 year-1). Hence the result of this study can also be said as expected result, still field verification and calibration are always necessary.

Another analysis was done according to the slope of the study area. The slope category prepared for analysis is as shown in table 7. The result shows that, as the slope increases, the erosion rate also increases. For the slope 0-10, the mean value of erosion is 39.65 whereas, the mean erosion value is 162.77 for the slope degrees of 50-90. The result seems acceptable to the concept that the erosion increases with slope. However, this can also be related with cropping pattern and land cover.

Table 7: Soil erosion probability according to slope degrees.

S. N.	Slope Degrees	Max	Mean
1	0 - 10	171	39.65
2	10 - 20	216	66.91
3	20 - 30	258	80.88
4	30 - 40	281	84.30
5	40 - 50	206	80.84
6	50 - 90	292	162.77

3.2. Discussion

Result of this study gives an erosion range of 0.03-292.878 tons/ha/yr. Definitely, the value is dependent on different parameter values that were taken, in particular, the slope classes, the C and P-factor. For more comparable results, decisions regarding reasonable factor values must be made. This will require further empirical research to determine these values.

To analyze the result, we can see that the mean erosion value ranges between 2.34 in urban area to 40.40 in cultivation area. Analysis done by Shrestha (1997) in Likhu khola watershed shows that the soil erosion ranges from 3.4 in degraded forest to 34.6 in rainfed cultivation area. Research by Uddin et. al. (2016) in Koshi basin shows that the mean erosion values ranges from 3.9 in shrub land to 21.8 in barren land. The result of this research, Uddin et. al. and that done by Shrestha shows consistent range. This shows that the result obtained from this study is valid.

4. Conclusion

In conclusion, the potential source of prediction error is in selecting factor values. It is possible to spatially and quantitatively analyze multi-layer of data within a watershed using GIS. Using GIS technology in combination with remote sensing to generate land cover data can provide systematic data in dynamic manner for decision-support system. The annual soil loss predictions range between 0 and 292.878 tons ha-1 year-1. GIS platform provides a faster and better method for spatial modeling and gives output maps that can be understood better. Implementation of Universal Soil Loss Equation using integration procedures of GIS enabled the prediction of potential and actual soil loss rates and in the identification of units for suitable protection measures.

Geographic Information System (GIS) and Remote Sensing are emerging most effective tools for analyzing spatial distributed information in different dimensions. The use of the USLE model integrated to GIS and RS is an effective tool than the time-consuming conventional methods for assessing the soil loss vulnerability. The all USLE parameter R, K, LS, C and P factor maps were combined together for creating the annual average soil loss map of the upper Bagmati river basin.

There were no field data on soil erosion available, from the study area, hence, no calibration/verification of the results could be made. The study showed that forested areas show less soil loss compared to unprotected areas like fallow lands, which contribute to high soil loss. The soil erosion assessment technique used in the present study is helpful to evaluate the influence of different land cover and soil management factors in quantitative estimations of soil loss of the study area. The methods and the predicted amount of soil loss and its spatial distribution of the basin described in this study which are useful to formulate and further implement conservation program that will reduce soil loss from the basin.

REFERENCES

Bera, A., (2017). *Estimation of soil loss by USLE model using GIS and remote sensing techniques: A case study of Muhuri river basin, Tripura, India.* Eurasian Journal of Soil Science, 6(3) pp. 206-215, 2017.

Brhane, G. and Mekonen, K., (2009). *Estimating soil loss using Universal Soil Loss Equation (USLE) for soil conservation planning at Medego Watershed, Northern Ethiopia.* Journal of American Science, Marsland Press, Center for Development Research (ZEF), University of Bonn, Walter-Flex-Str. 3, D-53113 Bonn, Germany, 2009.

Dahal, R., Hasegawa, S., Nonomura, A., Yamanaka, M., Masuda, T. & Katsuhiro, N., (2008). *GIS-based weights-of-evidence modelling of rainfall-induced*

landslides in small catchments for landslide susceptibility mapping. Environmental Geology. 54. 311-324. 10.1007/s00254-007-0818-3.

Erencin, Z., (2000). *C-Factor mapping using remote sensing and GIS. A case study of Lom Sak/Lom Kao, Thailand*. International Institute for Aerospace Survey and Earth Sciences (ITC), 2000.

Jain, S. K., Kumar, S. and Varghese, J., (2001). *Estimation of Soil Erosion for a Himalayan Watershed Using GIS Technique.* Water Resources Management, DOI:10.1023/A:10122460292693, 2001.

Karim, J., (1995). *An introduction to GIS and its applicat*ion. In Proceedings of International Seminar of Water Induced Disaster, March 20-25, HMG/JICA.

Liengcharernsit, W., Songrakkiat, K. and Takemura, J., (2007). *Study of Soil Erosion in Songkhla Lake Basin, Thailand.*

Mongkolsawat, C., Thirangoon, P. and Sriwongsa, S., (1994). *Soil erosion mapping with Universal Soil Loss Equation and GIS.* Computer Centre, Kho Kaen University, Khon Kaen 4002, Thailand, 1994.

Oldeman, L. R., (1994). The global extent of land degradation. In: D. J. Greenland and I. Szabolcs (eds.) *Land Resilience and Sustainable Land Use*, 99-118 Wallingford: CABI.

Pokharel, A.K. and Hallett, J., (2015). Distribution of rainfall intensity during the summer monsoon season over Kathmandu, Nepal. *Weather,* Vol. 70, No. 9, pp 257-261.

Renard, K.G. & Foster, G.R., (1983). *Soil conservation: principles of erosion by water*. In: Degne HE and Willis WO (Eds.) Dryland Agriculture, Agronomy Monogr. 23, Am. Soc., Crop Sci. Soc. Am., and Soil Sci. Am Madison, Wisconsin, 1983:156-176.

Renard, K. G. & Jeremy, R.F., (1994). *Using monthly precipitation data to estimate the R-factor in the RUSLE*. Journal of Hydrology. 157. 287-306. 10.1016/0022-1694(94)90110-4.

Risse, L.M., Nearing, M.A., Nicks, A.D, Laflen, J.M., (1993). Error assessment in the Universal Soil Loss Equation. *Soil Science Society of America Journal*. **57**, 825-833, 1993.

Shrestha, D. P., (1997). *Soil erosion modeling, ILWIS 2.1 for Windows, Application Guide.* International Institute for Aerospace Survey and Earth Sciene, The Netherlands, pp. 323-341.

Shrestha, D. P., (1997). Assessment of soil erosion in the Nepalese Himalaya, A case study in Likhu Khola Valley, Middle Mountain Region. *Land Husbandary,* Vol 2, No. 1, pp. 59-80Oxford & IBH Publishing Co. Pvt. Ltd.

Shrestha, D. P., Yazidhi, B., and Teklehaimanot, G., (2004). *Assessing Soil Losses Using Erosion Models and Terrain Parameters, A Case Study in Thailand.* 25th Asian Conference on Remote Sensing, Thailand, 2004.

Sheikh, A. H., Palria, S., Alam, A., (2011). *Integratin of GIS and Universal Soil Loss Equation(USLE) for soil loss estimation in a Himalayan Watershed.* Geology and Geography, 2011, 3(3): 51-57.

Universal Soil Loss Equation. http://www.usask.ca/classes/ABE/432/assignments/ 04% 20USLE.pdf retrieved on 4th Feb, 2008.

U.S. Department of Agriculture (USDA), (1980). *Predicting soil loss using Universal Soil Loss Equation,* USDA

soil conservation service, Arkanas, 1980.

Wischmeier, W. H. and Smith, D. D., (1965). *Predicting rainfall-erosion losses from cropland east of the Rocky Mountains: guide for selection of practices for soil and water conservation.* Agriculture Handbook 282, U.S. Department of Agriculture (USDA), 1965.

Wischmeier, W. H. and Smith, D.D., (1978). *Predicting rainfall-erosion losses from cropland east of the Rocky Mountains: guide for selection of practices for soil and water conservation.* Agriculture Handbook 537, U.S. Department of Agriculture (USDA), 1978.

Wischmeier, W.H. and Meyer, L. D., (1973). *Soil erodibility on construction Areas*. Highway Research Board, Special Report 135: 20-20, 1973.

Author's Information

Name	:	Susheel Dangol
Academic Qualification	:	Master of Science in Geoinformation Science and Earth Observation for Land Administration
Organization	:	Survey Department
Current Designation	:	Deputy Director General
Work Experience	:	15 years
Published paper/article	:	12

Price of Maps

S.No.	Description	Scale	Coverage	No. of sheets	Price per sheet (NRs)
1.	Topo Maps	1:25 000	Terai and mid mountain region of Nepal	590	150
2.	Topo Maps	1:50 000	HIgh Mountain and Himalayan region of Nepal	116	150
3.	Land Utilization maps	1:50 000	Whole Nepal	266	40
4.	Land Capibility maps	1:50 000	Whole Nepal	266	40
5.	Land System maps	1:50 000	Whole Nepal	266	40
6.	Geological maps	1:125 000	Whole Nepal	81	40
7.	Districts maps Nepali	1:125 000	Whole Nepal	76	50
8.	Zonal maps (Nepali)	1:250 000	Whole Nepal	15	50
9.	Region maps (Nepali)	1:500 000	Whole Nepal	5	50
10.	Nepal (English)	1:500 000	Whole Nepal	3	50
11.	Nepal Map (Nepali)	1:1000 000	Nepal	1	50
12.	Nepal Map (Nepali)	1:2000 000	Nepal	1	15
13.	Nepal Map (English)	1:1000 000	Nepal	1	50
14.	Nepal Map (English)	1:2000 000	Nepal	1	15
15.	Physiographic Map	1:2000 000	Nepal	1	15
16.	Photo Map			1	150
17.	Wall Map (loosesheet)		Nepal	1 set	50
18.	VDC/Municipality Maps (Colour)		Whole Nepal	4181	50
19	VDC/Municipality Maps A4 Size		Whole Nepal	4181	5
20.	VDC/Municipality Maps A3 Size		Whole Nepal	4181	10
21.	Orthophoto Map		Urban Area (1:5000) and Semi Urban Area (1:10000)	-	1 000
22.	Outlined Administrative Map A4 size		Nepal	1	5

Price of co-ordinates of Control Points

Type	Control Points	Price per point
Trig.Point	First Order	Rs 3 000.00
Trig. Point	Second Order	Rs 2 500.00
Trig. Point	Third Order	Rs 1 500.00
Trig. Point	Fourth Order	Rs 250.00
Bench Mark	First & Second Order	Rs 1 000.00
Bench Mark	Third Order	Rs 250.00
Gravity Point	-	Rs 1 000.00

Assessment of Landcover Change of Kathmandu District, Nepal

Bimala Lama[1] & Basanti Kumpakha
bimalalama386@gmail.com, bkumpakha@gmail.com
[1]Forest Research and Training Centre

KEYWORDS

Landcover, Google Earth Engine, Remote Sensing, Urban Planning

ABSTRACT

It is necessary to understand land cover changes for managing and monitoring natural resources and development, especially urban planning. Remote sensing and geographical information systems (GIS) are proven tools for assessing land use and land cover changes, which helps planners advance sustainability. Google Earth Engine is used in this study to detect land cover changes in one of the rapidly growing cities in Nepal. It was discovered that from 2013 to 2019, 0.26% of the total area was increased by forests, 3.28% by settlement, 0.015% by wetland, and 1.21% by otherland. The overall accuracy and kappa coefficient of the landcover change study for 2013 are 80% and 0.74, and the overall accuracy and kappa coefficient of the study of landcover change for 2019 are 83.33% and 0.78. The status of the landcover change in Kathmandu district before and after the earthquake showed that forest covers the highest area, followed by cropland, and then settlement in both years 2013 and 2019. Forest, settlement, wetland, and other land have increased by 0.26%, 4.54%, 0.015%, and 1.21%, respectively. However, cropland and grassland have been decreased by 3.28% and 0.22% respectively.

1. BACKGROUND

Land is a delineable area of the earth's terrestrial surface, encompassing all attributes of the biosphere immediately above or below this surface, including those of the near surface, climate, soil, and terrain forms; the surface hydrology (including shallow lakes, rivers, marshes, and swamps); the near-surface sedimentary layers and associated groundwater reserve; the plant and animal populations; the human settlement pattern; and the physical results of past and present human activity (terracing, water storage or drainage structures, roads, buildings, etc.) (FAO, 1995).

Because all aspects of sustainability were meant to be captured, nine land use functions were considered, each of which was either societal, economical, or environmental. The societal land use functions are the provision of work, human health, recreation, and culture. The economic landuse functions are residential and land-independent production, land-based production, and transport. The environmental landuse functions are provision of abiotic resources, support and provision of biotic resources, and maintenance of ecosystem processes (Perez-Soba *et al.* 2008).

Although the terms "land cover" and "land use" are often used interchangeably, their

actual meanings are quite distinct. Land cover refers to the surface cover on the ground, such as vegetation, urban infrastructure, water, bare soil, etc. Identification, delineation, and mapping of land cover are important for monitoring studies, resource management, and planning activities. Identification of land cover establishes the baseline from which monitoring activities can be performed. Land use represents economic and cultural activities, for example, recreation, wildlife habitat, agriculture, residential, etc. Land use applications involve both baseline mapping and subsequent monitoring, since timely information is required to know what current quantity of land is in what type of use and to identify land use changes from year to year. This knowledge will help to develop strategies to balance conservation, conflicting uses, and developmental pressures. (Ravisankar, 2017).

Land-use and land-cover change are two of the main driving forces behind global environmental change. They have a high influence on a variety of environmental and landscape attributes, including water quality, land and air resources, ecosystem function, and the climatic system itself through greenhouse gas changes and surface albedo effects (Lambin *et al.* 2000).

Green space coverage has substantial importance for the quality of life as it has a significant impact on ecosystem functions, local microclimate, air quality, recreation, and aesthetic perceptions (Vatseva et al. 2016). Green spaces and other nature-based solutions provide innovative approaches to increasing the quality of urban settings, enhancing local resilience, and promoting sustainable lifestyles while at the same time improving the health and well-being of urban residents. Well-planned and managed urban green spaces ensure adequate opportunities for exposure to nature. Urban biodiversity is maintained and protected. Similarly, environmental hazards such as air pollution or noise are reduced. Various extreme weather impacts, such as heat waves, extreme rainfall, or flooding, are mitigated (WHO, 2017).

Urban expansion has increased the exploitation of natural resources, changing land use and land cover patterns. Understanding land use and land cover changes has become a necessity in managing and monitoring natural resources and development, especially urban planning.

In this regard, remote sensing and geographical information systems are proven tools for assessing land use and land cover changes that help planners advance sustainability (Lee et al. 2018). Geographic Information Systems (GIS) and remote sensing are powerful means for mapping and analyzing green space coverage at various spatial and temporal scales. It is a cost-effective and precise alternative to studying landscape dynamics. The transformation of Earth observation data into useful information is necessary for green space planning and decision-making. This can be done with the availability of high-resolution remote sensing images and multi-source geospatial data. Due to improvements in satellite image quality and availability, it has been easier to perform image analysis at a much larger scale than in the past. Thus, remote sensing and GIS have greater scope for the conception of dynamic models of physical environmental processes (Jensen, 2005).

According to the preliminary results of the National Census 2078, the population of Nepal stands at 29,192,480, which is 2,697,976 more than the population of 26,494,504 ten years ago (2068). Nepal's population has grown by 10.18%. The annual growth rate for the last ten years is 0.93%, compared to 1.35% in the previous census. As per UN-HABITAT (2013), the last quarter of the 20th century saw a fast expansion of Kathmandu Valley, reflecting the trend of urban growth dominant in the Himalayan region and elsewhere in South Asia (UN-HABITAT, 2013).

The study conducted by Maharjan (2018) using Landsat images for the years 2006, 2013, and 2017 identified that forest areas have been in relatively stable condition and that aggressive urban growth has somewhat slowed down in the last 5 years. However, mostly agricultural lands were converted into settlement areas, and other areas increased by about 68.15% from 2006 to 2017. Also, due to the 2015 earthquake, co-seismic surface deformation was reported along with its effects on the natural environment, such as landslides and liquefaction (Maharjan, 2018).

Thus, the study will compare how landcover change has occurred with the increasing population in 2013 and 2019, and will also explore the status of landcover change before and after earthquakes by using a globally reliable and fast remote sensing method, i.e., Google Earth Engine, which gives robust results. It will help urban planners and researchers make assessments of landscape development and change for continuous monitoring, well-planned development, and management of natural resources.

2. METHODOLOGY

2.1. Study area

The map of study area is shown in figure 1.

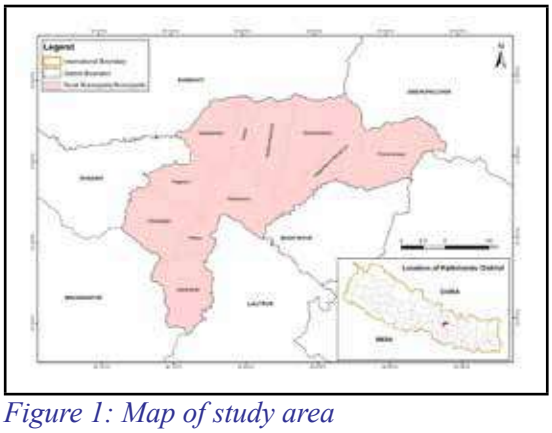

Figure 1: Map of study area

Kathmandu district is taken as the study area in this research. Kathmandu is one of the 77 districts of Nepal and covers an area of 433.61 km2. It is located in the Kathmandu Valley, Bagmati Province, of Nepal, a landlocked country in South Asia. The total number of people in the district is 2041578 (as per the census of 2021). Kathmandu Metropolitan City is the headquarters of this district, which is also the capital of Nepal. It is one of the three districts located in the Kathmandu Valley. It is located from 27°27′E to 27°49′E longitude and from 85°10′N to 85°32′N latitude. The district is surrounded by Bhaktapur and Kavrepalanchok in the east, Dhading and Nuwakot in the west, Nuwakot and Sindhupalchok in the north, and Lalitpur and Makwanpur in the south (http://ddcktm.gov.np/). The altitude of the district ranges from 1,262 m to 2,732 m above sea level. The temperature fluctuates between 32 °C in summer (June–July) and -2°C in winter (December–January) in the urban center. The district includes 11 municipalities, which are Budhanilkantha, Chandragiri, Dakshinkali, Gokarneshwar, Kageshwar Manohara, Kathmandu, Kirtipur, Nagarjun, Shankharapur, Tarakeshwar, and Tokha.

The main reason to choose Kathmandu as the study area is that it is the most developed area among other cities and towns in Nepal. A huge number of people have migrated from rural to urban areas, and the rapid increase in population has resulted in challenging problems such as crowding and landuse conflicts (e.g., competitive demands for land use have an adverse effect on neighboring landuses) and problems in urban planning and management (Bakrania, 2015). This case study analyzes the land cover of Kathmandu district using remote sensing Landsat data for the years 2013 and 2019.

For this study, Google Earth Engine (GEE) scripts followed by Forest Research and Training Centre in the study of National Land Cover Monitoring System was customized as per requirements. The methods for this study is described in figure 2 as follows:

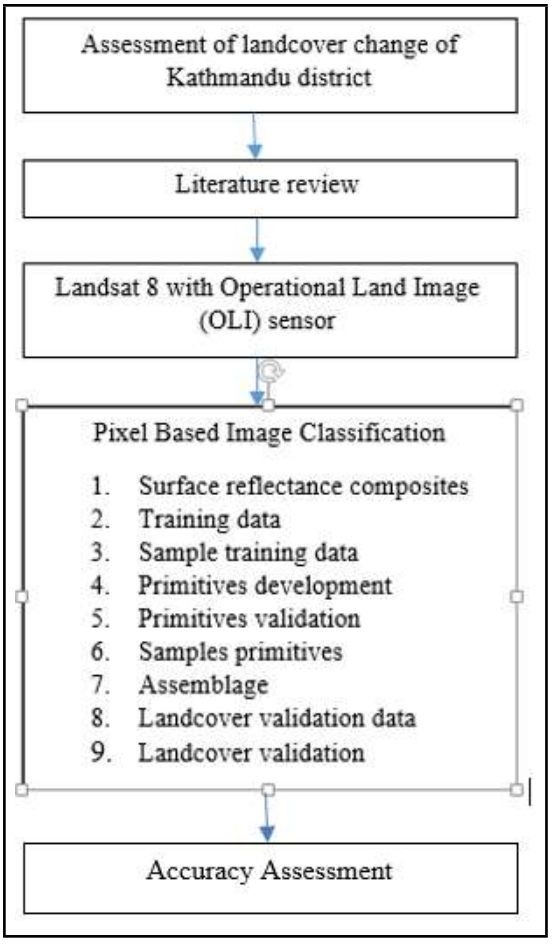

Figure 2: Methodology flowchart

2.2. Pixel based image classification

Landsat 8 with Operational Land Imager (OLI) sensor was acquired through the commonly used high power planetary-scale raster analysis utilities of Google Earth Engine (GEE) (Sidhu et al., 2018) and further landcover mapping and classification work was carried out in QGIS 3.24.1. The detail of satellite data is given in table 1.

Table 1: Characteristics of landsat image

Satellite	Sensor	Path-Row	Date	Resolution (m)	Band
Landsat 8	Operational Land Imager (OLI)	141-41	2013 and 2019	30	1 to 8

2.2.1. Surface reflectance composites

It involves image pre-processing such as shadow and cloud masking Bidirectional Reflectance Distribution Function (BRDF) and topographic correction. For composites preparation, Landsat 8 was used. After this, image composites were created which consists of all the information that is required to capture the information in the study area throughout the year. Composites image for 2013 and 2019 of Kathmandu district was created. These data were hosted in the Earth Engine data archive and have approximately 30 meters ground resolution, multiple bands spanning visible to thermal wavelengths, and approximately 16-day revisit time.

2.2.2. Training data

The training data points of Forest, Cropland, Wetland, Grassland and Settlements were generated. Rest of the land was taken as other land. Top level landcover categories in the good practice guidance of International Panel on Climate Change (IPCC) were followed (IPCC, 2003). Total 519 points i.e., 160 points for forest, 5 points for grassland, 2 points for wetland, 150 points for cropland and 192 points for settlement for 2013 were selected with high certainty.

510 points i.e., 158 points for forest, 20 points for grassland, 12 points for wetland, 165 points for cropland and 155 points for settlement for 2019 were collected from the 0.4*2 km grid spread over the entire district with the help of high-resolution satellite imagery. This kind of high-resolution earth observation data allows us to select location with extended coverage. It involves identification of typology for the specific country on the basis of which reference data were being collected.

2.2.3. Sample training data

The data which were used to perform classification called covariates. However, these data were added to our reference points so that the classifier can use these to train the model. Covariate dataset were extracted on the pixel where reference points (which are actually our "known" points) so that they can

be used to train a classifier which is actually predicting class of other pixels (which are actually our unknown points).

2.2.4. Primitive development

The sampled reference points were used to create primitive layers. For this, random forest classifier was used. Since the classification is the probability of a certain biophysical feature existing within that pixel, classification was performed using only two classes i.e. 1. Class that specifies that said a certain feature exists 2. Class that specifies that said feature doesn't exist. For instance, for tree cover primitive generation, points were set that symbolize tree cover as a class 1 and other points such as settlement, river etc. as class 0.

2.2.5. Primitive validation

For the validation of the primitives, stratified random samples i.e. 13 points for forests, 16 points for cropland, 4 points for grassland, 6 points for wetland and 11 points for settlement for 2013 were generated to validate the developed primitive. Similarly, 13 points for forests, 17 points for cropland, 4 points for grassland, 8 points for wetland and 11 points for settlement for 2019 were generated to validate the developed primitives.

2.2.6. Sample primitives

Quality check of primitives using validation points was done by plotting probability distribution of points throughout a certain primitive over 2013 and 2019. This gives the distribution of probabilities throughout the points that are supposed to be of same class vs. those that are supposed to be of different class.

2.2.7. Assemblage

A decision tree was prepared with the help of assembler based on user specified thresholds which can be tuned based on visual assessment as well as primitive assessment plots. The order of primitives in the list denotes the order in which primitives are placed in the decision tree with the first primitive placed on the top and so forth which means that if a pixel has high probability on two primitives (according to specified threshold) the final class will be based on the primitive that is higher up on the decision tree.

2.2.8. Landcover validation data

Primitive of each landcover class was formed and landcover class map of 2013 and 2019 was produced. Land cover of 2013 was validated with the help of stratified sample points. 8 points for forest, 8 points for cropland, 1 point for grassland, 2 points for wetland and 6 points for settlement were collected in GEE. Similarly, 8 points for forest, 9 points for cropland, 1 point for grassland, 2 points for wetland and 6 points for settlement were collected in GEE for the validation of landcover of 2019.

2.2.9. Landcover validation

After having a set of landcover map, its quality was checked for which the accuracy assessment of the map was done. For this, a set of data separated for validation purposes was used which are not used to train the model. Analyzed data was presented in maps and bar diagrams through statistical calculation showing LULC changes area wise in 2013 and 2019 and interpretation was done accordingly.

2.4. Accuracy Assessment

The overall accuracy and overall kappa coefficient of the classification was assessed. The overall accuracy of the classified image compares how each of the pixels is classified versus the definite land cover conditions obtained from their comparing ground truth (Rwanga and Ndambuki, 2017). Kappa coefficient is a degree of how the classification results compare to values assigned by chance. So, higher the kappa coefficient, higher the accuracy of the classification is (Ukrainski, 2019). Further, producer's accuracy and user's accuracy will be assessed. Producer's accuracy is the accuracy of the map from the point of view of the map maker (the producer).The user's accuracy is the accuracy of the map

from the point of view of a map user, not the map maker.

Besides, the satellite images for image classification and image base analysis, other primary and secondary data were also collected. Secondary data were collected from various published journals, articles, reports, books, websites, thesis, officials' records etc.

2.5 Data analysis

Collected information and data was presented and interpreted with the help of bar diagrams using MS Excel 2013.

3. RESULT AND DISCUSSION

3.1. Status of landcover of Kathmandu district of 2013 and 2019

The study provided an empirical and explicit land cover map of 2013 and 2019, depicting the land cover change of Kathmandu district in Nepal (Figures 3 and 4).

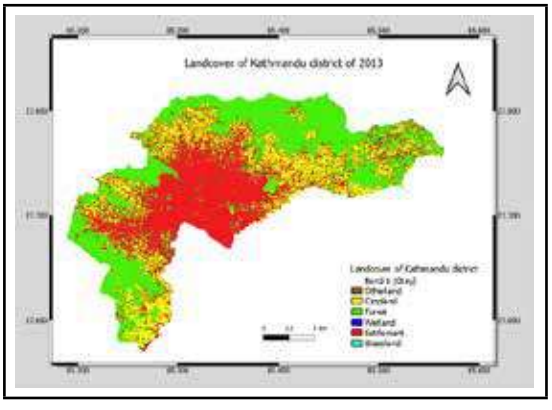

Figure 3: Landcover map of 2013

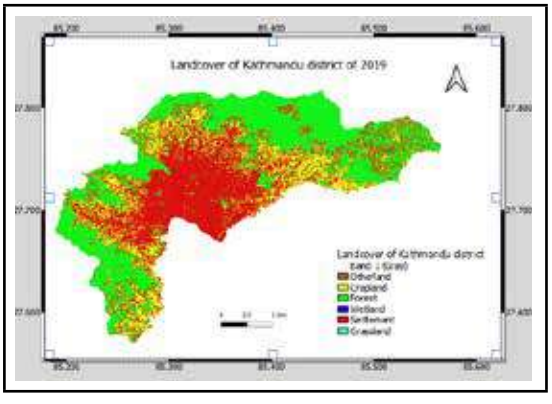

Figure 4: Landcover map of 2019

The study revealed that the major portion of landcover in both years 2013 and 2019 was covered by forest, cropland and settlement. The largest area is covered by forest. Cropland occupies the next largest area after forest, followed by settlement. The remaining areas are covered by otherland, grassland and wetland. The status of landcover change in Kathmandu district between 2013 and 2019 are illustrated in Table 2 and Figure 5.

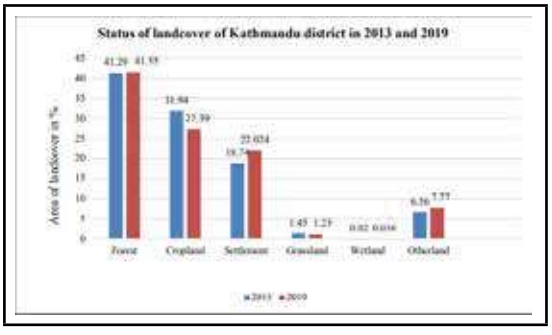

Figure 5: Status of landcover of Kathmandu district of 2013 and 2019

In 2013, the forest covered 170.987 km², or 41.29% of the entire area of Kathmandu district. Following the forest, cropland takes up the second largest land area at 132.27 km², accounting for 32.94 % of the total area. Settlement covers 77.61 km² i.e. 18.74% of the total area. Otherland and grassland cover 27.172 km² and 6.012 km² of land, accounting for 6.56 % and 1.45 % of the district's total area, respectively. Only 0.089 km² i.e. 0.02% wetland are available.

Whereas, in 2019, forest occupied 172.065 km², which is 41.55 % of the total area of the Kathmandu district. The cropland occupies 113.45 km², corresponding to 27.39 % of the total area. After that, settlement occupies 91.21 km² (i.e., 22.02 % of the total area). Otherland and grassland cover 32.167 km² and 5.098 km² of land, representing 7.77% % and 1.23% of the district's total area, respectively. With respect to wetland, this analysis only covers 0.152km² which corresponds to 0.04%. Grasslands are the most difficult land cover to recognize in photographs (Zhao *et. al*., 2017).

Table 2: Status of landcover of Kathmandu district in 2013 and 2019

Landcover class	Area in 2013 (Sq. Km.)	Area in 2019 (Sq. Km.)
Forest	170.987	172.065
Cropland	132.27	113.449
Settlement	77.61	91.209
Grassland	6.012	5.098
Wetland	0.0894	0.152
Other land	27.172	32.167
Total	414.14	414.14

Table 3: Status of landcover change of Kathmandu district in 2013 and 2019

Landcover class	Change in area (Sq. km.) (2013-2019)	Change in area (%)
Forest	1.078	2.73
Crop land	-18.821	-47.68
Settlement	13.599	34.45
Grassland	-0.914	-2.32
Wetland	0.062	0.16
Other land	4.995	12.66

The landcover change analysis showed landcover changes based on the respective initial year 2013 as a reference. The result indicates that forests, otherland, wetland, and settlements have increased, whereas cropland and grassland have decreased. Forest, wetland, settlement, and other land have been expanded by 0.19 km2, 0.015 km2, 16.39 km2, and 5.19 km2, respectively. Cropland and grassland, on the other hand, have shrunk to an area of 20.92 km2 and 0.914 km2, respectively. The status of landcover change in Kathmandu district between 2013 and 2019 is shown in Table 3. The study of the landcover change matrix of 2013 and 2019, i.e., after the earthquake, shows the conversion of each landcover as follows (Table 4)

Table 4: Landcover change matrix of Kathmandu district of 2013 and 2019

Landcover class		2013						
		Other land	Crop land	Forest	Wetland	Settlement	Grass land	Total
		(Area in Sq. Km.)						
2019	Other land	22.01	9.01	0.31	0.01	0.81	0.02	**32.17**
	Cropland	3.05	109.29	1.08	0	0.03	0.003	**113.45**
	Forest	1.51	1.45	168.25	0.00	0.01	0.85	172.07
	Wetland	0.02	0.05	0.002	0.08	0	0	0.15
	Settlement	0.58	12.46	1.32	0	76.76	0.089	91.21
	Grassland	0.002	0.01	0.025	0.00	0.01	5.05	5.10
	Total	27.17	132.27	170.98	0.09	77.61	6.01	414.14

(Note: This study used the mapped area of 414.14 km² applying WGS 84 map projection.)

The forest cover has been increased by 0.26 %. The major land cover conversion into the forest is from otherland (0.36 %) and cropland (0.35%). Likewise, 0.21% of grassland, 0.001% of settlement and 0.00009% of wetland area are converted into forest. However, forest cover is converted into otherland (0.075%), cropland (0.261%), wetland (0.0005%), settlement (0.32%) and grassland (0.006%). Thus, area of total forest gain and total forest loss of Kathmandu district is 3.82 km² and 2.74 km² respectively. According to ward level analysis of landcover conversion of Kathmandu district, major forest gain areas are Sheshnarayan-9, Jitpurphedi-5, Sundarijal-1 and Saukhel -9 and major loss areas are Kabhresthali-3, Sangla-8, and Bhimdhunga-2.

The cropland area has decreased by 4.54%. The land cover conversion into the crop is from otherland (0.74%), forest (0.26%), settlement (0.006%), and grassland (0.0007%). However, cropland is converted into otherland (2.18%), forest (0.35%), wetland (0.012%), settlement (3.008%), and grassland (0.002%). Thus, the area of total cropland gain and total cropland loss in Kathmandu district is 4.16 km2 and 22.98 km2, respectively. Major cropland gain areas are Lapsiphedi-9, 3, Sundarijal-5, and Nanglebnhare-6, and major cropland loss areas are Matatirtha-9, Kirtipur-17, and Dahachowk-3.

The area of settlement has been increased by 3.28%. The landcover conversion into the settlement is from otherland (0.14%), cropland (3.008%), forest (0.32%), and grassland (0.02%). However, settlement is converted into otherland (0.196%), cropland (0.006%), forest (0.001%), and grassland (0.002%). Thus, the area of total settlement area gain and total settlement area loss is 14.45 km2 and 0.85 km2, respectively. Major settlement gain areas are Tokha Chandeshwari-5, Kirtipur-14, and Matatirtha-2, and major settlement loss areas are Gothatar-6, Balambu-4, and Kirtipur-6.

The rapid increase in built-up area confirms past reports by the United Nations Department of Economic and Social Affairs and subsequently by other researchers (Khanal *et al.,* 2019; Ishtiaque et al., 2017; and Poudel et al., 2016), who asserted that urbanization is the main cause for the conversion of agricultural and forest lands into built-up areas in Kathmandu valley. The increase in urban growth has been increased in adjacent areas of the cities and built-up areas along the main roads by creating new cores. Khanal et al. (2019) reported that the rate of urbanization in Kathmandu increased rapidly after the civil war ended in 2006.

The area of grassland has decreased by 0.22%. The landcover conversion into grassland is from otherland (0.0005%), cropland (0.002%), forest (0.006%), wetland (0.0005%), and settlement (0.002%). However, grassland is converted into otherland (0.005%), cropland (0.0007%), forest (0.21%), and settlement (0.021%). Thus, the area of total grassland gain and total grassland loss is 0.048 km2 and 0.962 km2, respectively. Major grassland gain areas are Kathmandu-31, 35, and 9, and major grassland loss areas are Kathmandu-35, Dakshinkali-6, and Chhaimale-9.

The area of wetland has been increased by 0.02%. The landcover conversion into the wetland is from otherland (0.005%), cropland (0.012%), and forest (0.0005%). However, wetland is converted into otherland (0.002%), forest (0.0009%), and grassland (0.0005%). Thus, the area of total wetland gain and loss is 0.072 km2 and 0.009 km2, respectively. Major wetland gain areas are Dakshinkali-6, Kathmandu-1, and Chalnakhel-9, and major wetland loss areas are Kirtipur-15, Kathmandu-1, and Gongabu-1.

The area of otherland has increased by 1.21%. The landcover conversion into otherland is from cropland (2.18%), forest (0.07%), wetland (0.002%), settlement (0.19%), and grassland (0.005%). However, other land is converted into cropland (0.74%), forest (0.36%), wetland (0.005%), settlement (0.14%), and grassland (0.0005%). Thus, the area of total otherland gain and total otherland loss is 10.16 km2 and 5.16 km2, respectively. Major other land gain areas are Matatirtha-9, Kirtipur-17, and Dahachok-3, and major other land loss areas are Lapsiphedi-1, Sundarijal-1, and Nanglebhare-1.

Landcover changes are regarded as a main source of environmental changes such as soil degradation, greenhouse gas emissions, climate change, and biodiversity loss. Therefore, land cover change can be considered an important issue in the present context. Among various landcovers, forests are vital to addressing these kinds of global concerns.

The error matrix generated from the accuracy assessment of 2013 and 2019 landcover is presented in tables 5 and 6, respectively. The overall accuracy of the classification and the overall kappa statistic achieved were 80% and 0.74, respectively, for 2013, whereas the overall accuracy of the classification and kappa statistic achieved 83.33% and 0.78, respectively, for 2019. In 2013, the user's accuracy of wetland, settlement, and grassland was 100%, 100%, 80%, and 100%, respectively, whereas the producer's accuracy of wetland, settlement, and grassland was 100%, 100%, 80%, and 100%, respectively. Similarly, in 2019, the user's accuracy of wetland, settlement, and grassland is 100%, 100%, 80%, and 100%, respectively, whereas the producer's accuracy of wetland, settlement, and grassland is 100%, 100%, 83.33%, and 100%, respectively.

During the study, a few sample points in the case of grassland and wetland were taken in comparison to other classes. Even though those sample points were few in number, they were taken with high certainty. However, the data that falls under cropland was not fully covered while collecting data, as some areas of cropland were left accounting for bare soil, due to which

the areas of other land automatically rose in both years. The NLCMS study conducted by FRTC in 2022 shows that there is no bare soil in Kathmandu district. The result of this study regarding cropland area is less (-31.26 km2 in 2013 and 56.93 km2 in 2013) than the result of FRTC, which indicates that some landcover parts that fall under the category of cropland were left while collecting data. Due to this, those left areas were automatically added to other land as bare soil, due to which cropland has the lowest user's accuracy obtained, i.e., 62.5% in 2013 and 55.56% in 2019. However, forest, wetland, and grassland have the highest accuracy obtained, followed by settlement in both 2013 and 2019.

Table 5: Accuracy assessment of landcover of 2013

	Other land	Crop land	Forest	Wetland	Settlement	Grass land	Total	User's (%)
Otherland	0	0	0	0	0	0	0	0
Cropland	2	5	0	0	1	0	8	62.5
Forest	0	0	8	0	0	0	8	100
Wetland	0	0	0	2	0	0	2	100
Settlement	1	0	0	0	4	0	5	80
Grassland	0	0	0	0	0	1	1	100
Column Total	3	5	8	2	5	1	24	
Producer's accuracy (%)	0	100	100	100	80	100		

Table 6: Accuracy assessment of landcover of 2019

	Otherland	Cropland	Forest	Wetland	Settlement	Grassland	Total	User's (%)
Otherland	0	0	0	0	0	0	0	0
Cropland	3	5	0	0	1	0	9	55.56
Forest	0	0	8	0	0	0	8	100
Wetland	0	0	0	2	0	0	2	100
Settlement	1	0	0	0	5	0	6	80
Grassland	0	0	0	0	0	1	1	100
Column Total	4	5	8	2	6	1	26	
Producer's accuracy (%)	0	100	100	100	83.33	100		

4. CONCLUSION

Land cover is a critical factor in the environmental study of Nepal. This analysis states the current status of forests and other different land cover classes in 2013 and 2019. Based on the results derived from this assessment, the calculated results for forests, settlements, wetlands, and grassland are reliable. However, further studies are necessary to generate more reliable results in terms of cropland and other land.

REFERENCE

FAO, (1995). *Planning for sustainable use of land resources: towards a new approach* (No. 2). Food & Agriculture Organization of the UN (FAO)

Bakrania, S., (2015). *Urbanisation and urban growth in Nepal.* Governance, Social Development, Humanitarian Response and Conflict (GSDRC), Applied Knowledge Services of University of Birmingham, Birmingham, UK. http://www. gsdrc. org/wp-content/ uploads/2015/11/HDQ1294. pdf.

UNHabitat, (2013). *State of the world's cities 2012/2013: Prosperity of cities. Routledge*

Jensen, J. R., (2005). *Introductory Digital Image Processing: A Remote Sensing Perspective.* Upper Saddle River, Prenice Hall. Inc. 525p.

Lambin, E. F., Rounsevell, M. D. and Geist, H.J., (2000). Are agricultural land-use models able to predict changes in land-use intensity? *Agriculture, Ecosystems & Environment*, 82(1-3), pp.321-331.

Lee, J. K., Acharya, T. D. and Lee, D. H., (2018). Exploring land cover classification accuracy of Landsat 8 image using spectral index layer stacking in hilly region of South Korea. *Sensors and Materials*, 30(12), pp.2927-2941.

Maharjan, A., (2018). *Land use /Land cover of Kathmandu valley by using remote sensing and GIS.* M.Sc. Thesis, Central Department of Environmental Science, Institute of Science and Technology, Tribhuvan University, Kritipur, Kathmandu, Nepal.

Pérez-Soba, M. et al. (2008). Land use functions — a multifunctionality approach to assess the impact of land use changes on land use sustainability. In: Helming, K., Pérez-Soba, M., Tabbush, P. (eds) *Sustainability Impact Assessment of Land Use Changes.* Springer, Berlin, Heidelberg. https://doi.org/10.1007/978-3-540-78648-1_19

GoN, (2021). *National Population and Housing Census 2021.*

Ravisankar, T., (2017). *Land use Land cover Mapping.* National Remote Sensing Center (NRSC)/ISRO Hyderabad-500625 India.

Rwanga, S.S. and Ndambuki, J.M., (2017). Accuracy assessment of land use/ land cover classification using remote sensing and GIS. *International Journal of Geosciences,* 8(04), p.611.

Sidhu, N., Pebesma, E. and Câmara, G., (2018). Using Google Earth Engine to detect land cover change: Singapore as a use case. *European Journal of Remote Sensing*, 51(1), pp.486-500.

Ukrainski, P., (2019). *Classification accuracy assessment. Confusion matrix method.*

Vatseva, R., Kopecka, M., Otahel, J., Rosina, K., Kitev, A. and Genchev, S., (2016). *Mapping urban green spaces based on remote sensing data: Case studies in Bulgaria and Slovakia.* In Proceedings of 6th International Conference on Cartography and GIS (pp. 569-578).

WHO, (2017). *Urban green spaces: a brief for action.* World Health Organization.

ACKNOWLEDGEMENT

I would like to express gratitude to Ms. Basanti Kumpakha for her immense support, sincere attention and guidance throughout my research period. I am also thankful to Mr. Rajaram Aryal for his advices on my research. I am greatly thankful to Dr. Narayan Prasad Koju for all the encouragement. I owe my great debt to Ms. Sangita Shakya, Mr. Amul Kumar Acharya, Mr. Dipesh Kumar Sharma and Mr. Prakash Lamichhane for their support in successful completion of this research work.

Author's Information

Name	:	Bimala Lama
Academic Qualification	:	B.Sc. Forestry and M.Sc. Natural Resources Management
Organization	:	Forest Research and Training Centre, Babarmahal, Kathmandu
Current Designation	:	Assistant Research Officer
Work Experience	:	[9 years]
Published paper/article	:	[6]

Can GNSS Derived Height Replace Levelling Height? - A Case of Low-Land of Nepal

Shankar K.C.[1], Stallin Bhandari [1], Sandesh Upadhyaya [1], Sanjeevan Shrestha [1]
shankarkc01@gmail.com, stallin.bhandari@gmail.com, sandeshupadhya1@gmail.com, shr.sanjeevan@gmail.com
[1]Survey Department

KEYWORDS

GNSS derived orthometric height, GNSS, geoid, precise levelling, ellipsoidal height

ABSTRACT

Orthometric height is the generally adopted type of height worldwide and in geomatics community. Precise levelling has been the method of obtaining orthometric height in past for most of the country, so as the Nepal. However, due to wide usage of Global Navigation Satellite System (GNSS), the alternative approach of combining GNSS derived ellipsoidal height with geoid undulation to get GNSS derived orthometric height, has been used extensively. In Nepal, this technique was officially adopted in 2020 for Everest height measurement and understood as the efficient way to comply with levelling height. In this study, GNSS surveying was conducted on 15 stations located at the lowland region of Nepal and orthometric heights were obtained from GNSS and geoid method. When compared GNSS derived orthometric height with precise levelling height, the difference remained within threshold of 5cm for majority of observation stations. However, these differences are not sufficient to support the standards set for the third order levelling by Survey Department (SD). The accuracy of GNSS derived orthometric height can be significantly affected by various environment and existing resources such as existing accuracy of geoid, nature of precise levelling height. Considering the revisit upon these conditions, we expect GNSS-levelling as a strong alternative to time consuming, tedious, and costly precise levelling which is most suitable method of obtaining orthometric height in lowland topography at a precision less than 4 cm.

1 INTRODUCTION

1.1 Background

The global navigation satellite system (GNSS) is one of the most popular surveying techniques for determining 3D-position of various objects. This includes establishment of control points for detailed surveying as well as mapping purposes. Despite the fact that GNSS produces accurate 3D position on the earth, its height refers to the ellipsoidal height and does not refer to the vertical datum. The mean sea level (MSL) is the most common local vertical datum and spirit levelling has been employed continually to provide orthometric heights that always coincide with the local vertical datum. Although constructing a vertical datum for practically every country require substantial effort and financial investment, levelling procedures are employed to determine height. It is now feasible to obtain orthometric height using the GNSS technology, also known as GNSS-derived height, thanks to the development of accurate local geoid

(Menegbo, 2017). In many countries, like the United States of America, Australia, Japan, Korea, etc., it has been widely employed as a replacement for spirit levelling since it is more time and cost efficient (Lee et al., 2021).

Through Geodetic Survey Division (GSD), the Survey Department (SD) of Nepal is constantly striving to construct a geodetic network by carrying out several activities across the nation, including precise levelling, astronomical survey, gravity survey, GNSS and other geodetic survey work activities. Focusing on the vertical reference system, vertical datum of Nepal has been realized from extensive network of levelling networks of around 7600 km along the major roads at a period of around half century. Owing to the issues of existing vertical reference system which is passive by nature, continuously deformed as a result of seismic deformation and secular and annular shifts, in-sufficient levelling network due to time and cost intensive in nature etc.- SD is aiming to develop hybrid geoid model for vertical datum. As a starting point, SD has prepared a locally constrained nationwide geoid and used a GNSS-derived height determination approach to determine the height of Mount Everest. The establishment of a permanent bench mark (PBM) and its orthometric height using GNSS observation is one of the potential uses of the hybrid geoid model in the future. To do this, it is necessary to guarantee the GNSS based height's precision and efficiency in comparison with the levelling-based height. Although levelling work has been replaced by GNSS based height in many countries (Featherstone, 2008; Even-Tzur & Steinberg, 2009; Ampatzidis *et. al,* 2018; Oluyori *et. al,* 2018; Sikder et. al, 2020), there has been no research on this topic in Nepal. Conseqeuntly, in order to examine the prospect of replacing levelling height with GNSS-derived height, the study evaluates the precision of the GNSS derived orthometric height in low-land of Nepal by comparing it with levelling based height.

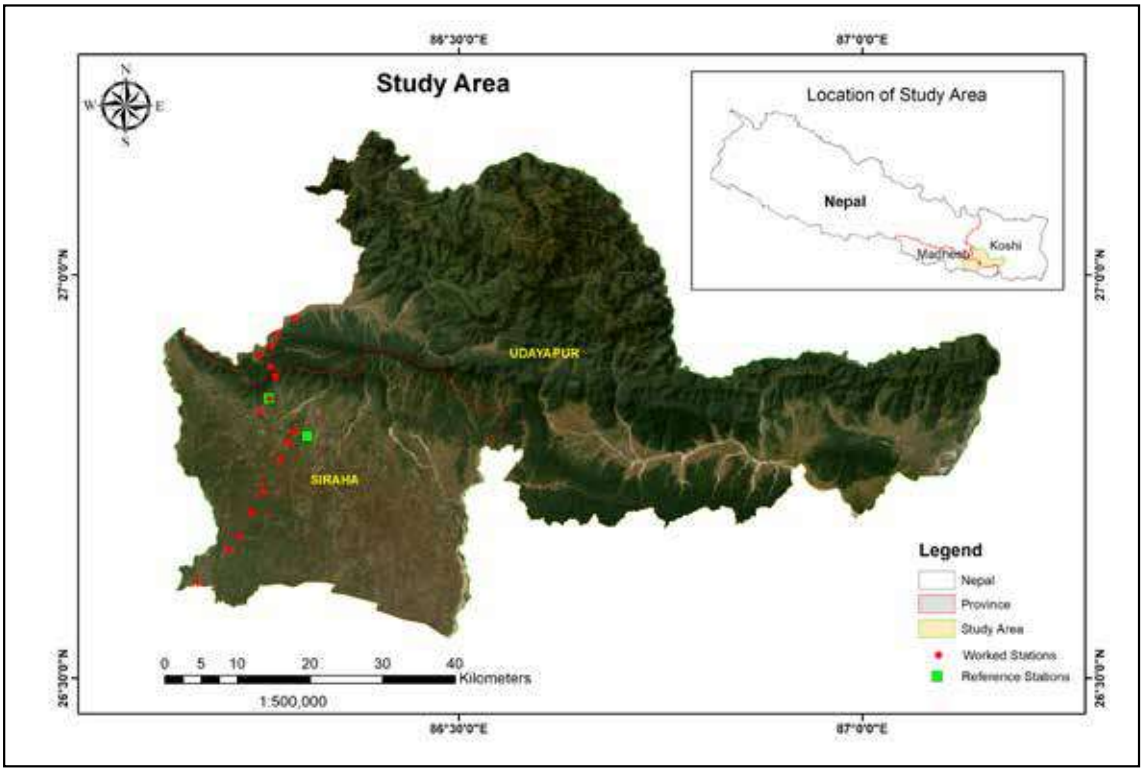

Figure 1 : Study Area

1.2. Study Area

The study area is located at the lowland region of the Terai, Nepal. In this study, 15 permanent levelling benchmarks (PBM) were surveyed and used. The lowland belongs to Siraha district and Udayapur district. The spatial extent of study area is: 26° 37' 7.6368" N to 26° 56' 46.9464" N in latitude and 86° 10' 30.4752" E to 86° 18' 44.5824" E in longitude. The elevation range of selected PBMs in the study area is around 180m (178.19m), with lowest and highest PBMs at an elevation of 8.65m and 186.84m respectively.

These PBMs are located along Chorhawa Siraha Madar Road, East-West Highway, and Mirchaiya-Katari Road. Since a refined geoid of this region was developed during Sagarmatha Height Measurement project, this site was chosen for the study purpose.

2. Methodology

Table 1: Survey Strategy for GNSS-derived height determination in Lowland of Nepal

Parameter	Specification
Observation period per session	4 hours
Number of sessions	2
Data logging interval	15s
Survey type	Static, Differential
Receiver	Multiple frequency
Check for the consistency of baseline processing results	Smaller than 3 cm between 4 h solutions of the first and second session
Geoid model	Geoid model prepared during Sagarmatha Height Measurement Project

2.1. Data Acquisition Strategy

For determination of GNSS-derived height, two stations were run daily as reference stations, namely: base 1 & base 2, while in PBMs, GNSS survey was carried out in differential GNSS mode. Therefore, base 1 and base 2 serve as master stations, while other PBMs were used as rover stations. Every PBM was surveyed twice with two sessions of 4 hours period separated by a time interval taken to shuffle the receivers and restart the survey. For example, 3 BMs were occupied by 3 GNSS receivers for the first 4 hours of a day and then GNSS receivers were shuffled between those same 3 BMs and occupied for the next 4 hours. The intention of the second occupation at the same station was to make separate observations in different scenario, so that, the geometry of satellite and the receiver changes at different session. These different scenario provides the redundant observations. In addition to redundancy, occupying the same stations twice offers independent check of the recorded observations. The general specification of surveying strategy is shown in Table 1.

2.2 Data Processing Strategy

Following the observation, GNSS data processing was carried out using the RTKLIB (*RTKLIB: An Open Source Program Package for GNSS Positioning*, n.d.) and Trimble Business Center (TBC) software. The detailed explanation are discussed in following sections.

2.2.1 Data Preparation/Data Cleaning:

This stage involved downloading data from the GNSS receivers; conversion to Receiver Independent Exchange (RINEX) format, and checking and making corrections to station metadata, such as proper naming, instrument height etc. as needed.

2.2.2 Precise Point Positioning (PPP) of Reference Stations:

Two reference stations' positions were determined using the PPP (Teunissen & Kleusberg, 1998) approach. The PPP technique was implemented using RTKLIB. The location of a station was calculated in standalone and absolute mode in PPP approach. Processing was done on the dual frequency signal's

pseudorange and carrier phase data. Errors are meticulously fixed using IGS precise satellite orbit and clock products. Both receiver phase center offset (PCO) and phase center variation (PCV) for the relevant antenna model were used during processing. Ionosphere error was removed by Ionosphere-Free combination method while troposphere error was corrected using standard model and residual troposphere error was estimated along with carrier phase ambiguity, coordinate and receiver clock. The error in position due to earth and ocean tide was corrected using tidal loading models.

2.2.3 DGNSS Positioning of PBMs:

The position of each PBMs were computed relative to the reference stations based on the Differential GNSS positioning method (*Differencing | GEOG 862:*, n.d.) in TBC platform. DGNSS is applied in a short baseline scenario where double differencing is used to eliminate errors from the satellite and atmosphere, such as satellite orbit error, satellite clock error, relativity error, ionosphere error, and troposphere error. This is due to the fact that both satellite and atmospheric errors remain common at two end of the short baseline. Based on this differential positioning technique, the absolute positions of PBMs were derived relative to the base stations.

The final coordinates of PBMs were calculated after performing network adjustment with fixed coordinates of reference stations. These final adjusted coordinates in the form of triplets (Latitude, Longitude and ellipsoidal height) were used for further analysis.

The GNSS observations were collected and processed over the course of two different sessions to properly detect and correct blunders. Since the study aims to work on vertical component of the result, the study focused on the uncertainty of the ellipsoidal height. The difference between the vertical precision obtained from first session was compared to second session and the baselines with difference falling within 3cm (Lee *et al.,* 2021) were accepted for further processing.

2.2.4 Precise Levelling Height:

The precise levelling heights of individual PBMs along the alignments under the study were obtained from the Levelling and Gravity Section, GSD, of SD, Nepal. These precise levelling heights were compared against the GNSS-derived orthometric height calculated from GNSS and geoid approach.

2.2.5 Extraction of Geoid Undulation

Geoid undulation values at the PBMs, required for deriving orthometric heights, were extracted from Nepal Geoid 2021 with an accuracy of around 8 cm within the study area (unpublished). The geoid was fitted to local MSL obtained from precise leveling heights. The orthometric heights were calculated from both fitted and non-fitted geoid. The geoid fitting job had a mean of 2.141 cm and a standard deviation of 4.1 cm.

2.2.6 Computation of Orthometric Height

Equation 1 was used to derive the orthometric height from the ellipsoidal height obtained from GNSS observations using geoid undulation values (Heiskanen & Moritz, 1967).

$$H = h - N \quad \ldots\ldots\ldots\ldots\ldots\ldots\ldots\ldots\ldots\ldots\ldots\ldots\ldots\ldots\ldots\ldots \quad (i)$$

Where, H is orthometric height, h is ellipsoidal height, and N is geoid undulation (fitted and non-fitted both).

2.2.7 Comparison of Precise Levelling Heights & Orthometric Heights

The comparison of GNSS derived orthometric height and precise levelling height were performed in two ways. Firstly, the orthometric height and precise levelling height at each benchmark was compared by computing difference and the nature of such difference was examined. Secondly, the consecutive difference in GNSS derived orthometric

height and in precise levelling height between consecutive pair of PBMs were computed and compared against third order levelling tolerance prescribed by GSD in levelling instruction book (Shrestha, 1988) as well as tolerance prescribed by ICSM guideline, Australia (Intergovernmental Committee on Surveying and Mapping, 2020). The formula for the tolerance set by GSD and ICSM for third order levelling can be derived from the equation (2) and (3) respectively.

$$\text{Tolerance} = 5.0\sqrt{k}\text{mm} \quad \text{(3rd order leveling)} \quad (ii)$$

$$\text{Tolerance} = 12.0\sqrt{k}\text{mm} \quad \text{(3rd order leveling)} \quad (iii)$$

Where, K is length of levelling alignment in km.

3. Results:

3.1 Precision Analysis

In this section, the vertical precisions of baseline processing acquired in both sessions were compared to check the consistency. In this comparison, the baseline from base 2 to Madar had a significant variance, measuring 3.8 cm. The comparison for other baselines showed differences below 3cm. It suggested consistency in vertical accuracy for baseline processing of the observation. Thus, data of both sessions were merged and processed to get the final horizontal position and ellipsoidal height of PBMs.

Figure 2 shows the differences between GNSS derived orthometric height (from fitted geoid) and those obtained from precise levelling for the 15 unknown stations (BM's) located at the lowland of terai area. As shown in figure 2, 10 out of 15 stations (67%) observation showed difference smaller than 3 cm. The difference was smaller than 1, 2, 3 and 4 cm at five stations (33%), six stations (40%), 10 stations (67%) and 12 stations (80%). Only 20% (3 stations) of observation showed the difference in the range of 4-10 cm with maximum difference of 8.04cm at station 203-014.1.Thus, the mean absolute difference was calculated to be approximately 2.93cm.m

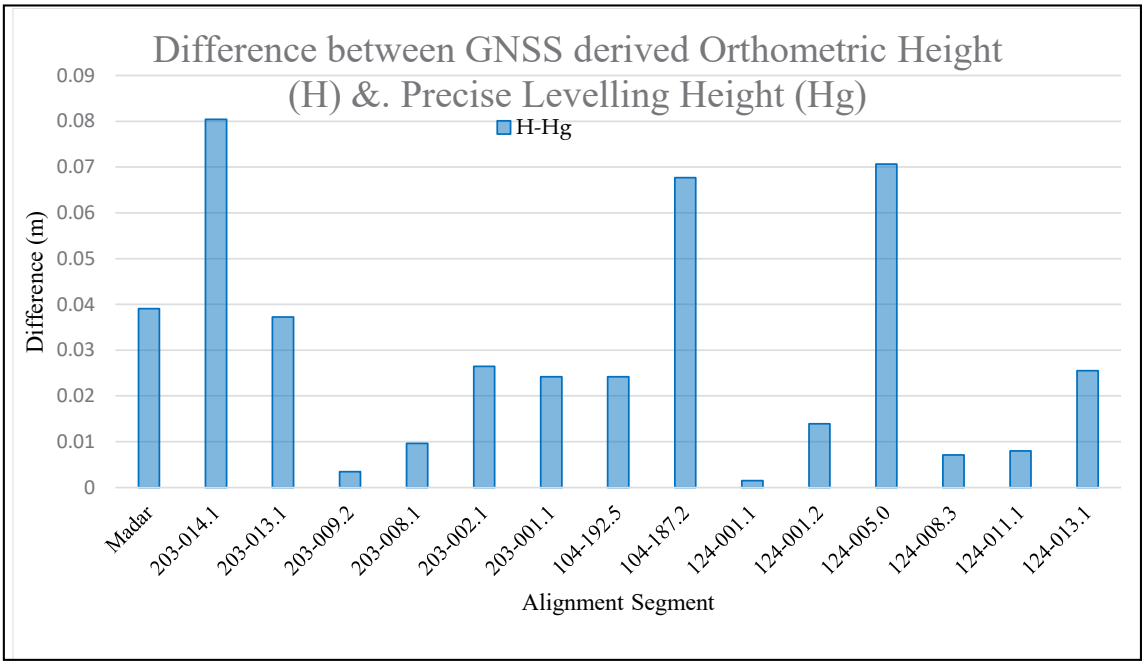

Figure 2: Plot of difference between GNSS derived orthometric height (from fitted geoid) and precise levelling height at each benchmark (Each bar corresponds to each BM and represent difference between orthometric height obtained from GNSS/geoid method and corresponding precise levelling height at that BM. The black horizontal line represents difference of 0.05m.)

3.2 Possibility of substituting GNSS derived orthometric height for third order levelling

Relative height differences between each successive station were calculated for both precise levelling heights and orthometric heights. This relative difference has been called consecutive height difference here. Difference of these two consecutive height differences was then compared with tolerance of third order levelling. The difference of relative difference of orthometric height and relative difference of precise levelling height (from both fitted and non-fitted geoid), the Tolerance of third order levelling set by GSD (equation (2)) and tolerance of third order levelling set by ICSM (equation (3)) are shown in Figure 3.

The result of relative differences from fitted geoid shows that only 6 segments (43%) fall within tolerance set by ICSM and only 4 segments (28%) fall within in tolerance set by GSD (see Figure 3). Whereas, The result from non- fitted geoid shows that only 6 segments (43%) segments fall within tolerance set by ICSM and only 4 segments (28%) fall within in tolerance set by GSD (see Figure 3).

The differences between GNSS derived orthometric heights from fitted geoid and precise leveling heights shows that only 7 segments (50%) fall within tolerance set by ICSM and only 4 segments (29%) fall within tolerance set by GSD. The remaining segments mostly deviate from the tolerance value.

The result refers that, based on present scenario, GNSS derived orthometric height cannot replace the third order levelling in lowland of Nepal. This may be due to the fact that GNSS derived orthometric height determination is largely affected by the site specific environmental conditions and available infrastructure for GNSS height derivation, the detailed explanation is placed in section 4..

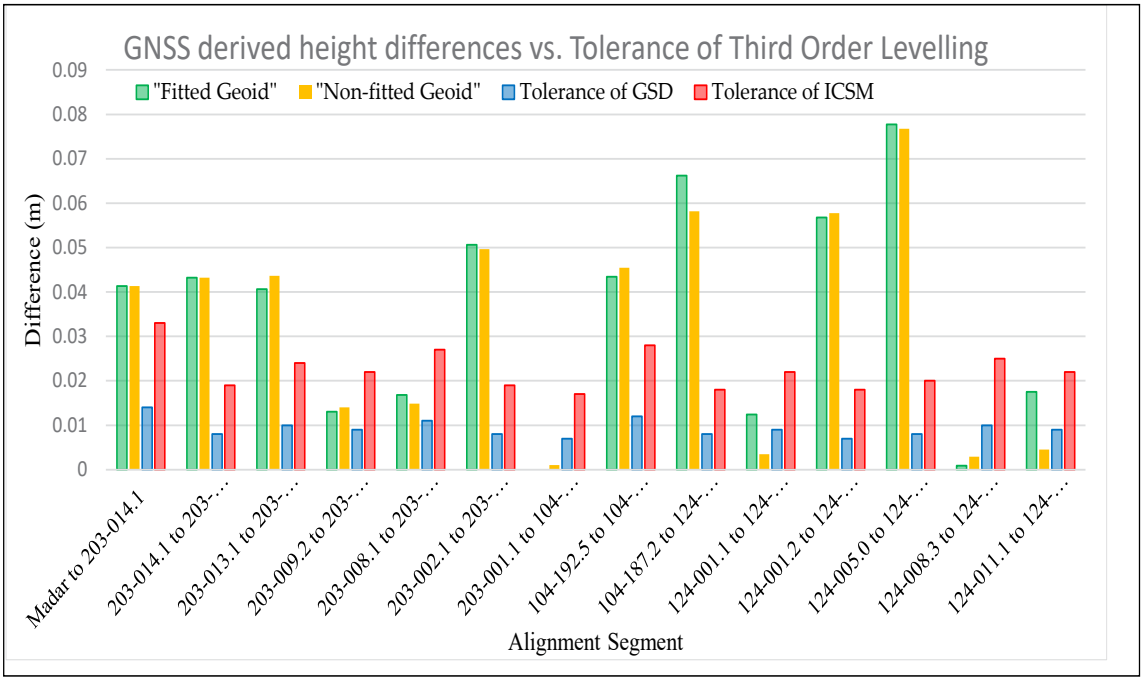

Figure 3: Plot of comparison of GNSS derived orthometric height differences (both from Fitted geoid and non-fitted geoid) with Tolerance of third order levelling, set by GSD and ICSM (At each segment, the difference of difference in orthometric height and difference in precise levelling height is computed and compared against tolerance of third order levelling according to GSD and ICSM.)

4. DISCUSSION

In this section the potential sources that could have deteriorated the precision of GNSS derived orthometric height has been discussed in detail.

4.1 Site Conditions and Multipath Effect

Referring to the Figure 1, only at 3 stations- 203-014.1, 104-187.2, and 124-005, the orthometric heights deviates from its precise levelling heights by more than 4cm. Examining the site condition of these stations, it was found that these stations were substantially effected by multipath conditions, as shown in figure 4. This is due to the fact that, the PBM stations are generally constructed to avoid unwanted intervention to keep PBMs safe. So, there are several cases where the PBMs are unfit for GNSS survey, resulting in significant multipath errors, which is the case in aforementioned stations.

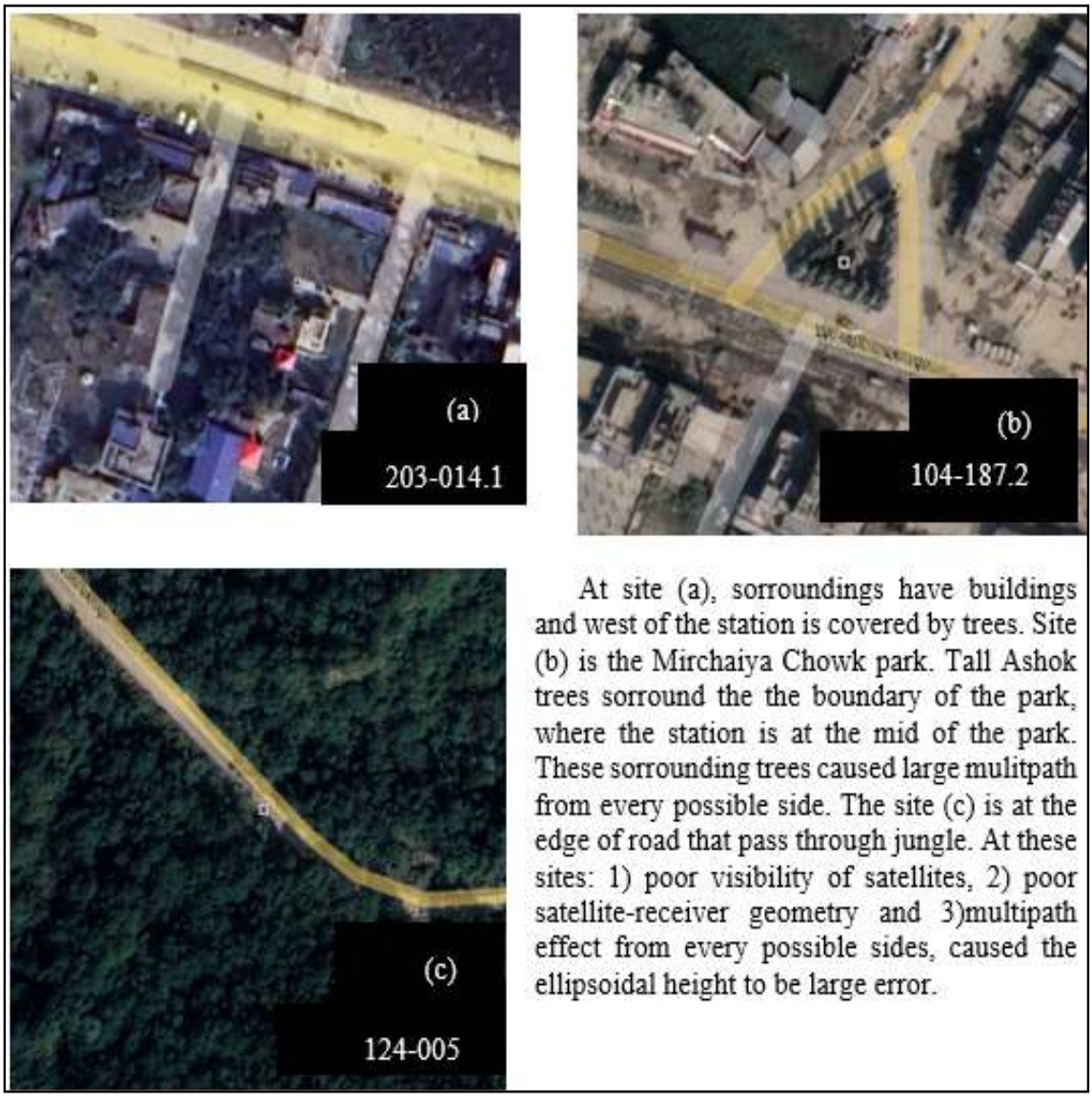

Figure 4: Site condition of PBMs whose ellipsoidal height has large errors

4.2 Precision of Existing Geoid

The precision of geoid has large role on the resulting accuracy from GNSS derived orthometric height. Reportedly, Korea has developed a geoid called KNGeoid18 having degree of fit of 2.3 cm and obtained the precision of around 3 cm in GNSS derived orthometric height determination approach (Lee et al., 2021). Similary, Australia has created its own geoid, known as the AUSGeoid, which is accurate to within 4-8 cm. Australian height datum (AHD) can be computed directly from the GNSS and AUSGeoid of accuracy of 6-13 cm (Intergovernmental Committee on Surveying and Mapping (ICSM), 2021) Additionally, Thailand's gravimetric geoid model 2017 (THAIG17) has rmse of 4.9 cm, which results in accurate heights of at least 10 cm accuracy level or better (Dumrongchai et al., 2021). However, the study used the geoid (geoid 2021) to extract the geoid undulation has reported accuracy of only about 8 cm in the sagarmatha region and 4 cm in the current study area. This demonstrates that the majorities of the countries that have employed geoid for GNSS-levelling work have prepared the geoid precise with greater precision than we have achieved so far. Therefore, we can conclude that the current geoid lacks the precision for GNSS-levelling works up to the precision of third order levelling.

4.3 Accuracy of Precise Levelling Height

In Nepal, the heights obtained from precise leveling height are actually geometric heights. Gravity correction must be applied to geometric height to derive pure orthometric height which is a physical height in a true sense. Therefore, the GNSS derived orthometric height cannot be easily compared with them given the nature of the precise levelling height that is currently available. Moreover, these heights are not network adjusted height either. The significant disparity in relative differences between them may have also been brought on by these conditions.

5. CONCLUSIONS

This study compared orthometric heights obtained from GNSS and geoid approach (both fitted and non-fitted) with precise levelling heights at 15 BMs which are located at lowland of Terai of Nepal. When GNSS-derived height, from fitted geoid, of 15 unknown points (BMs) were determined based on surveying for 4h/day for two different sessions, it is found that around 78% of points showed differences smaller than 4 cm as compared to the precise levelling results. Though the maximum difference was 8.04cm, the mean absolute difference remained within 2.93 cm. Those 3 stations which have difference larger than 4 cm were found to be situated at places with poor site conditions. If such site conditions are avoided and heavy multipath potentiality is avoided, the difference between orthometric height and precise levelling height can be restrained below 4cm in the lowlands of Nepal.

In addition, comparing the relative difference of GNSS derived orthometric height (from both fitted and non-fitted geoid) and relative difference between precise levelling heights between successive PBMs with tolerance of third order levelling prescribed by GSD and ICSM, it is found that, 28% (4/14 of leveling segments) falls within tolerance of GSD and 43% (6/14 of leveling segments) falls within tolerance of ICSM.

The result shows that GNSS derived orthometric height cannot replace the third order levelling in lowland of Nepal in present scenario as the accuracy of geoid in the study area was found to be around 4 cm only. Moreover, it should be noted that the tolerance set by other countries is higher than that set by GSD.

6. RECOMMENDATIONS

The study demonstrated that, unlike other countries, our current infrastructure supporting the vertical reference system prevents us from substituting GNSS derived orthometric height

for precise levelling height of the third order. Therefore, the suggestions listed below are made to improve the situation so that GNSS derived orthometric height can be used instead of precise levelling height for third order levelling or lower.

- The current site conditions, on which levelling points are constructed, are usually unfavorable for GNSS observation leading to a large vertical position discrepancy. Therefore, it is recommended to establish the levelling points for the future with GNSS observation in mind.
- The available precise levelling height at present is geometric height without network adjustment. It is recommended that such geometric height be subjected to gravimetric correction to convert these into physical height. In addition, network adjustment should be applied to these heights. This makes the orthometric heights acquired using GNSS-geoid technique and the height achieved via precise levelling equivalent.
- The precision of the current geoid cannot be compared to the geoid prepared by the rest of the countries utilizing GNSS levelling as a substitute. Therefore, it is advised to increase geoid's precision in the future.
- When compared to the tolerance set for the same order of levelling by other countries, it can be seen that SD's tolerance for different order levelling is very low. Therefore, it is recommended to review the current levelling guidelines to align with global settings.
- This study used the reference collocated points at the low-land of Nepal, having height difference of nearly 180 m. The study's conclusion might not be precise given the wide diversity of heights in Nepal. Therefore, it is advised to continue the study using the contiguous points that cover every physiographic region of Nepal.
- Additional surface gravity surveys should also be conducted throughout the country to improve accuracy of gravimetric geoid as only certain protion of Nepal has been covered during Western Terai LiDAR Mapping Project and Everest Height Measurement Project. (Bhandari et al, 2022)

REFERENCES

Ampatzidis, D., Bitharis, S., Pikridas, C., & Demirtzoglou, N. (2018). On the improvement of the orthometric heights via GNSS-levelling:. *Geodäsie Geoinf. Landmanag.*, 235-241.

Bhandari S, KC S & Upadhyaya S (2022). *Gravimetry in Survey Department: A brief history and current practices.* Journal of Land Management and Geomatics Education, 34-38.

Differencing | GEOG 862: GPS and GNSS for Geospatial Professionals. (n.d.). Retrieved April 23, 2023, from https://www.e-education.psu.edu/geog862/node/1727

Dumrongchai, P., Srimanee, C., Duangdee, N., & Bairaksa, J. (2021). The determination of Thailand Geoid Model 2017 (TGM2017) from airborne and terrestrial gravimetry. *Terrestrial, Atmospheric and Oceanic Sciences*, *32*(5.2). https://doi.org/10.3319/TAO.2021.08.23.01

Even-Tzur, G., & Steinberg, G. (2009). Using an official undulation model for orthometric height acquisition by GNSS. *Survey Review*, 292-300.

Featherstone, W. (2008). GNSS-based heighting in Australia: Current, emerging and future issues. *Journal of Spatial Science*, 115-133.

Heiskanen, W. A., & Moritz, H. (1967). *Physical Geodesy* (3rd ed.). W.H. Freeman and Company.

ICSM, (2020). *Guideline for Control Surveys by Differential Levelling v2.2*. Intergovernmental Committee on Surveying and Mapping. https://www.icsm.gov.au/sites/default/files/2020-12/Guideline-for-Control-Surveys-by-Differential-Levelling_v2.2.pdf

ICSM, (2021). *Australian Vertical Working Surface (AVWS)*. Intergovernmental Committee on Surveying and Mapping (ICSM), Geodesy Working Group (GWG).

Lee, J., Kwon, J. H., & Lee, Y. (2021). Analyzing Precision and Efficiency of Global Navigation Satellite System-Derived Height Determination for Coastal and Island Areas. *Applied Sciences*, *11*(11), 5310. https://doi.org/10.3390/app11115310

Menegbo, E. (2017). Determination of orthometric elevations using gnss-derived height with the egm2008 geoid height model. *International Journal of Advanced Geosciences*, *5*(1), 13. https://doi.org/10.14419/ijag.v5i1.7190

Oluyori, P., Ono, M., & Eteje, S. (2018). Computations of Geoid Undulation from Comparison of GNSS/Levelling with EGM 2008. *International Journal of Scientific and Research Publications*, 235-241

RTKLIB: An Open Source Program Package for GNSS Positioning. (n.d.). Retrieved April 23, 2023, from https://rtklib.com/

Shrestha, N. N. (1988). *Levelling Instruction Book*. Survey Department, Geodetic Survey Branch.

Sikder, M., Wu, F., Ahmed, W., Thodsan, T., & Zhao, Y. (2020). Assessment of Orthometric Height Derived from Levelling, GNSS. In Proceedings of the 2020 15th IEEE International Conference on Signal Processing, (pp. 689-694). Beijing, China

Teunissen, P. J. G., & Kleusberg, A. (Eds.). (1998). *GPS for Geodesy*. Springer Berlin Heidelberg. https://doi.org/10.1007/978-3-642-72011-6

Author's Information

Name	:	Shanker KC
Academic Qualification	:	BE in Geomatics
Organization	:	Geodetic Survey Division, Survey Department
Current Designation	:	Survey Officer
Work Experience	:	5 years
Published paper/article	:	4

Challenges of Current National Reference Frame (NRF) and Map Sheet Layout in Nepal Cadastral Mapping

Sushil Narsingh Rajbhandari[1] & Damodar Dhakal[1]
sushil.n.rajbhandari@gmail.com, rajddhakal@gmail.com
[1] Survey Department

KEYWORDS

Cadastral Survey, National Reference Frame, Projection System, Transformation Parameter

ABSTRACT

Systematic Cadastral mapping in Nepal used to be carried out using local coordinates. Later National Reference Frame (NRF) and a map sheet layout is being used to improve the situation. Current trend of use of GNSS in establishing control points demands a set of transformation parameters. The coordinates in NRF which are obtained by transforming the GNSS results, does not give expected accuracy to be used for large scale mapping. In addition, map sheet layout is being used not in line with the guidelines due to complications at the margins of projection zones. The conclusion is the current NRF and map sheet layout is not appropriate to use further for large scale mapping – which demands improvements in reference frame as well as projection system.

1. BACKGROUND

Systematic cadastral surveying and mapping in Nepal started in year 1964/65 (Dhakal, 2021) after enactment of Land (Survey Measurement) Act, 1963. During those periods, mapping was based on so called "Local Reference Frame", in which base lines were established locally. These maps are termed as "Island Maps". Use of National Reference Frame (NRF) was not in place. The basis for integration of these maps are the common objects in adjoining maps and their shapes at the map boundaries. This job is not possible in the areas where accumulation of error is considerably high or mapping of neighboring area is absent. In summary, due to absence of geometric basis for georeferencing, integrating such maps is cumbersome task and sometimes impossible.

For overcoming such issues, mapping in the remaining areas has been initiated using coordinates in NRF. An institution was established for establishing nationwide control network of NRF and develop geographic information base, initially with the name "Trigonometrical Survey Branch" in 25 September 1970. Later, name was changed to "Geodetic Survey Division". The division is under the national mapping organization (NMO) of Nepal – "Survey Department".

Details of establishment of control points in NRF and use of map sheet layout for mapping at different scales have been specified in Triangulation Instruction Book (DOS, 1976) as described below in sections 2 and 3 respectively.

This study tries to identify - how the NRF and map sheet layout is being currently

implemented and what are the challenges present in actual practices. The study has been limited to limitation of map sheet layout design (specifically in the zone margins) and NRF.

2. NATIONAL REFERENCE FRAME

For surveying and mapping, NRF and a set of square grid map sheet layout have been adopted. For this purpose, Everest 1830 ellipsoid was used with semi-major axis a = 6, 377, 276.345 m., semi-minor axis b = 6, 356, 075.413 m. and inverse flattening 1/f = 300.8017. The NRF is adopted based on Transverse Mercator (TM) Projection with zones of 3° longitudinal widths (Krakiwsky, 1973). Three such zones have been considered for covering whole area of the Nepal. The central meridians of those zones are 81° E, 84° E and 87° E (Figure 1) with extents of 79°30' - 82°30' E, 82°30' - 85°30' E and 85°30' - 88°30' E; and zone numbering as 44.0, 44.5 and 45.0 respectively. The scale factor at each of the central meridians is 0.9999.

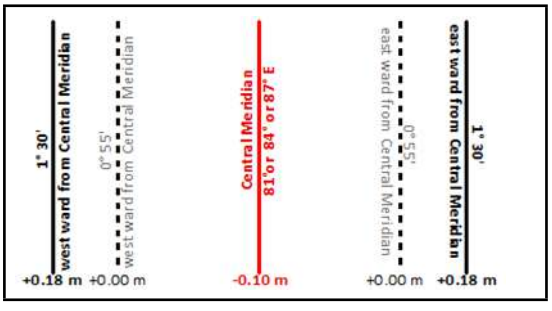

Figure 1:Transverse Mercator Zones.

In each of the zones, distortions per kilometer at the central meridian, at the meridians where the projecting cylinder intersects with the ellipsoid (which are at 0°55' apart eastward and westward from central meridian), and at the edges (which are at 1°30' apart eastward and westward from central meridian) are taken as the values -0.10 m., 0.00 m. and +0.18 m. respectively. Since wider zone consist larger distortion, the modified version of the UTM system (MUTM) with three zones was adopted.

3. MAP SHEET LAYOUT

Coordinate extents of each of the zones is between 350000-650000 m. in easting and 2900000-3400000 m. in northing, each of which spaces has been divided into square grids of 50 km. X 50 km. wide. This resulted in forming 10 rows and 6 columns for each zone. Numbers from 001 to 060, 061 to 120 and 121 to 180 have been assigned to respective grids of the zones starting at north west corner and ending at south east corner (Figure 2).

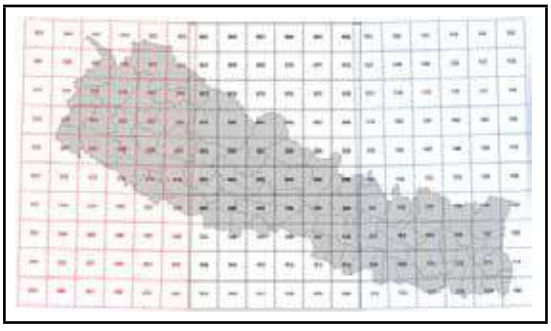

Figure 2: Grids of 50 Km X 50 Km.

Large scale maps are defined to be from 1:2,500 to 1:500. One of the grids of 50 km X 50 km is divided into 40X40 grids to form total 1600 grids of 1,250 m X 1,250 m sheets for mapping at a scale of 1:2,500 (Figure 3). Assignment of number for these sheets started from 0001 at the north-west corner to 1600 at the south-east corner assigning the map sheet number for first grid as 102-0001 and for last as 102-1600.

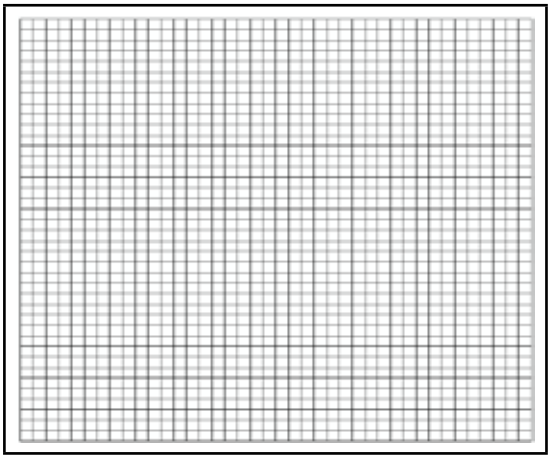

Figure 3: Grids for mapping in scale 1:2500

One of the sheets of 1,250 m. X 1,250 m. is divided into 4 sheets of 625 m X 625 m for mapping at a scale of 1: 1,250. Assignment of number for these grids starts from 1 at the north-west corner and ends at 4 in the south-east corner (Figure 4) assigning the map sheet number for first grid as 102-0001-1 and for last as 102-0001-4.

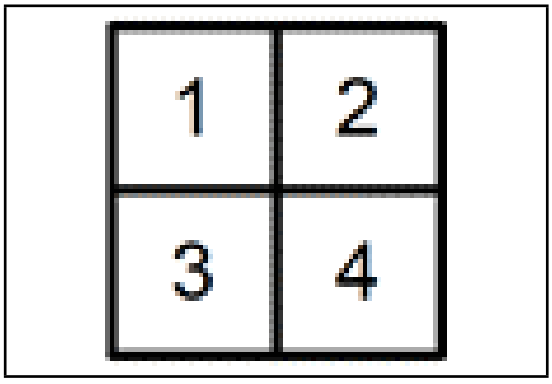

Figure 4: Grids for mapping in scale 1:1250

In the similar manner, same sheet of 1,250 m X 1,250 m is divided into 25 grids of 250 m X 250 m for mapping at a scale of 1:500. Assignment of number for these grids starts from 01 at the north-west corner and ends at 25 in the south-east corner (Figure 5) assigning the map sheet number for first grid as 102-0001-01 and for last as 102-0001-25.

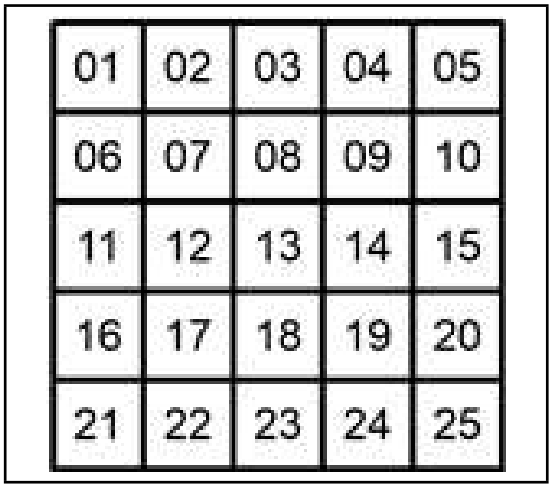

Figure 5: Grids for mapping in scale 1:500.

Map sheet numbering system has been designed in such a way that, for any map whose sheet number (identifier) is known, then its scale, the grid number to which it belongs and the subsequent map sheet can also be identified. For example, if a map has an identification number 085-0254 then the scale of the map is 1: 2,500 and its source grid is 085. If a map identification number is 085-0254-3 then its scale is 1:1,250, its source grid is 085 and its source map sheet at scale 1: 2,500 is 0254. In a similar manner, if a map identification number is 085-0254-13 then its scale is 1:500, it belongs to grid 085 and source map sheet at scale 1: 2,500 of 0254. Apart from this, the location coordinate of a specific map sheet can also be calculated.

4. CONTROL POINTS, COORDINATES AND TRANSFORMATION PARAMETER

For mapping an area, a network of control points has to be established and accurate coordinates of those are needed. During previous periods, traditional technologies such as triangulation, trilateration, traversing were used for such purpose. Recent trend is to use modern technology like GNSS to establish control networks. From the accuracy, economy and time perspective, this technology is efficient which is based on WGS84 Spheroid (with parameter values a = 6, 378, 137.000 m., b = 6, 356 752.314 m. and 1/f = 298.2572). From the use of GNSS technology we can expect relatively higher level of accuracy.

As the ellipsoids of current NRF and GNSS system are different, a set of transformation parameters are needed for transforming coordinates between the two systems. Based on the observation on existing control network, a set of computed transformation parameters to transform coordinates from WGS84 to Everest 1830 has been calculated using Bursa-Wolf method (Manandhar, 2015) as shown in table 1.

Table 1:Transformation parameters.

Translation		
dx=124.3813	*dy=-521.6700*	*dz=-764.5137*
Rotation		
X=-17.1488"	*Y=8.1154*	*Z=-11.1842*
Scale factor=2.1105 ppm		

(Source: Manandhar, 2015)

Manandhar (2015) identified the difference between the existing and computed values of coordinates as 0.77912 m. (minimum), 2.7737 m. (maximum) and 0.872848 m. (average) and also, suggested that these parameters are well enough to map at the scale of 1: 3,500 and smaller, and a need of further improvement of the parameters.

Other sets of parameters are from ESRI which is published and used in its software system. 3 sets of parameters for converting coordinates between the above-mentioned systems are defined (ESRI, 2012) as shown in table 2.

Table 2: Transformation parameters from ESRI.

WGS_1984_To_Nepal_Nagarkot _1_EPSG (Method: Geocentric Translation)		
dx=-293.17 m	*dy=726.18 m*	*dz=-245.36 m*
WGS_1984 _To_ Nepal_Nagarkot_1 (Method: Geocentric Translation)		
dx=-296.00 m	*dy=732.00*	*dz=-273.00 m*
WGS_1984 _To_ Nepal_Nagarkot_2 (Method: Geocentric Translation)		
dx=-296.207 m	*dy=731.245 m*	*dz=-273.001 m*

ESRI also has published the list of accuracies of these parameters as: 0.30 m, 10 m and 5 m respectively.

5. SHEETS AT THE EDGES OF TWO ZONES

The cadastral map sheets at the margins of two projection zones with central meridians 81° E and 84° E covering the part of Rolpa District (Figure 6) is considered for this study. Black line is the boundary between zones. Coverage of this district is the limits of grids 030, 036, 085 and 091. The grids 030 and 036 are in the zone with central meridian 81° E. and the grids 085 and 091 are in that with central meridian 84° E. Between these two zones, almost 5 map sheets of 1: 2,500 scale are overlapped to each other. As the map is in the projection system with central meridian of 84° E, grids those lying in this zone is aligned with the coordinate system where as grids in neighboring zone is not aligned with coordinate system (map is prepared by taking TM projection with 84° E. as central meridian).

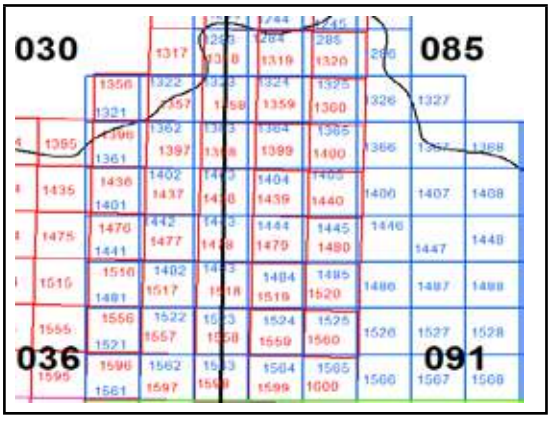

Figure 6: Sheet lying at the edges of two zones.

6. IMPLEMENTATION OF SHEET LAYOUT

Cadastral maps of Rolpa district are prepared in the scale of 1: 2,500. Figure 7 is the map sheet layout used for cadastral surveying in Rolpa District. This implementation of sheet system has been taken as the key example in current study for analysis.

Figure 7: Sheet layout of cadastral map of Rolpa.
(Source: Survey Office, Rolpa)

Form this figure we can visualize, how the actual implementation is different from the criteria specified in triangulation instruction book. Figure 8 is the part of the figure 7 in which it shows that how the concept of sheet layout has been realized differently in practice.

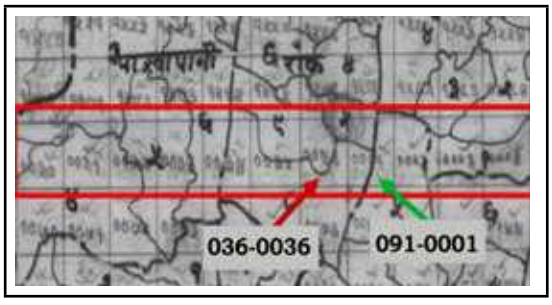

Figure 8: Part of sheet layout from figure 7.

In grid 091, the first-row maps have been started from the number 0001 where as in grid 036 the first-row maps have ended at 0036. From the figure, we note that map sheets 036-0036 and 091-0001 are neighbors. But as per specified criteria, which should be as shown in figure 6, they should overlap each other. All along the edge upwards and downwards, the same practice can be seen. These sheets are aligned with the coordinate system in practice.

It is also of greater interest to take a look at these two cadastral maps sheets 036-0036 and 091-0001. Both of these maps are prepared using a same coordinate system and they come together as like in left of the figure 9. But as per specification, these map sheets should overlap to each other as shown in right of the figure 9.

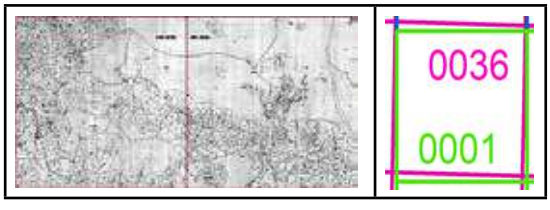

Figure 9: Cadastral map sheets 036-0036 & 091-0001.

7. CONCLUSION AND SUGGESTIONS

The study shows that the coordinates of a zone beyond its limit cannot be used due to exceeding distortion values. But the practice is not in line with this concept. Taking the example of Rolpa district, huge effort has been seen in making seamless map of the cadastral sheets within a single district. It shows that problem was already identified in early stage of adoption of NRF for cadastral mapping and the appropriate solution was also provided for that time. Transformation parameter has also been defined but still need more refinement. Results of GNSS is converted to NRF using computed local transformation parameters based on existing NRF which shows that results of higher accurate data are converted into a lower accurate one. Besides this, the current map sheet layout design has some technical shortcomings in generating seamless geographical information base of whole of the nation showing some discrepancy at the margins of zones.

Based on these conclusions, need of more appropriate coordinate system and map sheet layout design can be suggested, so that they can be implemented in otherwise than specified. Since from the study it is seen that lagging in getting expected accuracy is due to the transformation parameters that are being used to transform from WGS 84 to Everest 1830 spheroid. Hence if WGS 84 system can be adopted then error due to transformation parameter can definitely be reduced. Besides this, projection system can also be adopted so as to reduce the distortions. Shrestha (2021) proposed Lambert Conformal Projection (LCC) with two standard parallel which showed that, distortion produced by LCC is less in compared to MUTM at major portion of the country region. There is no need of three different projection parameters as in MUTM in the case of LCC and sheet overlap problem will also be eliminated. Hence, the use of this projection system can be further studied and make necessary decision on adoption of new projection and the map sheet layout accordingly.

REFERENCES

Dhakal, S., (2021). *Cadastral System in Nepal*. https://www.researchgate.net/ (Accessed: November 01, 2022).

DOS, (n.d.). https://dos.gov.np/office/geodetic (Accessed: November 08, 2022).

DOS, (1976). *Triangulation Instruction Book*. Geodetic Survey Division, Survey Department, Government of Nepal.

ESRI, (2012). *Geographic Transformations*. Environmental System Research Institute, 2012.

Krakiwsky, E. J., (1973). *Conformal Map Projection in Geodesy*.

Manandhar, N., (2015). A Review of Geodetic Datum Transformation of Nepal and Transformation Parameters for WGS84 to Geodetic Datum of Nepal. *Nepalese Journal on Geoinformatics* - Number:14, 2015.

Shrestha, S.M., (2021). *Cartography and geographic information system*. ISBN 9789937093897

Author's Information

Name	:	Sushil Narsingh Rajbhandari
Academic Qualification	:	Professional Master Degree in Geo-information Science and Earth Observation (Specialization: Cartography and Geo-information Visualization)
Organization	:	Survey Department
Current Designation	:	Deputy Director General
Work Experience	:	27

Price of Aerial Photograph

Data	size	NRs. Rate	remarks
Aerial Photo (Scan Copy)	23cm X 23cm	350	

Price of District Level Land Use Digital Data

Data	Unit	Rate	remarks
Present Land Use	Per sq. Km.	5	
GIS Data for Land Resource	Per sq. Km.	5	Except Land Use Zoning Data
Profile	per piece	200	

Price of Local Level Land Use Digital Data

Data	Unit	Rate	remarks
Present Land Use	VDC/Municipality	300	
GIS Data for Land Resource	VDC/Municipality	300	Except Land Use Zoning Data
Profile	VDC/Municipality	200	
Soil Map Data	VDC/Municipality	300	

GIS data for land resource map is available for 20 districts of terai region, Illam and Dhankuta District

Price of Digital Topographic Data Layers

LAYER	Rs/Sheet
Administrative	Free
Transportation	200.00
Building	60.00
Landcover	300.00
Hydrographic	240.00
Contour	240.00
Utility	20.00
Designated Area	20.00
Full Sheet	1000.00

S.N	Data	Price
1	Seamless Data whole Country	Rs. 300000.00
2	Seamless Data (Layerwise- whole country)	
2.1	Administrative Boundary	Free
2.2	Building	Rs. 15000.00
2.3	Contour	Rs. 65000.00
2.4	Transportation	Rs. 60000.00
2.5	Hydrographic	Rs. 70000.00
2.6	Landcover	Rs. 87000.00
2.7	Utility	Rs. 2000.00
2.8	Designated Area	Rs. 1000.00
3	1:1000000 Digital Data	Free
4.1	Rural Municipality (Gaunpalika) unitwise- all layers	Rs. 1000.00
4.2	Municipality (Nagarpalika) unitwise- all layers	Rs. 2000.00
5	District Data (Topographical) 1:100k (Per District)	Rs. 2000.00

Price of Printed maps

S.No	Maps	Unit	Rate (In NRs)
1	Political and Administrative Map of Nepal (2019)	Whole Nepal	150
2	Topographic Base Map (1992-2001)	Sheet	150
3	Topographic Map (1950s)	Sheet	50
4	District Map (1980s)	Sheet	50
5	Land Utilization Map (LRMP)	Sheet	50
6	Land Capability Map (LRMP)	Sheet	50
7	Land System Map (LRMP)	Sheet	50
8	Pysiographic Map of Nepal		50

Image Data:

Digital orthophoto image data of sub urban and core urban areas mintained in tiles conforming to map layout at scales 1:10000 and 1:5000, produced using aerial potography of 1:50000 and 1:15000 scales respectively are also available. Each orthophotoimage data at scale 1:5000 (covering 6.25Km2 of core urban areas) costs Rs. 3,125.00. Similarly, each orthophotoimage data at scale 1:10000 (covering 25 Km2 of sub urban areas) costs Rs 5,000.00.

Price of SOTER Data	Whole Nepal	NRs : 2000.00.

Obituary

All the officials of Survey Department pray to the almighty for eternal peace to the departed soul of the following officials of the department and this department will always remember the contribution they have made during their service period in this department.

Madhur Man Maskey
Then Survey Officer
Shrawan 2079

Ganesh Bahadur Mulmi
Then Survey Officer
11 Aswoj 2079

Madan Shakya
Then Chief Survey Officer
29 Aswoj 2079

Jagendra Karna
Surveyor
29 Aswoj 2079

Krishna Raj Adhikari
Then Deputy Director General
18 Poush 2079

Sarju Sahi
Driver
29 Baisakh 2080

Estimation of Above Ground Biomass and Carbon Stock using UAV images

Sandesh Upadhyaya[1], Prabin Gyawali[2], Sambhav Sapkota[3], Nishan Neupane[4], Manoj Neupane[5]
sandeshupadhya[1]@gmail.com, prabngyawali@gmail.com, sambhavsapkota@gmail.com, nishhan.neupane@gmail.com, mnzneups@gmail.com
[1]Survey Department, [2]Dronepal Pvt. Ltd, [3]Fanshawe College,
[4]Wuhan University, [5]Western Regional Campus

KEYWORDS

Above Ground Biomass, Carbon Stock, Pinus Wallichiana, Photogrammetry, UAV

ABSTRACT

Forests have a vital role in maintaining global climate stability by removing greenhouse gases like carbon dioxide from environment. Estimation of carbon stock is crucial in quantifying the amount of carbon that is present in the forest. The estimation of forest biomass and carbon stock through field measurements is a challenging and time-consuming task. Here in this scenario, our study aims to estimate carbon stock in a forest area using the hybrid technique i.e., aerial survey and ground survey. We used low-altitude remote sensing data acquired by UAV to estimate biomass and carbon stock in an efficient way compared to the traditional techniques. We developed an orthomosaic from the collected aerial imageries and manually delineated tree crowns to obtain crown projection area (CPA) for the entire study area using GIS tools. Our study area contained a mixed species with Pinus Wallichiana to be the dominant species while other species are negligible. Using field-measured tree height and diameter at breast height (DBH) as input, we estimated above-ground biomass (AGB) with an allometric equation and then used a factor value to estimate carbon stock or above-ground carbon (AGC) for six sample plots. Next, we developed a relationship between CPA and carbon stock and validated it by comparing the carbon stock values obtained from the allometric equation for the remaining four sample plots. Among the various developed model, 4th order Polynomial model was chosen due to its highest coefficient of correlation. After the model validation was done the AGC of whole study area was obtained by using the CPA delineated manually from the orthomosaic image. The total AGC and AGB obtained for our study area which was about 7 hectare was 210.7480 tons and 448.4 tons respectively.

1. INTRODUCTION

Forest plays a vital role in keeping the soundness of the global climate. Trees play a pivot role in removing large amount of Carbon dioxide (CO_2), Green House Gases (GHG) from the atmosphere as they develop themselves consuming the carbon and storing those carbon in the biomass of their stems, branches, roots, leaves, etc. So, through the sustainable management of forests, we can reduce CO_2, GHG from the environment (WHRC, 2011). Forest can act both as carbon consumer as well as carbon emitters depending on how we manage the forest. If forest is burned by any means, then forest act as a carbon emitter and if forest consume the carbon for

growing then they act as a carbon consumer. Forest biomass is a significant component of worldwide carbon emission estimations. However, such estimations require accurate and viable methods to estimate Above Ground Biomass (AGB). The above ground carbon in tropical forests represents about 40% of total carbon stocked in forests worldwide (Gibbs et al., 2007) .There is a significant sum of carbon present in the forests of Nepal as about 40% of total area of Nepal is covered by Forests (Oli & Shrestha, 2009) Biomass estimation of Forest ecosystem empowers us to appraise how much CO_2 can be concealed from the atmosphere by the forest. AGB and Carbon Stock estimation can be done through field measurement, remote sensing, and GIS methods (Vashum, 2012). For the biomass estimation a statistical relationship is established between the ground-based measurement and the information extracted from the Unmanned Aerial Vehicle (UAV) imageries. In any case, the most reliable strategy for the assessment of biomass is through cutting of trees and weighing of their parts, which is tedious and costly for large regions (Nordh, 2004) . This destructive method is frequently used to approve other less obtrusive and less expensive techniques such as measurement of carbon stock using remote sensing (Nordh, 2004) . The non-destructive method for AGB assessment includes measuring different parameters such as: diameter at breast height (DBH), height of the tree, volume of the tree, wood density, crown projection area (CPA), etc. and calculating the biomass using allometric equations which are developed for biomass estimation by laying out the relationship between different above mentioned parameters for different tree species (Ravindranath & Ostwald, 2008) .Different equations have been created by different researchers for the assessment of biomass of different tree species. Remote Sensing techniques offers a method for assessing AGB in which a statistical relationship between satellite extracted tree parameters and ground based measurements are used. The information obtained involving a UAV based platform has a high functional adaptability regarding cost, time and repeatability contrasted with the satellite-based platform and conventional manned photographic operations. Among all the biophysical parameters of the tree, DBH is one of the fundamental parameters to assess biomass and carbon since it makes sense of over 95% variety in biomass (Gibbs et al., 2007) .Therefore, this study aimed to assess the estimation of AGB and Carbon Stock using high resolution UAV images through regression models and allometric equations.

2. MATERIALS AND METHODS

2.1 Study area

The forest area of Gosaithan, Banepa Municipality, Nepal has been selected. The forest has large area but only 7 hectare is chosen for our study as this area contains major *Pinus Wallichiana* tree species. The climate of study area is classified as warm and temperate. Other tree species such as Schima Wallichi and Alnus Nepalensis are also present, but they were negligible interms of height and density i.e., other species had the coverage of just 1% compared to *Pinus Wallichiana.*

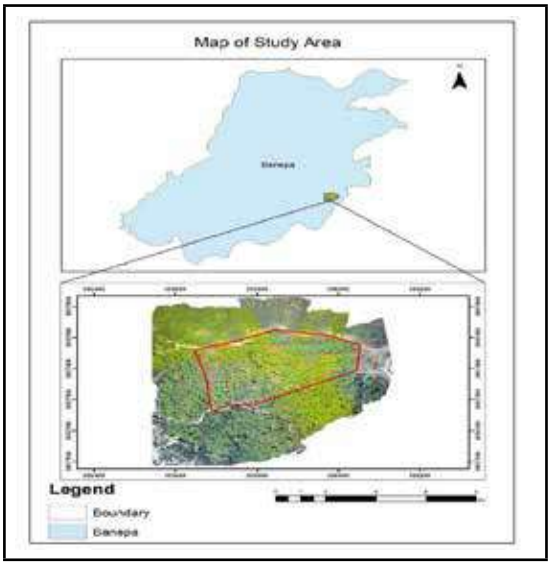

Figure 1 Study area map

2.2 Research method

The methodology consists of three major steps to fulfill the objectives of the study. The first step is field measurement while others are remote sensing and statistical analysis. Field Measurement part was carried out by Differential Global Positioning System (DGPS) survey and biometric data collection. DGPS survey was done to establish control points and biometric data collection was done to collect different tree parameters such as: measurement of DBH, tree height, etc. while the Remote Sensing part includes capturing digital images using UAV, processing the images to generate the orthophoto and mosaicking. Statistical Analysis includes developing the Non-linear regression model between CPA and Carbon Estimation followed by giving input of different parameters in allometric equation to estimate AGB.

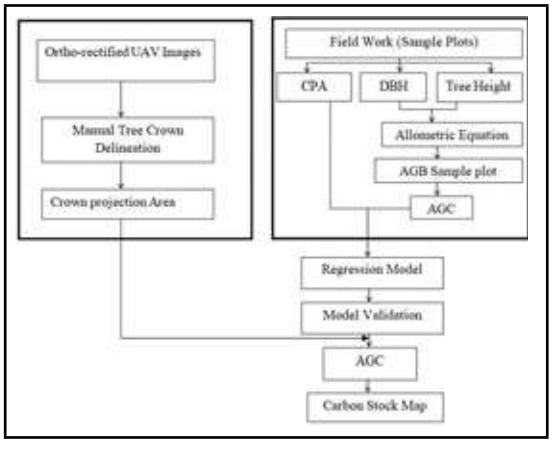

Figure 2 Methodological flowchart

2.2.1 Pre-field work

First, planning was done on how our study will be carried out. Planning includes general framework of the project such as: Establishment of Ground Control Points (GCP), survey method to establish GCP, Flight mission planning, GCP marker to be used during flight mission, Biometric Data collection and so on. Possible plots were identified in Google Earth Pro such that it covers the whole study area, and the coordinates of sample plot centers were noted.

2.2.2 DGPS survey

The ground control points were established using the Static DGPS survey. The established ground control points are required for accurate geo-referencing of the Orthomosaic. A total of 13 ground control points were established.

2.2.3 Biometric data collection

For the data collection of different tree parameters such as: DBH, CPA and height, field works were carried out. According to the study conducted by (Ruiz et al., 2014) ,if the plot size is increased above 500m^2, no significant difference in result could be found. Bigger plot sizes don't fundamentally increase the accuracy of models, yet they increment the expense of fieldwork. So, circular plots of area 500 m^2 (radius 12.62m) were used to collect the biometric parameters of the trees. The radius of the plots was measured by measuring tape.

The diameter at breast height (DBH) was measured using measuring tape at 1.3m above ground as usually DBH is measured at mentioned height above ground (Brown, 2002) . The tree height was measured using the Remote Elevation Measurement (REM) function of the total station. The tree having DBH equal to or greater than 10cm was considered because the trees that have DBH less than 10cm cannot contribute a role significantly in assessing aboveground biomass (Brown, 2002). Measurement of DBH, CPA, and tree height of 113 trees from 10 sample plots was done.

2.2.4 UAV flight planning

Map Pilot Pro was used to plan the photogrammetric flight for the DJI Phantom 3 aircraft. The flight planning took major parameters like flight height, overlap and flight speed into consideration that had direct impact on the quality of imageries that the aircraft would capture (Dandois et al., 2015). The flight mission parameters used is tabulated below:

Table 1 Flight Planning Parameters

Application Name	Map pilot
Type of mission	Singe grid
The geometry of flight mission	Polygonal
Flying height	70m
Resulting resolution	3cm/pixel
Forward Overlap	90%
Side overlap	70%

2.2.5 Ground control point (GCPs)

We selected the spots for GCPs such that there was enough open space in the sense they are visible in UAV images. The ground control points were used for geo-referencing of the orthomosaic. As, the number and distribution of GCPs influence image orientation (Hashem, 2019) so, the GCPs were established such that they cover the area of our study and will be sufficient for geo-referencing.

2.2.6 DGPS data processing

GCPs were established using the Static DGPS survey. Here, established GCPs were computed using the reference station at National Trig point of Nepal. The rover stations at GCP were kept at least 1 hour at a single station. The collected raw data were processed using GNSS Solution by Spectra Precision.

2.2.7 UAV image processing

The software used for image processing was Pix4D Mapper. It was used to generate 3D dense point cloud and orthophoto from UAV images. This software used SfM and stereomatching algorithms for 3D feature reconstructions. SfM represents the process to obtain a 3D structure of a scene of an object from a series of digital images. SfM uses a sequence of overlapping images to produce a sparse 3D model of a scene (Curtis, 2008). Initially, the software executed the keypoints extraction, keypoint matching and camera calibration. In the second stage, point cloud densification was done. The point cloud was used to develop the orthophoto.

2.2.8 Manual tree crown delineation

After obtaining Orthomosaic from image processing, Manual Tree Crown Delineation was done to obtain the CPA of individual trees of the whole study area using Quantum GIS (QGIS).

2.2.9 Data analysis

Different Statistical methods such as coefficient of correlation, regression analysis was done to statistically analyze the obtained data.

2.2.9.1 Estimation of aboveground biomass

The most common method of AGB estimation is by using an allometric equation in a non-destructive way. Various researchers have developed allometric equation based on a destructive method to estimate biomass and carbon in the different forest ecosystem and different tree species (Curtis, 2008). The generic allometric equation developed by (Chave *et al*., 2014) was considered a suitable equation to estimate above-ground biomass of the forest area. A study conducted by (Shrestha et al., 2014) also used the same allometric equation for aboveground tree biomass estimation.

The equation used is:

$$AGB = 0.0559 \times (\rho D^2 H) \quad \ldots\ldots\ldots\ldots i$$

Where,

AGB= estimated above ground biomass (kg),

D= diameter at breast height (cm),

H= tree height (m),

ρ= wood density (gm/cm³) = 0.357 (for Pinus Wallichiana) (Lu & Sinclair, 2006)

2.2.9.2 Estimation of carbon stock

The estimated biomass can be converted to carbon stock by using a factor value. Various factors have been defined but for our study biomass is multiplies by the factor of 0.47 to estimate the carbon stock (Mc Growdy *et.al*., 2004).

The carbon stock is calculated by using the equation below:

$$Carbon\ stock = 0.47 * AGB \text{.....ii}$$

3. RESULTS

This research was performed in a well-formatted methodology to gain the potential outcomes identified during the desk study. All the results obtained during various stages of the research are briefed hereafter.

3.1 Regression Model Development and Validation

3.1.1 Regression model development

Data collected from the field observations in six sample plots were now used as input parameters in the global allometric equation to estimate the AGB. Different equation models were evaluated against each other to get the most suitable one. Among the tested models, the Fourth Order Polynomial Equation was chosen to be the best as it had the highest correlation coefficient (R^2) among all. A detail comparison of the models is tabulated below:

Table 2 Model Comparison

Model	Equation	R^2
Linear	*Carbon (kg)=4.31016*CPA-8.3818*	0.6591
Logarithmic	*Carbon (kg)=98.973*ln CPA-211.3*	0.5571
Exponential	*Carbon (kg)=32.975*$e^{0.0387*CPA}$*	0.5578
Quadratic	*Carbon (kg)=0.1169*CPA^2-2.3297*CPA+72.49*	0.7105
3rd Order Polynomial	*Carbon (kg)=-0.0013*CPA^3+02237*CPA^2-5.05*CPA+93.24*	0.7111
4th Order Polynomial	*Carbon (kg)=-0.0005*CPA^4+0.0593*CPA^3-2.150*CPA^2+33.08*CPA-116.8*	0.7217

The following graph shows the scatter plot diagram of the data with the best-fitting fourth-order polynomial curve (dotted).

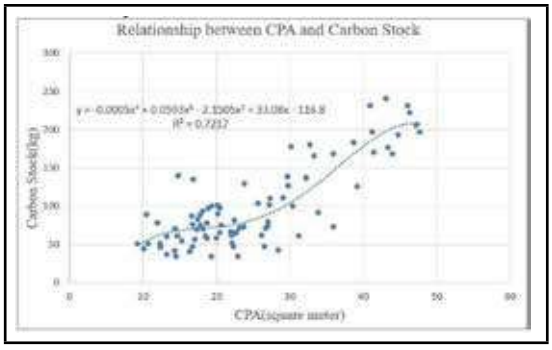

Figure 3 Scatter plot diagram of the chosen model

3.1.2 Model validation

The manually delineated CPA of the trees of the remaining 4 sample plots obtained from the image were used as input in the established regression equation to obtain carbon stock. The field measured DBH and tree height of the same sample plots were used in the allometric equation to estimate the value of carbon stock. This value was compared with the value obtained from regression equation.

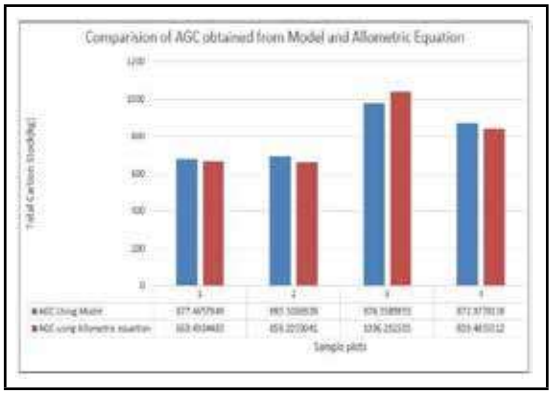

Figure 4 AGC Comparison Chart

3.1.3 Estimation of AGC and AGB of the study area

After the model validation was done the AGC of the whole study area was obtained by using the CPA delineated manually from the orthomosaic image. The total AGC obtained was 210.7480 tons. While the equation 2 resulted in the AGB of 448.4 tons.

3.1.4 Carbon stock mapping

A few numbers of trees that contributed more than 400 kg of carbon were present whereas

most of the trees contributed to less than 100 kg of carbon.

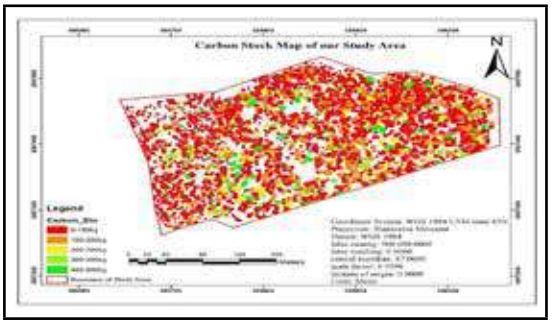

Figure 5 Carbon Stock Map

4. DISCUSSION

Almost all related studies tend to focus on evaluating the accuracy of each step involved in measuring biomass and carbon stock, but often overlook the careful consideration of error propagation in the results (Chave *et al.,* 2014). So, we must identify and assess the influence of various sources of error on biomass and carbon estimation.

Errors and uncertainties from various sources such as inaccuracies in tree parameter measurements, error in allometric equations, and data processing errors can impact the final estimated biomass. A previous study identified four types of errors when assessing the biomass and carbon, which include errors in tree measurements, selection of allometric equations, selection of the sampling plot size, and the representation of the landscape at a larger scale (Chave et al., 2014).

4.1 Limitations

Some of the significant limitations are mentioned below which would serve as recommendations while conducting this type of research in the future. To establish control points and place the GCP markers inside the forest enough open space is required. In forests, it is a very challenging task to find enough open space to place the GCP markers. Because of the low accuracy of handheld GPS identification of the correct location of sample plot centers is challenging. During tree crown delineation it is difficult to delineate a tree crown where tree crowns of two or more trees overlap. The suppressed trees which are covered by dominant trees aren't considered.

4.2 RECOMMENDATION

To enhance the accuracy of the carbon stock estimation model, certain improvements should be made before developing the model in future. Some of the major recommendations are briefed below:

As an equation developed by (Chave *et al.,* 2014) was used due to the lack of local level allometric equations, the error can be reduced by using a local level allometric equations. Thus, it is highly recommended to develop allometric equations for the forests of Nepal to estimate carbon stock accurately.

The high speed of UAV produces motion blur, while the polygonal flight path can result in tilted images at the corner flight paths, which can affect the accuracy of orthomosaic resulting in degrading accuracy of CPA which is directly related to AGC as per the developed model. Therefore, it is suggested that a moderate speed be chosen as a parameter when flying UAV to achieve better results.

5. CONCLUSION

Assessing the productivity and sustainability of forest ecosystems requires an accurate estimation of AGB. The primary aim of this study was to create a carbon stock estimation model and compare the predictions against the one generated from allometric equation. To achieve this, CPA of the individual trees which was the main factor was manually delineated from the orthomosaic.

There exists a reasonable relationship between the CPA and the carbon stock. The obtained relationship has the coefficient of determination (R^2) of 0.7217. Hence, the total aboveground carbon and biomass obtained for our study area are 210.7480 tons and 448.4 tons respectively.

REFERENCES

Anderson, S. C., Kupfer, J. A., Wilson, R. R., & Cooper, R. J., (2000). Estimating forest crown area removed by selection cutting: A linked regression-GIS approach based on Stump Diameters. *Forest Ecology and Management*, *137*(1-3), 171–177. https://doi.org/10.1016/s0378-1127 (99)00325-4

Brown, S., (2002). Measuring carbon in forests: Current status and future challenges. *Environmental Pollution*, *116*(3), 363–372. https://doi.org/10.1016/s0269-7491 (01)00212-3

Brown, S., Sathaye, J., Melvin, C. M. G. R., & Kauppi, P. E. (1996). Mitigation Actions. In *Mitigation of carbon emissions to the atmosphere by forest management* (1st ed., Vol. 75, pp. 80–91). essay, Commonwealth Forestry Association.

Chave, J., Réjou-Méchain, M., Búrquez, A., Chidumayo, E., Colgan, M. S., Delitti, W. B. C., Duque, A., Eid, T., Fearnside, P. M., Goodman, R. C., Henry, M., Martínez-Yrízar, A., Mugasha, W. A., Muller-Landau, H. C., Mencuccini, M., Nelson, B. W., Ngomanda, A., Nogueira, E. M., Ortiz-Malavassi, E., Vieilledent, G., (2014). Improved allometric models to estimate the aboveground biomass of tropical trees. *Global Change Biology*, 20(10), 3177–3190. https://doi.org/10.1111/gcb.12629

Dandois, J., Olano, M., & Ellis, E. (2015). Optimal altitude, overlap, and weather conditions for Computer Vision UAV estimates of forest structure. *Remote Sensing,* 7(10), 13895–13920. https://doi.org/10.3390/rs71013895

Dhital, N. (2009). Reducing Emissions from Deforestation and Forest Degradation (REDD) in Nepal: Exploring the Possibilities. *Journal of Forest and Livelihood,* 8(1), 56–61. Retrieved from https://www.nepjol.info/index.php/JFL/article/view/1884

Gibbs, H. K., Brown, S., Niles, J. O., & Foley, J. A., (2007). Monitoring and estimating tropical forest carbon stocks: Making REDD a reality. *Environmental Research Letters,* 2(4), 045023. https://doi.org/10.1088/1748-9326/2/4/045023

Gschwantner, T., Schadauer, K., Vidal, C., Lanz, A., Tomppo, E., di Cosmo, L., Robert, N., Englert Duursma, D., & Lawrence, M., (2009). Common tree definitions for National Forest inventories in Europe. *Silva Fennica*, 43(2). https://doi.org/10.14214/sf.463

Hashem, M.A., (2019). *Estimation of aboveground biomass/carbon stock and carbon sequestration using UAV imagery at Kebun Raya Unmul Samarinda education forest, East Kalimantan, Indonesia.* Faculty of Geoinfromation Science and Earth Obsrevation of University of Twente. Retrieved from http://essay.utwente.nl/83721/1/hashem.pdf

Huynh, T., Lee, D. J., Applegate, G., & Lewis, T., (2021). Field methods for above and below ground biomass estimation in plantation forests. *Methods X*, 8, 101192. https://doi.org/10.1016/j.mex.2020.101192

Kachamba, D., Ørka, H., Gobakken, T., Eid, T., & Mwase, W., (2016). Biomass estimation using 3D data from unmanned aerial vehicle imagery in a tropical woodland. Remote Sensing, 8(11), 968. https://doi.org/10.3390/rs8110968

Koh, L. P., & Wich, S. A., (2012). Dawn of Drone Ecology: Low-cost autonomous aerial vehicles for conservation. *Tropical Conservation*

Science, 5(2), 121–132. https://doi.org/10.1177/194008291200500202

Lu, P., & Sinclair, R. W., (2006). Survival, growth and wood specific gravity of interspecific hybrids of pinus strobus and P. Wallichiana grown in Ontario. *Forest Ecology and Management,* 234(1-3), 97–106. https://doi.org/10.1016/j.foreco.2006.06.027

Nordh, N., (2004). Above-ground biomass assessments and first cutting cycle production in willow (Salix sp.) coppice: A comparison between destructive and non-destructive methods. *Biomass and Bioenergy,* 27(1), 1–8. https://doi.org/10.1016/ j.biombioe.2003.10.007

Oli, B. N., & Shrestha, K., (2009). Carbon Status in Forests of Nepal:An Overview. *Journal of Forest and Livelihood,*8(1), 62–66. Retrieved from https://www.nepjol.info/ index.php/JFL/article/view/1885

Ravindranath, N. H., & Ostwald, M., (2008). Carbon inventory methods handbook for greenhouse gas inventory, carbon mitigation and roundwood production projects. https://doi.org/10.1007/978-1-4020-6547-7

Ruiz, L., Hermosilla, T., Mauro, F., & Godino, M., (2014). Analysis of the influence of plot size and LIDAR density on forest structure attribute estimates. *Forests,* 5(5), 936–951. https://doi.org/10.3390/f5050936

Saatchi, S. S., Harris, N. L., Brown, S., Lefsky, M., Mitchard, E. T., Salas, W., Zutta, B. R., Buermann, W., Lewis, S. L., Hagen, S., Petrova, S., White, L., Silman, M., & Morel, A., (2011). Benchmark map of forest carbon stocks in tropical regions across three continents. *Proceedings of the National Academy of Sciences*, 108(24), 9899–9904. https://doi.org/10.1073/pnas.1019576108

Shrestha, S., Karky, B., & Karki, S., (2014). Case study report: REDD+ pilot project in community forests in three watersheds of Nepal. *Forests,* 5(10), 2425–2439. https://doi.org/10.3390/f5102425

Vashum, T. K., (2012). Methods to estimate above-ground biomass and carbon stock in natural forests - A Review. *Journal of Ecosystem & Ecography,* 02(04). https://doi.org/10.4172/2157-7625.1000116

Author's Information

Name	:	Er. Sandesh Upadhyaya
Academic Qualification	:	Bachelor in Geomatics Engineering
Organization	:	Survey Department
Current Designation	:	Survey Officer
Work Experience	:	1.5 years
Published paper/article	:	1

Restoration of Land Parcels using Land Consolidation & Readjustment: A Case of Resilience after Flood Disaster

Tanka Prasad Dahal[1], Susheel Dangol[1], Purna Bahadur Nepali[2], Reshma Shrestha[2]
tpdahal@gmail.com, susheel.dangol@nepal.gov.np, purna@kusom.edu.np, reshma@ku.edu.np
[1]Survey Department, [2]Kathmandu University

KEYWORDS

Land consolidation, Land readjustment, Resilience, Flood disaster, Land Use Policy, Land ownership

ABSTRACT

Millions of people are affected from natural disaster leading to loss of land tenure around the world. People affected from the disaster leading to loss of land tenure are often excluded from post disaster assistance. The parcel boundary may change or obliterated because of disaster or also from some infrastructure development. Re-establishing of the cadastral boundary is very crucial and challenging task to re-establish the tenure rights and other cadastral details. This paper focuses on the restoration of land parcels after flood. Paper highlights the impact of flood in parcel boundary and proposes a concept for restoration of those obliterated parcels of Melamchi bazar, Sindupalchok, Nepal which was affected from the flash flood on 15th June 2021. The model for restoration of land parcel using the concept of land consolidation and re-adjustment has been recommended focusing on land pooling, creating a regular shape of the parcel. This paper also evaluates the current legal provisions for restoration of land parcels after land use change due to flood.

1. BACKGROUND

Millions of people are affected from natural disaster around the world. According to Internal Displacement Monitoring Centre, 32.4 million people were displaced due to natural disaster according in the year 2012 only (Yonetani, 2013). The affect is seen more in South Asia. Among different disasters, flood bounces multiple effects like; people are prevented from access to land because of extended flooding period, damage to buildings, infrastructures, crops which impact on the livelihood of the people (Mitchell, 2011). Effect of natural disaster lead to displacement of human settlement including arable land leading to loss of land tenure. Thus, without the legal proof of land rights, people are often excluded from post disaster assistance and other services.

Disaster recovery activities in different region to restore land tenure shows that land is foundation to build disaster resilience where disaster hit-people can get back in their feet rebuilding the house and the livelihood (Ochong, 2019). Most of the relief activities focus on the group or community with documentation of land ownerships and ignore those who lack documentation (Caron, *et.al*, 2014). Post disaster assessment shows that land tenure insecurity, weak formal land administration system, outdated land records increases the difficulty in restoring land or other

property (Caron, 2009). The study of Shrestha *et al*. (2016) also highlighted about the weak land governance that can effects the informal settlements in post disaster. The different case study was mentioned in which informal settlements being excluded from various post disaster intervention related to reconstruction. Not only in the case of disaster recovery, this issue also effects in infrastructure development as well. Permanent inundation of land due to sea level rise is legally referred as obliterated land in Indonesia which creates uncertainty or loss of the former land ownership of the people and hence creating disputes during land acquisition for road construction (Pinuji, *et. al.,* 2023).

Disaster response as well as recovery require information about land tenure which are not up to date in most of the cases and as a result of this, vulnerable groups are often passed over by the government during risk management activities (Unger, *et al.,* 2019). Land information tells in detail about what, who, where, how much, and other key attributes of a property, the information without which, is almost impossible for cities and communities to develop proper disaster response (Wellenstein & Torhonen, 2018). At present there exists no dedicated tool for supporting land tenure recordation of all people-to-land relationships for the purposes of disaster risk management (Unger, *et. al*., 2019). Despite of this shortcoming, delineation of the cadastral boundary to identify the land right is basic and crucial step towards restoration of the cadastral data in affected area. According to the Pinheiro Principles, displaced people have the right to return to their lands when the emergency response is completed and each person should have rights to land that are at least as good as the situation prior to the disaster (Mitchell, 2011).

Community led participatory mapping was conducted in Aceh, Indonesia after 2004 Tsunami to reestablish cadastral boundary where neighbors' boundary is identified on the reference of other neighborhood which are then after digitization, shared to the communities, reviewed by each community and finally formalized by national land agency (Caron, *et. al.*, 2014). UN-HABITAT (2007) also recognized the community-based approach to re-establish tenure security, said that the government organizations should be sufficiently capable of replacing records through provisional certificates with reference to other records such as land tax payments and electricity bills on the basis of strong legal background. Mitchell (2011) consider cadastral maps as the basis for restitution of cadastral boundary through adjudication and verification process.

Correction of each land boundary was proposed so that there is no discrepancy in land record at the registry office and the ground situation (Sekine & Nanjo, 2012). The paper recognized two different methods for cadastral map correction. One is the block correction where several locations have irregular movement in a block. In this method block points are surveyed and each boundary point in a block are corrected as Helmert conversion. Another method is the cadastral map regeneration where every boundary has moved irregularly. In both of the method regeneration of cadastral map is done rather than readjustment. Cities like Osaka and Edo were rehabilitated after war and fire by expanding roads accompanied by changes in land ownership (Yanase, 2018) which is in line with the concept of readjustment. Marije, *et. al.*, (2022) also recognized land consolidation as a land management instrument used for management of agricultural development based on the formation of regular shape parcels which lead to the concept of readjustment. Land consolidation was conducted in the Netherlands to protect the community from river flood problem where total number of parcels were reduced from 2415 to 718 (Hoeksema, 2006). Charoenkalunyuta (2011) conducted the study on elements on resilient from land tenure perspective after flood in the case of Nepal and concluded that land consolidation is not feasible since land came under the river permanently. Hence, land

readjustment method can be an alternate solution. This is the process of reorganization, rearrangement and readjustment of land parcels rather than just a consolidation process of titles (De Souza, 2018b)

According to FIG, one of land policy instrument consider spatial developments in a coherent and comprehensive approach, integrating various sectorial policy domains is called Land consolidation. Land consolidation plan focus on the new layout of land parcels, related land rights and the right holders. it is a planned readjustment and rearrangement of fragmented land parcels and their ownership.

Land consolidation is often carried out in rural areas with fragmented land holdings, where small land parcels are difficult to manage and inefficient for agricultural production. The process can also help to reduce land degradation, improve the environment, and enhance biodiversity by promoting sustainable land use practices. It consists of a range of activities, including the physical realignment of land parcels, the creation of access roads and other infrastructure, the improvement of soil fertility and water management, the establishment of new property rights, and the provision of support services to farmers

Land readjustment is basically used to redefine the parcel boundary where existing or former land boundary has some issues and the restoration of parcel with improved tenure security (Hong & Brain, 2012). This is cheaper than gathering all required land by purchasing or by expropriation for land development (Yomralioglu, *et.al.,* 2018) This also gives out the urban development pattern as per desire, increase land value, distribute the value to the involved ones and also limits displacement (Hong & Brain, 2012). Land ownership is altered but not expropriated and public infrastructure, road access is developed in land readjustment (Linke, 2018). In land readjustment case of India, 40% of land was used for road network and public infrastructure and remaining 60% is allocated for land owners where no any land owners are deprived from a piece of land (Manohar, *et. al*., 2018). The concept in Japan started centuries back with the objective to reorganize agricultural land and develop transport facility and irrigation channel to improve productivity (Matsui, n.d.). Later on, land readjustment is considered for controlling urban sprawl, development of new town, urban rehabilitation, development of urban infrastructure and disaster reconstruction (Hosono, 2018). This is also considered as the public-private partnership where government and public bear cost and benefit by replotting the land to change location, size and format of land (De Souza, 2018).

Land readjustment in Angola was implemented after civil war reduced land conflicts where informal settlements were also incorporated in formal urban plan (Cain, *et. al*., 2018). In Bhutan, this concept was implemented for urban development with taking in consideration of: preserving interest of original land owners, incentive based urban management, participatory, environment protection and conservation of cultural heritage (Wangmo, 2018). In case of Nepal and Sweden, with the concept of land pooling, individual plots are combined into one single estate, road layout is planned, then after the estate is subdivided rationally with contribution from land owners for open space, road and finally including the facility of drinking water pipes, drainage system and electricity (Joshi & Shrestha, 2018, Osterber, 2018).

Land consolidation and readjustment (LCA) is a process that involves the rearrangement of land parcels to create larger, more efficient land holdings that are better suited to modern agricultural practices. The primary goal of LCA is to increase the productivity and profitability of agricultural land by reducing fragmentation and improving the quality of the land.

However, literature shows that most of the development activities in land readjustment is focused on urban development. This paper basically focused on the land consolidation and readjustment for effective parcel restoration after natural disaster.

2. STUDY AREA

Sindhupalchowk district is a part of Bagmati Province and one of the seventy-seven districts of Nepal, with an area of 2,542 km^2. There are 3 municipalities and 9 rural municipalities in this district. Among 12 local levels Melamchi is a municipality having total area of 160.63 km^2. The study area selected in Melemchi Bazar, the periphery of Melachi and Indrawati River damaged by the flood in 14 June 2021.

Flash flood hit this region which resulted in erosion and debris sedimentation. Damage of the arable land of this area due to sedimentation made the land unusable. More than 16m of sediment was accumulated in the Melamchi Bazar (WB & GFDRR, 2022). It also seems that the land cannot be rehabilitated and hence the damage looks like permanent leading to loss of land within the land holdings.

Melamchi flood is not from the single cause but a set of different process including heavy rain, snowmelt, glacial deposit erosion, old and new landslide triggered by earthquake to some extent, river bank erosion, debris deposition and inundation and with combination of all these factors, scale of damage was amplified (Maharjan, *et. al.,* 2021). Huge area of agricultural land, human settlement and their livelihoods, infrastructures like bridges, roads, hydropower, and electric poles were damaged. Numbers of people were dead along with 337 houses fully damaged and 525 families displaced (Maharjan, *et. al.,* 2021). Implementation of land readjustment adhering to the land use policy will help in successful and sustainable implementation of the concept (Viitanen, 2018).

Figure 1: Map of study area

Figure 2: Melamchi bazar before and after flood: (Source: WB & GFDRR, 2022)

The Melamchi river course before flood and cadastral parcels can be shown with following figure.

Figure 3: Pre-flood river course and the cadastral plots.

3. MATERIAL AND METHODS

3.1. Data source

Satellite images and the cadastral data of the study area are the primary data for the study. Freely available google image is used for analyzing pre and post flood scenario. Cadastral maps were collected from the survey office.

3.2. Data processing and information generation

Parcel information were generated by digitizing the paper maps collected from the survey office. Cadastral data and satellite images were overlaid for identification of flood damaged area. The legal provision for parcel boundary restoration study and development of new modality for restoration of the parcel boundary was carried out. The cadastral parcel layer and post flood image were overlaid to identify the number of parcels and area damaged by the flood. The restoration plan is based on consolidation of parcels of same owner within flood area and preservation of area of government land. The total number of parcels damaged by the flood was 270 and after restoration total number of plots were 145 Designed. The concept is based on the area of government land is placed as it is, and course of river was restored as in pre-flood course with making regular shape with minor modification from cadastral map.

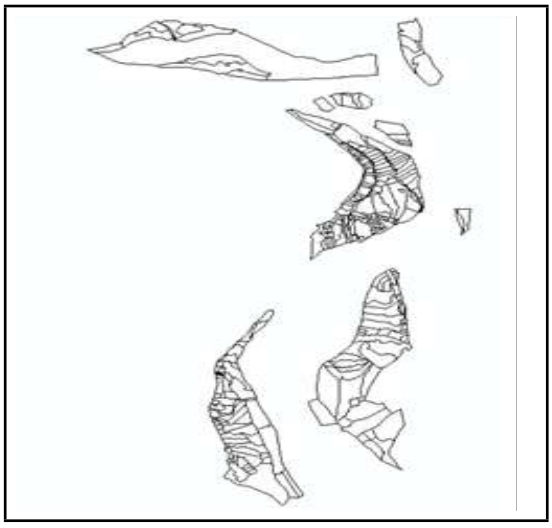

Figure 4: Parcel damaged during flood.

The conceptual framework of this study is based on change analysis during flood as following steps.

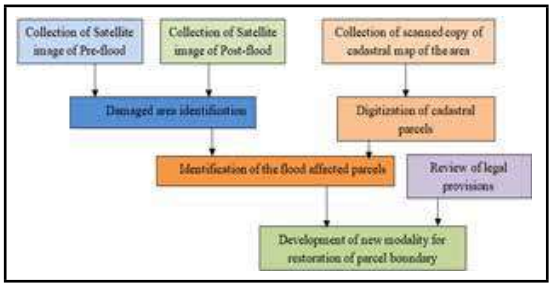

Figure 5: Conceptual framework.

4. RESULT AND DISCUSSION

The total parcel area damaged by the flood has been studied with using satellite image after flood. There are total 6 patches affected by the flood having 270 Number of parcels. The smallest and largest parcel area is 6.13 m^2 & 298383.78 m^2.

Figure 6: Damaged parcel over the google image.

4.1. Proposed Solution

It is seen that due to flood, all the parcel boundaries are obliterated at the study area. While referring to the cadastral maps, it shows that almost all the parcel boundaries are not in regular shape. Since there is no parcel boundary after flood, land use of all the parcels seems to be same. Hence, it is better to divide land parcels in regular shape with agricultural purpose road facility which is the concept of land consolidation and readjustment. Land readjustment involve transfer of land ownership to new parcels in replace of former parcel with some facility and the land registration is also revised according to the transfer of the ownership (Yanase, 2018). Objective of arable land readjustment everywhere doesn't mean urban planning but also could be to improve productivity by consolidating irregular and scattered parcels into the area with regular shape and access to road and irrigation system (Yanase, 2018). Same concept is proposed for this study area as well. Nominal percentage of land from land owner is deducted and used for agricultural purpose road development. This can be treated as land consolidation and land readjustment with an objective of agriculture purpose not only instead of settlement. Land value need to be considered for readjustment in order to control the conflicts. Cadastral records including information about land use and infrastructure information can support assessing the value and use of land (Charoenkalunyuta, 2011). With all these considerations, 145 cadastral plots were developed with consolidation two or more parcels assuming those having same ownership (Figure 4). This result is from the study of small portion of the affected area.

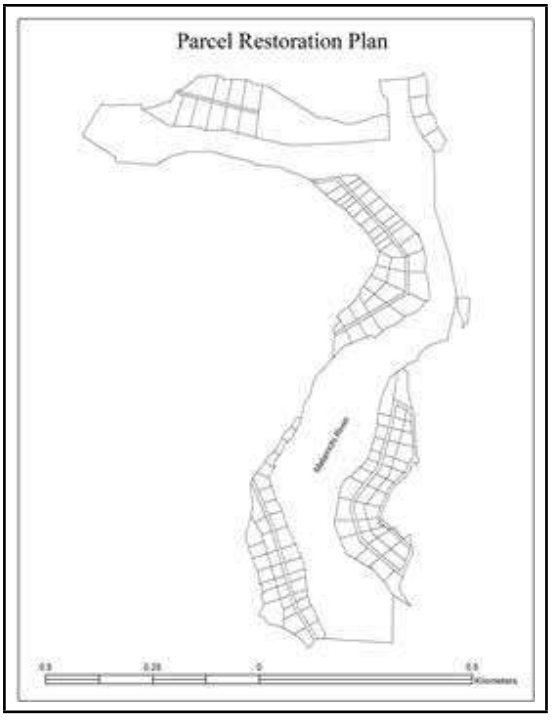

Figure 7: Land Parcel restoration plan for the affected area.

Steps for restoration of land parcels based on consolidation plan in ground.

1. Identification of Control point (or base boundary which was not damaged during flood)
2. Layout of the River boundary as in proposed plan
3. Layout of the planed road and Blocks
4. Demarcation of the planned parcels

4.2. Land Administration System

Land administration system should be good enough in terms of records and information in order to face less land dispute in post disaster scenario (Charoenkalunyuta, 2011) which will support in resilience of community after disaster. Nepal follows improved deed registration system. Cadastral survey, adjudication and first registration is conducted by survey office and after that attribute information about the land owner is transferred to land revenue office and cadastral maps and field books are kept in survey office. The land record includes all detail information about the

area, location, adjoining parcel, land owners, tenant's information and land use as well. All the land administration system is guided by major six acts and rules viz. Land (survey & measurement) Act & Rules and Land Revenue Act & Rules and Land Related Act & Rules. Besides these Acts and Rules, recently Nepal government formulated Land Use Act and rules which defines the major responsibility of local government to implement land use plan and policy. Hence while implementing land readjustment plan, there need to be strong coordination between the central government and the local government.

4.3. Legal Provision

The process of restoration of parcel boundary according to 'Land (Survey and Measurement) Regulation, 2001' can be listed as below;

1. The rule 33 states that the land owner has to apply for demarcation of his parcel boundary in Survey office with paying the charge.
2. The provision for charge is mentioned as "Any person or agency making survey or establishing mark for their own private purpose shall have to submit the amount as follows: –
    i. The amount equivalent to the daily and travel allowance of the employee and assistant deployed (assigned) for the survey of a land,
    ii. Fifteen percent added amount on the amount mentioned in Clause (i) for paper,
    iii. The amount prescribed by the Director General as for the rent of the equipment which shall be used for survey work."

After acceptance of application with demarcation charge, Survey office provides the date for demarcation and gives letter to local level for presence of their representative at the time of parcel demarcation.

The parcel demarcation is carried out by the surveyor apportioned by the office in the presence of land owner (applicant), land owner of surrounding parcels and representative of Local Level. After completion of the work the surveyor has to submit their report in written at the office. The base for demarcation of parcel is based on the cadastral map. Since there are no any boundary marks at the flooded area, this process is almost not possible. In this shortcoming of land survey rules, the issue can be undertaken by town development act.

The main features as discussed by the act are:

1. The parcel allocated is of regular shape
2. Each parcel has facility of agricultural road.
3. Numbers of parcels of same owner are consolidated and provided single parcel.
4. Land owner needs to contribute certain percentage of their land for development of road.

But the Town Development Act, 1998 is focused on urban development rather that arable land readjustment. Re-survey according to land survey and measurement act also cannot solve the problem as the Act directs to verify the existing cadastral maps and present parcel boundary and since there is no parcel boundary at ground, verification cannot be done. Hence, land consolidation and readjustment is proposed as good solution for the issue.

Land readjustment in Japan was only successful because of strong legal background i.e. "enforcement of replotting" defined by Arable readjustment act enacted in 1989 (Yanase, 2018). Germany also enacted law to enforce expropriation and land readjustment to reconstruct the city of Hamburg after the fire in 1842 (Yanase, 2018). Different legal frameworks were defined before implementing land readjustment. Table 1 shows the list of countries which formulated legal framework before implementing land readjustment. Western Australia enacted Town planning and development act 1984, Sweden approved Joint land development act 1987, Finland

redefined procedure of land readjustment in Real property formation act 1995, Thailand promulgated Land Readjustment Act BE 2547 in 2004, Law on Urban Reform-1989 & Law on Urban and Territorial Development-1997 addresses the readjustment concept in Sri-lanka, Bhutan adopted Land pooling rules in 2009, Netherlands formulated Land law in 2016 to address urban land readjustment (De Souza, 2018b). These are only some of the examples to show that land readjustment should only be conducted only on the basis of strong legal background. Hence, as stated in some of the examples above, provision of readjustment of the land need to be addressed in Land (Survey and Measurement) Act besides land consolidation.

5. CONCLUSION

Flood and landslides are major disaster in mountain area, which damages the land parcel boundaries. According to Land (Survey and Measurement) Regulation, 2001 those damages parcels boundaries are restored based on the Cadastral Map, while owner request with application and depositing required fee for restoration of land parcel boundaries. After flood, all land parcels are of same categories without any boundary and hence it is better to use land consolidation and readjustment tool which helps to restore parcels with regular shape and facility of agricultural road. For this land consolidation and readjustment of agricultural/rural area there is lack of legal provision in Nepal. In case of Urban Development, the Town Development Act, 1998 can be used. In this paper it is suggested to include legal provision for land consolidation and readjustment for restoration of land parcels after flood on agricultural area. This need to be in line with Land (Survey and Measurement) Act, 1963 and Land Use Act, 2019. The concept of land consolidation and readjustment for arable land after disaster may face uncertainties and challenges. Despite of this, the concept definitely offers another option for policy makers to consider for post-disaster reestablishment of the affected community. Similarly, the concept of reshaping arable land can contribute in saving resource and effort for restoration land parcel after flood and other disasters.

REFERENCES

Caron, C., (2009). Left behind: Post-tsunami resettlement experiences for women and the urban poor in Colombo." In: Fernando, P., K. Fernando, and M. Kumarasiri (eds). *Forced to Move: Involuntary Displacement and Resettlement – Policy and Practice*. Colombo, Sri Lanka: CEPA.

Caron, C., Menon, G. & Kuritz, L., (2014). Land tenure and disasters: Strengthening and clarifying land rights in disaster risk reduction and post-disaster programming. *USAID Issue Brief,* Land tenure and property rights portal: http://usaidlandtenure.net

Cain, A., Weber, B. & Festo, M., (2018). Participatory and iclusive land readjustment in Huambo, Angola. *Land readjustment: Solving urban problems through innovative approach. De Souza, F. F.; Hosono, A., Ochi, T (eds),* pp-99-104. JICA research institute, Tokyo, 2018.

Charoenkalunyuta, C., (2011). *Land tenure in disaster risk management: Case of flooding in Nepal.* Master of Science thesis, ITC, University of Twente, Netherlands.

De Souza, F.F., (2018a). Concepts on land readjustment. *Land readjustment: Solving urban problems through innovative approach. De Souza, F. F.; Hosono, A., Ochi, T (eds),* pp-15-33. JICA research institute, Tokyo, 2018.

De Souza, F.F., (2018b). A brief history of land readjustment in the world and case studies. *Land readjustment: Solving urban problems through innovative approach. De Souza, F. F.; Hosono, A., Ochi, T (eds),* pp-81-96. JICA research institute, Tokyo, 2018.

GON, (1963). *Land Survey and Measurement Act 1963*. Nepal Law commission, Government of Nepal.

GON, (1998). *Town Developmetn Act, 1998.* Government of Nepal.

GON, (2001). *Land Survey and Measurement Rules, 2001*. Nepal Law commission, Government of Nepal.

GON, (2016). *Constitution of Nepal*. Nepal law commission, Government of Nepal.

Hoeksema, R. J., (2006). *Designed for dry feet: Flood protection and land reclamation in the Netherlands.* American Society of Civil Engineer, Virginia, USA.

Hong, Y.H. & Brain, I., (2012). Land readjustment for urban development and post-disaster reconstruction. *Land lines*. Lincoln Institute of Land Policy.

Hosono, A., (2018). Land readjustment: Making cities inclusive, safe, resilient and sustainable. *Land readjustment: Solving urban problems through innovative approach. De Souza, F. F.; Hosono, A., Ochi, T (eds),* pp-1-12. JICA research institute, Tokyo, 2018.

International Institute for Sustainable Development (IISD), (2006). *Addressing Land Ownership after Natural Disasters: An Agency Survey*. Winnipeg, CA: IISD. (http://www.iisd.org/; Accessed 3 March 2023).

Joshi, K.K. & Shrestha, S.B., (2018). Land readjustment in Nepal. *Land readjustment: Solving urban problems through innovative approach. De Souza, F. F.; Hosono, A., Ochi, T (eds),* pp-157-166. JICA research institute, Tokyo, 2018.

Linke, H.J., (2018). The land readjustment in Germany. *Land readjustment: Solving urban problems through innovative approach. De Souza, F. F.; Hosono, A., Ochi, T (eds),* pp-128-136. JICA research institute, Tokyo, 2018.

Maharjan, S. B., Steiner, J. F., Shrestha, A. B., Maharjan, A., Nepal, S., Shrestha, M. S., Bajracharya, B., Rasul, G., Shrestha, M., Jackson, M. & Gupta, N., (2021). The Melamchi flood disaster: *Cascading hazard and the need for multihazard risk management*. International Center for Integrated Mountain Development (ICIMOD).

Manohar, J., Peter, A. & Dave, H., (2018). Land readjustment in India. *Land readjustment: Solving urban problems through innovative approach. De Souza, F. F.; Hosono, A., Ochi, T (eds),* pp-136-140. JICA research institute, Tokyo, 2018.

Marije, L., de Vries, W. T. & Hartvigsen, M., (2022). *Land Consolidation – The Fundamentals to Guide Practice*.

Matsuy, M., (n.d.).*Case study: Land readjustment in Japan.*Tokyo Development Learning Center, The World Bank, Tokyo.

Mitchell, D., (2011). *Assessing and Responding to Land Tenure Issues in Disaster Risk Management*. FAO Land Tenure Manuals 3. Rome: Food and Agriculture Organization of the United Nations.

Ochong, R., (2019). *Opinion: Building resilience and securing land tenure in th face of disasters*. (www.news.trust.org: accessed on 21st March 21, 2023)

Osterbert, T., (2018). The failure of land readjustment in Sweden. *Land readjustment: Solving urban problems through innovative approach. De Souza, F. F.; Hosono, A., Ochi, T (eds),* pp-171-175. JICA research institute, Tokyo, 2018.

Pinuji, S., de Vries, W.T., Rineksi, T.W. & Wahyuni, W., (2023). Is Obliterated Land Still Land? Tenure Security and Climate Change in Indonesia. *Land* 2023, *12*, 478. https://doi.org/10.3390/

land12020478

Sekine, I. & Nanjo, M., (2012). *Readjustment of the cadastral map in the east Japan earthquake disaster area*. FIG working week 2012, Rome Italy, 6010 May 2012.

Shrestha, R., Tuladhar, A., & Zevenbergen, J., (2016). *Exploring land governance in post disaster: a case of informal settlement*: International Federation of Surveyors. Article of the month.

Unger, E., Zevenbergen, J., Bennett, R., & Lemmen, C., (2019). Application of LADM for disaster prone areas and communities. *Land Use Policy*, Volume 80, Pages 118-126, ISSN 0264-8377,https://doi.org/10.1016/j.landusepol.2018.10.012.

UN-HABITAT, (2007). *Scoping Report: Addressing Land Issues After Natural Disasters*. Geneva.

Viitanen, K., (2018). Urban land readjustment in Finland. *Land readjustment: Solving urban problems through innovative approach. De Souza, F. F.; Hosono, A., Ochi, T (eds),* pp-123-128. JICA research institute, Tokyo, 2018.

WB & GFDRR, (2022). *Melamchi flood disaster in Nepal.* World Bank and Global Facility for Disaster Reduction and Recovery.

Wangmo, T., (2018). Land readjustment, an urban planning tool in Bhutan. *Land readjustment: Solving urban problems through innovative approach. De Souza, F. F.; Hosono, A., Ochi, T (eds),* pp-104-110. JICA research institute, Tokyo, 2018.

Wellenstein, A. & Torhonen, M. (2018). *When disaster displaces people, land records and geospatial data are key to protect property rithts and build resilience*. (https://blogs.worldbank.org/sustainablecities: accessed on 21 March 21, 2023).

Yomralioglu, T., Uzun, B. & Nisanci, R. (2018). The shortcomings of land readjustment in Turkey. *Land readjustment: Solving urban problems through innovative approach. De Souza, F. F.; Hosono, A., Ochi, T (eds),* pp-183-188. JICA research institute, Tokyo, 2018.

Yonetani, M. (2013). *Global estimates 2012: People displaced by disasters*. Geneva: Internal Displacement Monitoring Centre.

Yanase, N. (2018). Land readjustment and post disaster reconstruction in Japan. *Land readjustment: Solving urban problems through innovative approach. De Souza, F. F.; Hosono, A., Ochi, T (eds),* pp-63-78. JICA research institute, Tokyo, 2018.

Author's Information

Name	:	Tanka Prasad Dahal
Academic Qualification	:	Master's Degree in Land Administration, Kathmandu University
Organization	:	Survey Department
Current Designation	:	Director
Work Experience	:	27 Years

Susceptibility Modeling for Potential Fire Risk Zone in Semi-Urban Area

Bikash Kumar Karna
bikashkumarkarna@gmail.com
Survey Department, Nepal

KEYWORDS

Spatial Modeling, Multi-criteria evaluation, Analytical hierarchy process, Fuzzy Membership Function

ABSTRACT

Fires inflict major losses in global forest resources as well as human lives and property. Forest fires and their tendencies have increased in recent years in Nepal that, necessity for adequate management actions. The fire risk zone is identified with the origin of the ignitions and the pattern of their occurrence, as well as by shared environmental variables that translate into the same risk potential. To reduce the detrimental impacts of fire, several strategies for preventing and combating fires have been implemented based on identified potential fire risk zone. The work is carried out in Shambhunath Municipality, Saptari. In this study, spatial modeling with integration of MCE, fuzzy and AHP is applied for susceptibility assessment for identifying the potential fire risk zone. In fire risk assessment index map shows that 21.14 percent of municipality extent land occurred in the fire risk in which the distribution of the high risk occupied 0.01 percent, medium risk, 0.49 percent, low risk 20.64 percent and remaining 79 percent land free from fire risk. The high risk of potential fire zone were identified along the east west highway surrounding to the high voltage transmission route and petrol pump location. Likewise, potential high risk of forest fire also found in the dense forest area in elevation greater than 400m.

1. INTRODUCTION

Fires cause significant losses in worldwide forest resources as well as human lives and property. It impacts on the global ecological balance and gained substantial (Zhang *et al.*, 2019). In recent years, the frequency and severity of fires have increased considerably in many countries with global warming, industrialization, and human interference (Crimmins, 2006; Running, 2006; Hantson *et al.*, 2015) mainly in forest region. Nepal predominantly faces forest fires and its trends increasing in the recent years that need proper management interventions (Ranabhat *et al.*, 2022). Fire incidence has generally occurred during the summer season (March-June) and caused the loss of life, injury or other health

impacts, property damage, loss of livelihoods and services, social and economic disruption, and environmental damage. It took place in the village houses made of thatched grasses as well as building through poor management of fire and randomly occurred from the electric circuit malfunction and high voltage transmission line circuit breakdown. Smokes due to burnings of houses, forest leaf litters and aerial parts have created the hazy environment and drab surrounding to the forest and adjoining villages. So, fire incidence damaged mainly the beautiful natural resource as forest and related other forest resources that resulting the loss of biodiversity and deterioration of forest condition. The spatial scale of fire occurrence analysis could provide new information to assist planning efforts and reduce fire risk (Yang *et al.*, 2007). Controlled burning is commonly used by rural landowners in developing nations to prepare pasture for renewal. However, improper planning and execution of controlled burns can lead to fire incident (FAO, 2006).

Several measures for preventing and combating fires have been adopted to minimize the negative effects of fire. Fire risks are a recurring problem in worldwide, and information on the spatial distribution of fires is necessary to improve fire prevention strategies and tactics (Tian *et al.*, 2013). A fire risk zone is identified based on the cause of ignitions and pattern of their occurrence, and it is identified by common environmental characteristics that translate into the same risk potential (Eugenio *et al.*, 2016). It is very important in the land use planning to manage forest resources sustainably and support in planning and management of forest for increasing environmental protection. Several measures that utilize information obtained from risk maps may help reduce fire occurrence, including higher surveillance in the at-risk areas, restricted access to these sites, construction of firebreaks, reorganization of management practices, and aid in firefighting, which includes the construction of roads for faster access to at-risk sites and resource allocation for firefighting at strategic points (Ferraz & Vettorazzi, 1998).

In recent, various methods and algorithm have been successfully applied in the production of forest fire risk maps using GIS based multi-criteria decision analyses (MCDA) with remotely sensed imaginaries. Fire analysis has carried out in GIS environment using MCE, fuzzy and AHP technique. In order to minimize the negative effects of fires, some measures have to be taken to prevent and combat fires. The preparation of a fire map can be a first, but important, step towards planning and managing the protection of forest regions. GIS based Multi-Criteria Decision Analysis (MCDA) techniques have become increasingly widespread in environmental modeling and natural hazard prediction. Combining GIS and MCDA is a powerful approach to forest fire risk mapping (Feizizadeh *et al.*, 2015). In order to model and assess forest fire risk and to identify the regions susceptible to fire, various studies have been carried out around the world. Among the methods that researchers have used for modelling forest fire risk are fuzzy logic (Pourghasemi *et al.*, 2016; Soto, 2012), analytical hierarchy process (AHP) (Pourghasemi *et al.*, 2016), fuzzy AHP (Sharma *et al.*, 2012), frequency ratio (Pourtaghi *et al.*, 2015), artificial neural networks (Bui *et al.* 2017), and logistic regression (Guo *et al.*, 2016; Pan *et al.*, 2016; Tien Bui *et al.* 2016). Likewise, machine learning (ML) approaches have the ability to provide better results for the spatial prediction of forest fires (Bar Massada *et al.*, 2013). In the last decade, various ML algorithms such as artificial neural networks (Dimuccio *et al.*, 2011; Bisquert *et al.*, 2012; Satir *et al.*, 2016), random forests (RF) (Oliveira *et al.*, 2012;

Arpaci *et al.*, 2014; Pourtaghi *et al.*, 2016), support vector machine (SVM) (Hong *et al.*, 2018), multilayer perceptron neural network (MLP) (Vasconcelos *et al.*, 2001; Satir *et al.*, 2016), kernel logistic regression (KLR) (Bui, Le, *et al.* 2016), naive Bayes (Elmas & Sonmez, 2011; Jaafari *et al.*, 2018), gradient boosted decision trees (Sachdeva *et al.*, 2018), and particle swarm optimized neural fuzzy (Tien Bui *et al.*, 2017) have been successfully developed and widely applied in susceptibility mapping of forest fire. In this study, fire analysis has carried out through spatial modeling with integration of MCE, fuzzy and AHP tools in GIS environment.

The performance of the proposed model was validated with benchmark methods using several statistical measure as receiver operating characteristic (ROC) curve, and area under the curve (AUC). Generally, ROC has used to quantify the quality of deterministic and probabilistic detections and to determine the accuracy of the spatial modeling (Akgun *et al.*, 2012). The ROC curve has drawn by plotting specificity on the X axis and sensitivity on the Y axis where sensitivity represents the false positive rate and specificity as the false negative rate based on the number of observed fire incident predicted accurately compare to the predicted fire risk zone. The AUC has used to identify the model accuracy based on the validation samples fire incident and ability in predicting future fire zone based on the training samples of fire incident. The range of the AUC ranges from 0.5 to 1 with the AUC of 1 representing perfect prediction and the closer the value of the AUC to this number, the better the performance of the model (Tehrany *et al.*, 2013). In general, AUC of range between 0.9–1.0 is excellent, 0.8–0.9 is good, 0.7–0.8 is fair 0.6–0.7 is medium and 0.5–0.6 is poor (Kantardzic, 2011). In the model evaluation by AUC, there has two evaluation process based on the success rate and the prediction rate. The results for the success rate have achieved on the basis of training data and the prediction rates has attained by a set of validation data. The results of the success rate have represented the fitness of the model for the training data; used in model building and not useful in assessing the predicting power of the model (Nohani, *et al.*, 2019).

2. STUDY AREA

Shambhunath municipality is declared by Government of Nepal on 18th May, 2014 which has formulated by integration of previous Village Development Committees (VDCs) of Khoksar Parbaha, Shambhunath, Mohanpur, Bhangha, Basbalpur and Rampur Jamuwa in Sapatari district. After formulation of new Nepalese Constitution, local level has reconstructed and Sambhunath municipality has expanded by emerging Arnaha VDC. It is connected with east west highway and located at the latitude from $26^0$23' 35" to 26^0 42' 36" and longitude from 86^0 37' 39" to 86^0 44' 54". It has elevation ranges from 81 m to 444 m above sea level. The total coverage of the municipality is 108.60 sq.km having 12 wards has its sub-units. The municipality headquarter office is located at Kathauna Bazar as previous headquarters of Mohanpur VDC. It had a population of 38018 people living in the municipality in 2017 according to Local Level Reconstruction Commission. The naming of the municipality as famous Shambhunath temple (main attraction for Nepal and Indian Pilgrims) is situated within the municipality. People are likely to come here in Bada Dashain. During month of Baisakh (The first month of Bikram Sambat) the people are celebrate here with joy and happiness. The study area of the work is shown in Figure 1.

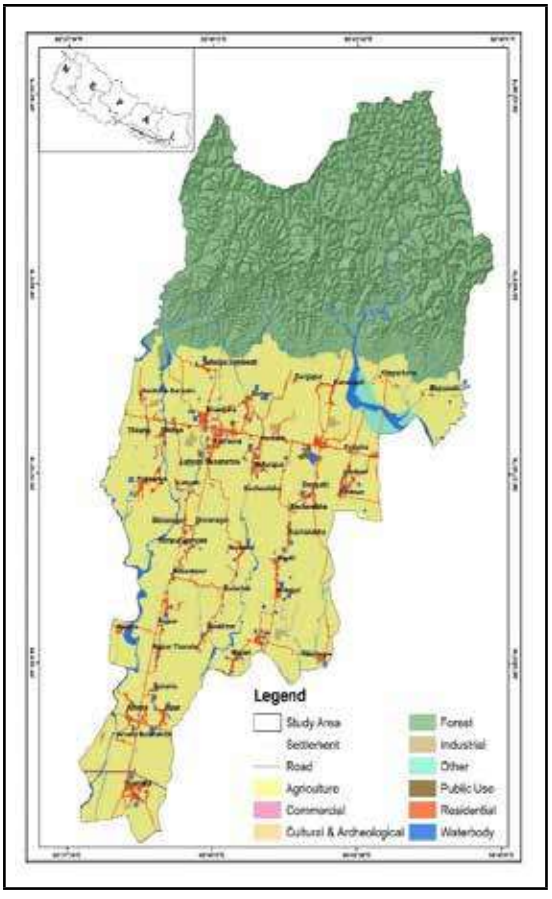

Figure 1: Study Area

3. METHOD & MATERIALS

3.1 Data used

The data collected from secondary source that utilized to create the influencing factors as criterion map and determine the potential site for susceptibility of forest fire (in Table 1).

Table 1: Data & data sources

Data Type	Compilation From	Year
World view satellite image, 2016	National land use project	2016
Land use map, scale 1:10000	National land use project	2017
Topographical map, scale 1:25000 & its digital layer	Survey department	1996
Climatic Data	Department of Hydrology and Metrology	2000-2017
Fire incident data	https://firms.modaps.eosdis.nasa.gov/download/create.php & District Disaster Committee	2000-2017

The previous fire locations were collected from the moderate-resolution imaging spectro-radiometer (MODIS) images for forest fire incident and house/building fire incidence from District Disaster Committee, Saptari.

3.2 Influencing Factor

The influencing factors used in fire risk analysis are: elevation, slope, aspect, annual precipitation (rainfall), wind speed, temperature, normalized difference vegetation index (NDVI), land use, distance from transmission line, and distance from petrol area from land use data, 2017. Three topographical related influencing factors were elevation, slope and aspect; which were derived from topographical contour of contour interval 10m. The climatic characteristics of an area affect the occurrence and intensity of forest fires (Moritz *et al.*, 2012). Three meteorologically related influencing factors were 17 years annual average precipitation, average wind speed, and maximum temperature from climatic data and secondary source. The climate related factors map has generated using the inverse distance weighted (IDW) interpolation method. The vegetation-related factor has NDVI which has identified as an important variable in forest fire modeling (Bajocco *et al.*, 2015) and reflected the vegetation's health and essentially the fuel load distribution (Yi *et al.*, 2013). The NDVI indices were derived from WorldView-2 satellite images. The human activities variables such as land use, distance from transmission line and distance from petrol area has used.

3.3 Priority Ranking of Factor

These fire incident location were used as reference fire location to correlate with the influencing factor. Multicollinearity technique was applied to estimate the correlation between the forest fire locations with influencing factors. The priority values within the influencing factor was computed and normalized through the fuzzy membership function for ranking the classes of the influencing factor with the given relationship (Gheshlaghi *et al.*, 2019).

$$\mu_{i,j} = \frac{PR_{i,j}}{Max(PR_{i,j})} \quad \text{.....}(i)$$

Where, μi,j is the fuzzy membership value of class, i of influencing factor, j and PRi.j is the priority value of class I of influencing factor j.

3.4 Computing weight of factor

In accordance with the advice of experts and local stakeholders, AHP a method is used to determine the weight of each criterion based on pairwise comparison with the scale of importance. Reciprocal pair-wise comparison were conducted based on the performance matrix. Each set of criteria in a pairwise comparison characterizes various attributes accordance with the specific qualities (Saaty, 1977; Shahabi & Hashim, 2015). The entries on the performance matrix use a 9-point rating system to rank each combination of criteria and relationship (Saaty, 1980). The rating scale's reciprocals represent the values in direct contrast to one another for each of the different criteria (Table 2). After comparing each interrelated combination of criteria pair-by-pair using the AHP approach, the criterion's weight is determined using numerical numbers. Consistency ratio is used to evaluate weight estimation. The performance matrix is thought to have a limited acceptance level if the consistency ratio is less than 0.1; otherwise, the pairwise relationship of the criterion is rejected (Karna *et al.*, 2021).

Table 2: Comparison rating scale

Intensity of importance	Description	Suitability class
1	Equal importance	Lowest suitability
2	Weak importance	Very low suitability
3	Moderate importance	Low suitability
4	Moderate to plus importance	Moderate low suitability
5	Strong importance	Moderate suitability
6	Strong to very strong importance	Moderate high suitability
7	Very strong importance	High suitability
8	Very strong to extreme importance	Very high suitability
9	Extreme importance	Highest suitability

(Source: Saaty, 1980)

3.5 Determination of potential fire zone

Based on the relationship between the acceptable performance matrix and the weight of the factor, the sum of the factor weights is maintained to be 1 in weighted linear combination (WLC) technique (Eastman, 2006). By dividing the weights supplied to each attribute factor by the scaled values given to the alternatives on those attribute classes of factor, then adding the results to get the total score for all attributes. Then, the weight and rank of influencing factors are converted into susceptibility index level in GIS using the weighted overlay function. According to the WLC result, the computed score categorizes the suitability susceptibility index level. The greatest score signified a class that was highly potential zone, and the lowest score indicated lesser potential risk zone.

4. RESULTS AND DISCUSSION

4.1 Influencing factor maps

The effective factors maps were created using geospatial methods and applied on the basis of

their significance in which the result of some criterion maps are described below.

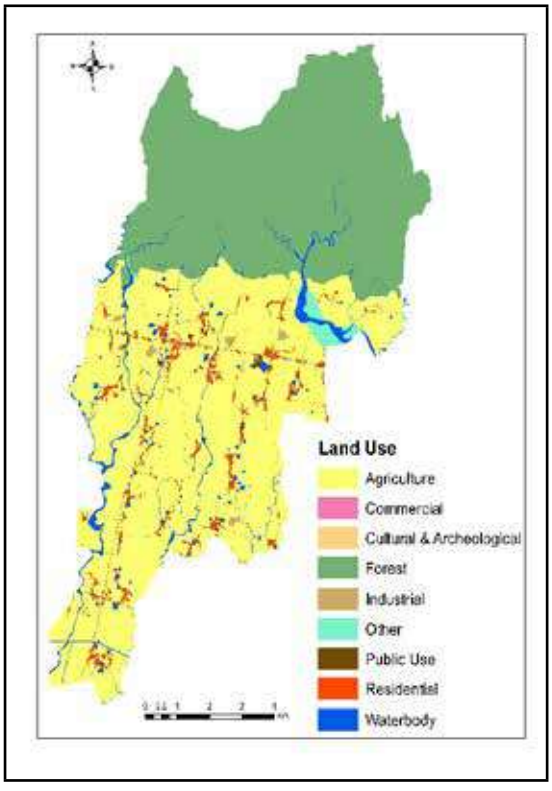

Figure 2: Land Use

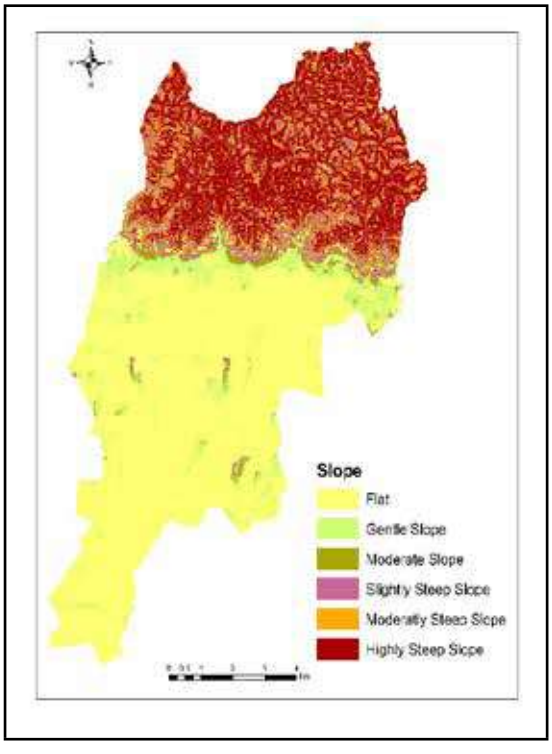

Figure 3: Slope

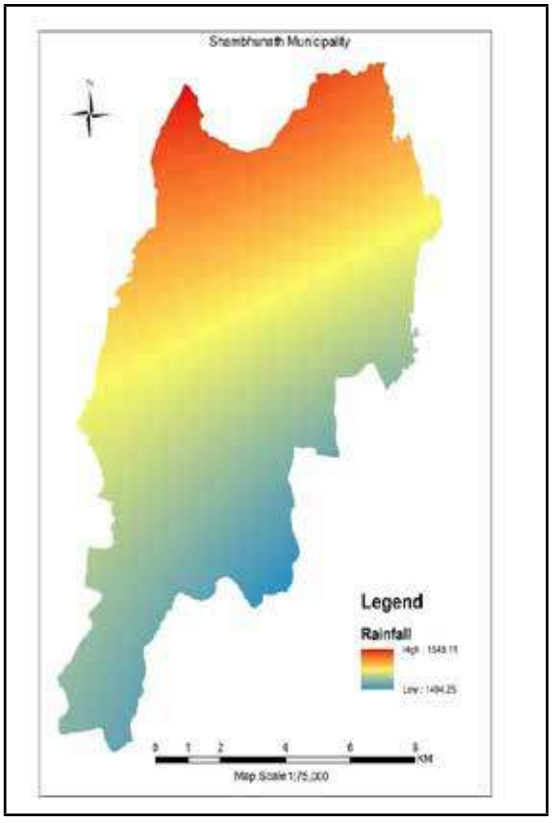

Figure 4: Annual Rainfall

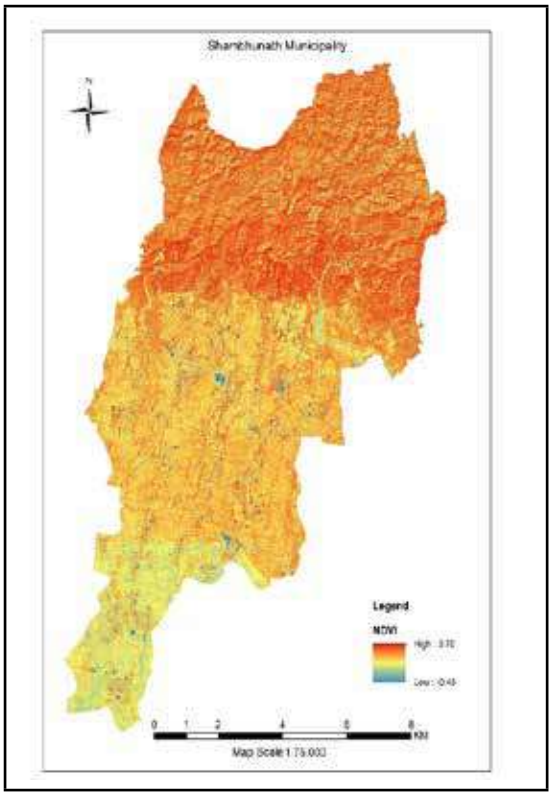

Figure 5: NDVI

Land use: About 3 percent having 251 hectares in the municipality is covered with residential areas. The pattern of land cover where residential practices are explained by human-related variables. It is crucial for residential use to manage infrastructure development operations, minimize development costs, improve socioeconomic condition, and increase the built-up area density in sustainable way.

Slope: Flat slope is occurred about 53 percent then highly steep slope area in Siwalik region in northern portion having 22 percent extent that are vulnerable area for residential use. Only 6 percent coverage belongs to moderate slope area having 5.74 sq. km. Similarly, moderately steep slope covers 8 sq. km having 7.72 percent; gentle slope covers 8 sq. km with 7.17 percent, and slightly steep slope covers 6 sq. km with 5.71 percent of municipality extent.

Precipitation: The average precipitation in terms of rainfall having more than 1500 mm per year area covers about 78.56 percent and remaining 21.45 percent area within the municipality occurs in average precipitation between 1000 to 1500 mm per year.

Normalized Difference Vegetation Index: The NDVI value less than 0 mainly waterbody or wetland area covered 1.25 percent, between 0 to 0.30 having bare soil, open area, built-up area, agriculture field, grass land etc. covered 32.55 percent, between 0.30 to 0.45 having shrubs, open forest area covered 38.88 percent and remaining 27.33 percent area having dense forest in the municipality.

4.2 Prioritized the factor

Based on its priority level, each factor data is ranked with risk level into subcategories of factors. The subcategories are normalized into uniformly ranking scales with fuzzy membership functions with priority rank and achieved in 1 to 4 values (in Table 2).

Table 2: Priority rank of factor

S.N.	Causative Factor	Classes	Risk	Rank
1	Slope (degree)	0-5	Very Low	0.00
		5-15	Low	0.25
		15-30	Moderate	0.50
		30-45	High	0.75
		< 45	Very High	1.00
2	Aspect	North	Low	0.25
		East	Moderate	0.50
		South	Very High	1.00
		West	High	0.75
3	Elevation (m)	< 200	High	1.00
		200-400	Moderate	0.67
		>400	Low	0.33
4	Wind Speed (km/h)	<21	Low	0.33
		21-23	Moderate	0.67
		>23	High	1.00
5	Temperature (^{0}C)	<35	Moderate	0.67
		>35	High	1.00
6	Annual Rainfall (mm)	<1500	Moderate	0.67
		>1500	High	1.00
7	NDVI	<0	Low	0.25
		0-0.30	Moderate	0.50
		0.30-0.45	High	0.75
		>0.45	Very High	1.00
8	Land Use	Water body	Very Low	0.00
		Built-up	High	0.75
		Agriculture	Moderate	0.50
		Open area	Low	0.25
		Forest	Very High	1.00
9	Dist. to Transmission Line (m)	<25	Very High	1.00
		25-50	High	0.75
		50-100	Moderate	0.50
		>100	Low	0.25
10	Dist. to Petrol Pump (m)	<100	Very High	1.00
		100-200	High	0.75
		200-500	Moderate	0.50
		500-1000	Low	0.25
		>1000	Very Low	0.00

4.3 Factor weight

In pair-wise relationships, various combinations of factor were created and examined according to the influencing factors. The weight of each influencing factor was determined by using the AHP technique. The calculated pairwise weights were assessed with consistency ratio and found to be the value of 0.08 which is within the acceptable threshold limit (0.10). The computed weight of the influencing factor is described in Table 3.

Table 3: Influencing factor weight

S.N.	Factors	Weight
1	Slope	0.1361
2	Aspect	0.0375
3	Elevation	0.0343
4	Wind Speed	0.1810
5	Temperature	0.1052
6	Rainfall	0.0377
7	NDVI	0.0528
8	Land Use	0.0588
9	Dist. to Transmission Line	0.1824
10	Dist. to Petrol Pump	0.1742

4.4 Potential fire risk zone

The potential fire risk assessment was carried out from the priority rank computed from fuzzy membership function and the weight computed from the AHP process using weighted overlay function in spatial analysis in GIS environment. The potential fire risk zonation map is shown in Figure 6.

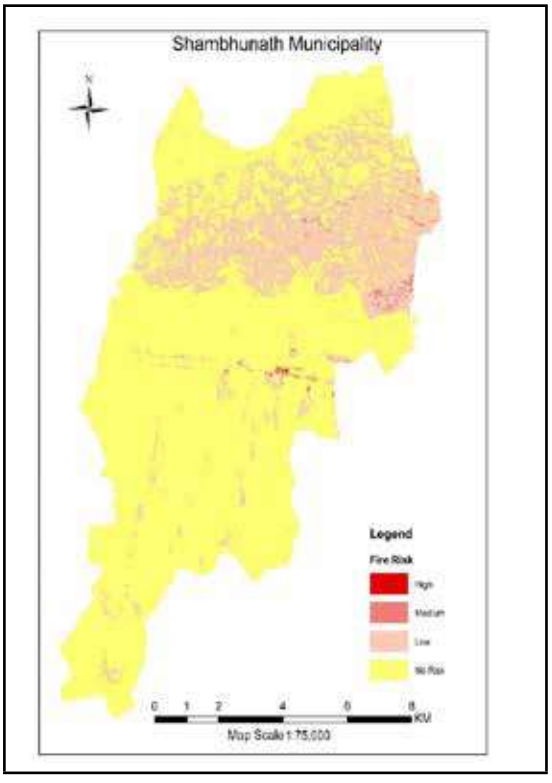

Figure 6: Potential Fire Risk Map

The municipality's fire risk assessment index map shows that 21.14 percent of municipality extent land occurred in the fire risk in which the distribution of the high risk occupied 0.01 percent, medium risk, 0.49 percent, low risk 20.64 percent and remaining 79 percent land free from fire risk. The high risk of potential fire zone were identified along the east west highway surrounding to the high voltage transmission route and petrol pump location. Likewise, potential high risk of forest fire also found in the dense forest area in elevation greater than 400m.

4.5 Validation of susceptibility model

The designed model was validated through ROC curve, and AUC through successive and prediction rate. The area under the curve of the success rate was found as 0.88 and prediction rate as 0.89 showing 89.5% prediction accuracy of the model. So, the produced susceptibility model of fire risk potential is reliable showing with all satisfactorily validation rates having good accuracy (in Figure 7).

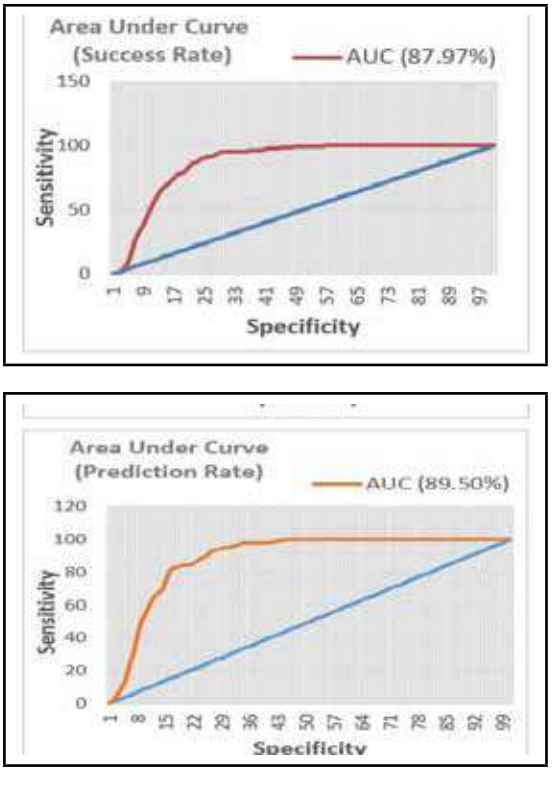

Figure 7: Model Validation

4.6 Impact of potential risk

The impact of potential fire risk assessment is carried out by the process of spatial overlay operation using zonal statistics of fire risk susceptibility layer with land use layer 2017. The potential fire risk in the land use categories is shown in Table 4.

Table 4: Impact of Fire Risk on Land Use

S.N.	Land Use Type	Fire Risk Susceptibility (in ha)				
		High	Medium	Low	Total	%
1	Agriculture	0.00	0.17	0.32	0.49	0.02
2	Forest	0.00	32.62	2037.12	2069.74	90.13
3	Water body	0.00	0.15	17.95	18.10	0.79
4	Residential	1.13	12.10	130.47	143.70	6.26
5	Other	0.00	0.77	14.15	14.92	0.65
6	Public Use	0.22	3.83	24.04	28.08	1.22
7	Industrial	0.00	2.29	12.93	15.22	0.66
8	Commercial	0.00	0.99	4.14	5.13	0.22
9	Cultural & Archeology	0.00	0.00	0.94	0.94	0.04
	Total	1.34	52.92	2242.06	2296.33	100.00

Among the municipality extent, about 21.14 percent of area is the fire risk prone zone. 47 percent of forest land use area is found to be risky by fire burn zone. 58 percent of total residential area is fire risk in which 13 ha residential area for high and moderate risk. Likewise, 38 percent of industrial land occurred under medium and low fire risk in which 12 ha industrial area along the surrounding of high voltage transmission line. Similarly, 27 percent of commercial area is occurred under the medium and low fire risk. 34 percent of total public use area is fire risk in which 4 ha residential area for high and moderate risk.15 ha other land use mainly open area and 1 ha cultural & archeological area are found under low fire risk threat. 33 ha forest land in medium risk and 2037 ha forest land in low risk are major affected area; these forest area need to be protected for environment sustainability. The risk of fire is reduced in the forest region to enhance the potential for protection of the environment and forest management sustainability. The incidents of forest fire are minimized through taking preventive measures in high and medium fire risk area.

5. CONCLUSION

In the context of Sambhunath municipality, the factor for forest risk assessment are established identified in the local situation. These factors might be used in fire risk susceptibility assessments of potential fire zone in different part of Nepal as well. The high risk of potential fire zone were identified along the east west highway surrounding to the high voltage transmission route and petrol pump location. Likewise, potential high risk of forest fire also found in the dense forest area in elevation greater than 400m. Also, in GIS environment, spatial modeling with integration of MCE, fuzzy and AHP is effectively and widely applicable in the fire risk susceptibility assessment. The developed susceptibility model provides an appropriate and acceptable framework for risk zonation.

REFERENCES

Akgun, A., Kincal, C. & Pradhan, B., (2012). Application of remote sensing data and GIS for landslide risk assessment as an environmental threat to Izmir city (west Turkey). *Environmental Monitoring Assess*, 184: 5453–5470.

Arpaci, A., Malowerschnig, B., Sass, O. & Vacik. H., (2014). Using multi variate data mining techniques for estimating fire susceptibility of Tyrolean forests. *Applied Geography,* 53: 258–270

Bar Massada, A., Syphard, S., Stewart, I. & Radeloff, V. C., (2013). Wildfire ignition-distribution modelling: a comparative study in the Huron–Manistee National Forest, Michigan, USA. *International Journal of Wildland Fire*, 22(2): 174–183.

Bisquert, M., Caselles, E., Sa´nchez, J.M. & Caselles, V., (2012). Application of artificial neural networks and logistic

regression to the prediction of forest fire danger in Galicia using MODIS data. *International Journal of Wildland Fire,* 21(8): 1025–1029.

Crimmins, M. A., (2006). Synoptic climatology of extreme fire-weather conditions across the southwest United States. *International Journal of Climatology*, 26(8): 1001–1016.

Dimuccio, L.A., Ferreira, R., Cunha, L. & Campar de Almeida, A., (2011). Regional forest-fire susceptibility analysis in central Portugal using a probabilistic ratings procedure and artificial neural network weights assignment. *International Journal of Wildland Fire,* 20(6): 776–791.

Eastman, J. R., (2006). *Idrisi 15 Andes, Guide to GIS and Image Processing*. Clark University; Worcester: MA 01610-1477 USA.

Elmas, C. & Sonmez, Y. (2011). A data fusion framework with novel hybrid algorithm for multi-agent Decision Support System for Forest Fire. *Expert Systems with Applications*, 38(8): 9225–9236

Eugenio, F. C., dos Santos, A. R., Fiedler, N. C., Ribeiro, G. A., da Silva, A. G., dos Santos, A. B., Paneto, G. G. & Schettino, V. R., (2016). Applying GIS to develop a model for forest fire risk: A case study in Espirito Santo, Brazil. *Journal of Environmental Management*, 173: 65-71.

FAO, (2006). Better Forestry, Less Poverty: a Practitioner's Guide. Food and Agriculture Organization of the United Nations, Roma.

Feizizadeh, B., Omrani, K., & Aghdam, F. B., (2015). Fuzzy analytical hierarchical process and spatially explicit uncertainty analysis approach for multiple forest fire risk mapping. *GI_Forum – Journal for Geographic Information Science*, 1: 72–80.

Ferraz, S. F. B. & Vettorazzi, C. A., (1998). Fire risk mapping in forests using a geographic information system (GIS). *Scientia Florestalis*, 53: 39-48.

Gheshlaghi, H. A., (2019). Using GIS to develop a model for forest fire risk mapping. *Journal of the Indian Society of Remote Sensing*, 47(7): 1173-1185.

Guo, F., Su, Z., Wang, G., Sun, L., Lin, F. & Liu, A., (2016). Wildfire ignition in the forests of southeast China: Identifying drivers and spatial distribution to predict wildfire likelihood. *Applied Geography*, 66: 12–21.

Hantson, S., Pueyo, S. & Chuvieco. E., (2015). Global fire size distribution is driven by human impact and climate. *Global Ecology and Biogeography*, 24(1): 77–86

Hong, H., Tsangaratos, P., Ilia, I., Liu, J., Zhu, A. X. & Xu, C., (2018). Applying genetic algorithms to set the optimal combination of forest fire related variables and model forest fire susceptibility based on data mining models. The case of Dayu County, China. *Science of the Total Environment*, 630: 1044–1056.

Jaafari, A., Zenner, E. K. & Pham, B.T., (2018). Wildfire spatial pattern analysis in the Zagros Mountains, Iran: A comparative study of decision tree based classifiers. *Ecological Informatics*, 43: 200–211.

Kantardzic, M., (2011). *Data mining: Concepts, models, methods, and algorithms*. New York: Wiley.

Karna, B. K., Shrestha, S., & Koirala, H. L., (2021). Land suitability analysis for potential agriculture land use in Sambhunath Municipality, Saptari,

Nepal. *The Geographic Base*, 8, 13-30.

Moritz, M. A., Parisien, M.A., Batllori, E., Krawchuk, M. A., Van Dorn, J., Ganz, D. J. & Hayhee, K., (2012). Climate change and disruptions to global fire activity. *Ecosphere*, 3, 1–22.

Nohani, E., Moharrami, M., Sharafi, S., Khosravi, K., Pradhan, B., Pham, B.T., Saro Lee, S. & Melesse, A. M. (2019). Landslide Susceptibility Mapping Using Different GIS-Based Bivariate Models. *Water*, 11: 1-22

Oliveira, S., Oehler, F., San-Miguel-Ayanz, J., Camia, A. & Pereira, J. M. C., (2012). Modeling spatial patterns of fire occurrence in Mediterranean Europe using Multiple Regression and Random Forest. *Forest Ecology and Management*, 275: 117–129.

Pan, J., Wang, W. & Li, J., (2016). Building probabilistic models of fire occurrence and fire risk zoning using logistic regression in Shanxi Province, China. *Natural Hazards*, 81, 1879–1899.

Pourtaghi, Z. S., Pourghasemi, H. R. & Rossi, M., (2015). Forest fire susceptibility mapping in the Minudasht forests, Golestan Province. Iran. *Environmental Earth Sciences*, 73, 1515–1533.

Pourghasemi, H., Beheshtirad, M. & Pradhan, B., (2016). A comparative assessment of prediction capabilities of modified analytical hierarchy process (M-AHP) and Mamdani fuzzy logic models using Netcad-GIS for forest fire susceptibility mapping. *Geomatics, Natural Hazards and Risk*, 7, 861–885

Pourtaghi, Z. S., Pourghasemi, H. R., Aretano, R. & Semeraro, T., (2016). Investigation of general indicators influencing on forest fire and its susceptibility modeling using different data mining techniques. *Ecological Indicators* 64: 72–84.

Ranabhat, S., Pokharel, A., Neupane, A., Singh, B. & Gahatraj, S., (2022). Forest fire risk assessment and proposal for fire stations in different geographical regions of Central Nepal. *Journal of Forest and Livelihood*, 21 (1):46-59.

Running, S.W., (2006). Is global warming causing more, larger wildfires? *Science*, 313(5789): 927–928.

Saaty, T. L., (1977). A scaling method for priorities in hierarchical structures. *Journal of Mathematical Psychology*, 15(3), 234–281.

Saaty, T. L. (1980). *The analytic hierarchy process*. McGraw-Hill, New York.

Sachdeva, S., Bhatia, T., and Verma, A. K., (2018). GIS-based evolutionary optimized Gradient Boosted Decision Trees for forest fire susceptibility mapping. *Natural Hazards,* 92(3): 1399–1418.

Satir, O., Berberoglu, S., and Donmez. C., (2016). Mapping regional forest fire probability using artificial neural network model in a Mediterranean forest ecosystem. *Geomatics, Natural Hazards and Risk*, 7(5): 1645–1658.

Shahabi, H., & Hashim, M., (2015). Landslide susceptibility mapping using GIS-based statistical models and Remote sensing data in tropical environment. *Scientific Reports*, 5, 1-15

Sharma, L.K., Kanga, S., Nathawat, M.S. & Sinha, S., (2012). Fuzzy AHP for forest fire risk modeling. *Disaster Prevention and Management*, 21(2):160-171.

Soto, M. E. C., (2012). The identification and assessment of areas at risk of forest fire using fuzzy methodology. *Applied Geography*, 35, 199–207.

Tehrany, M. S., Pradhan, B. & Jebur, M. N., (2013). Spatial prediction of flood

susceptible areas using rule based decision tree (DT) and a novel ensemble bivariate and multivariate statistical models in GIS. *Journal of Hydrology*, 504: 69–79.

Tian, X., Zhao, F., Shu, L. & Wang, M., (2013). Distribution characteristics and the influence factors of forest fires in China. *Forest Ecology and Management*, 310: 460-467.

Tien Bui, D., Pham, B. T., Nguyen, Q. P., & Hoang, N.D., (2016). Spatial prediction of rainfall-induced shallow landslides using hybrid integration approach of least-squares support vector machines and differential evolution optimization: A case study in Central Vietnam. *International Journal of Digital Earth*, 9, 1077–1097.

Tien Bui, D., Bui, Q. T., Nguyen, Q. P., Pradhan, B., Nampak, H. & Trinh, P. T., (2017). A hybrid artificial intelligence approach using GIS-based neural-fuzzy inference system and particle swarm optimization for forest fire susceptibility modeling at a tropical area. *Agricultural and Forest Meteorology,* 233: 32–44.

Vasconcelos, M. J. P. de, Silva, S., Tome M., Alvim, M. & Perelra, J. M. C., (2001). Spatial prediction of fire ignition probabilities: Comparing logistic regression and neural networks. *Photogrammetric Engineering & Remote Sensing*, 67(1): 73–81.

Yang, J., Healy, H. S., Shifley, S. R. & Gustafson, E. J., (2007). Spatial patterns of modern period human-caused fire occurrence in the Missouri Ozark Highlands. *Forest Science,* 53: 1-15.

Zhang, G., Wang, M. & Liu, K., (2019). Forest fire susceptibility modeling using a convolutional neural network for Yunnan Province of China. International *Journal of Disaster Risk Science*, 10: 386–403.

Author's Information

Name	:	Bikash Kumar Karna
Academic Qualification	:	M. Tech. in Remote Sensing & GIS
Organization	:	Survey Department
Designation	:	Chief Survey Officer
Work Experience	:	24 Years
Published Article/Paper	:	11

Topographic Base Map Update in Nepal: Overview, Accomplishments and Way Forward

Tina Baidar[1], Buddha Lama[1], Rajeev Gyawali[1], Girija Pokhrel[1]
tina.baidar13@gmail.com, lama.boodha3@gmail.com, rajeev1994.gna@gmail.com, girija.pokhrel12@gmail.com
[1] Survey Department

KEYWORDS

Topographic Base Maps, Survey Department, ZY-3, Image Processing, Feature Update, Map Compilation, Map Validation

ABSTRACT

The latest series of topographic base map of Nepal were prepared by Survey Department of Nepal during 1992-2001 A.D and preparation of their digital database namely National Topographic Database started in 1999 A.D. Understanding the utmost need of updating these maps and database, the department started update process in a rapid pace from fiscal year 2075/76 B.S based on ZiYuan-3 Survey and Mapping (ZY-3) satellite images with 2.1 m panchromatic and 5.8 m multispectral spatial resolution. The overall update procedure includes satellite image processing, feature update, field verification, field data compilation, finalization, map and database approval from Mapping Technical Subcommittee and finally map reproduction. The technical aspects of this whole process is based on standard specification document namely "Specifications for 1:25000 and 1:50000 Topographic Base Maps". First level of update and field verification of all grid sheets covering Nepal was completed by fiscal year 2078/79 and is now in the phase of approval by Mapping Technical Subcommittee and reproduction. At the end of 2079 B.S, around 250 number of sheets have been approved and are made available by the department. With the completion of this update series, there are further opportunities to produce thematic data/maps as well as administrative maps of smaller scales. Furthermore, with the availability of higher resolution images through LiDAR, UAV and other resources, the department has opportunities to work on large scale mapping in coming days.

1. INTRODUCTION

In Nepal, topographical base maps were prepared by Survey of India (SOI) for the first time during 1950s and 1960s at the scale of one inch to a mile. However, these maps were not updated later and therefore do not represent the current topographical scenario of the country (Shrestha, 2021). Later in 1993, with the technical and financial assistance of Government of Japan through Japan International Cooperative Agency (JICA), Survey Department of Nepal published 81 sheets of topographic base maps covering Lumbini Zone at the scale 1: 25,000 using aerial photographs of 1990 (Pradhananga, 2003). These maps were produced in five colors namely red, green, blue, brown, and black.

Topographical base maps for the rest of the 13 zones were prepared in two projects

namely Eastern Nepal Topographic Mapping Project (ENTMP) during 1992-1997 and Western Nepal Topographic Mapping Project (WNTMP) during 1996-2001. 255 map sheets in a scale of 1:25000 for terai and middle mountains and 37 map sheets in a scale of 1:50000 for high mountains and himalayan region were prepared using aerial photographs of 1992 during ENTMP while WNTMP published 254 map sheets in a scale of 1:25000 for terai and middle mountains and 79 map sheets in a scale of 1:50000 for high mountains and himalayan region using aerial photographs of 1995-1996 (Shrestha, 2009). These maps were prepared by Survey Department with technical and financial support of Government of Finland through Finnish International Development Agency

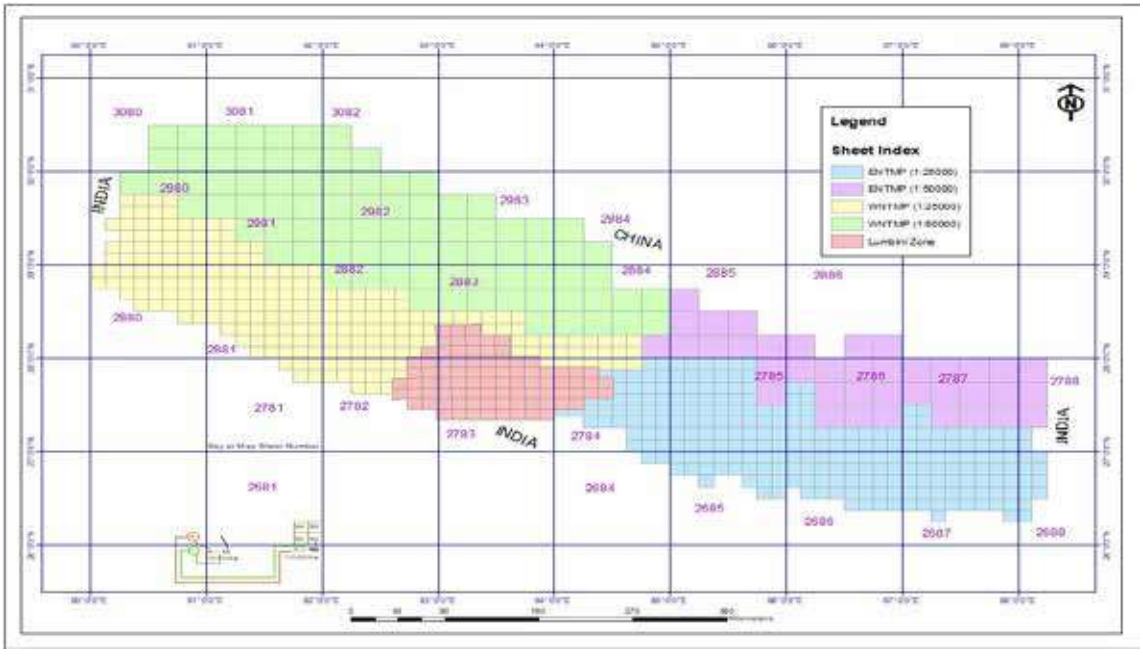

Figure 1: Topographic Mapping Series of Nepal with Sheet Index
(Data Source: Topographic Survey and Land Use Management Division)

(FINNIDA). The contents of these maps were depicted in six different colors (red, blue, green, yellow, brown and black).

In total, 706 maps sheets covered the whole Nepal including 590 sheets in 1:25000 scale and 116 map sheets of 1: 50000 scale in Modified Universal Transverse Mercator (MUTM) projection system. Figure 1 shows the topographic mapping series of Nepal with details of sheet index. These topographical base maps included different natural and artificial features, which can be classified into the point (triangulation point, transmission tower, buildings, temples, hospital, schools, etc.), line (roads, transmission line, contours, streams, administrative boundaries, etc.) and polygon features (land cover) in the context of digital mapping. In addition to these, annotations were added to make the maps more meaningful and readable. Furthermore, in January 1999, Survey Department started digitization of all 1:25000 and 1:50000 scale topographic maps to create National Topographical Database (NTDB) (Shrestha, 2021). These datasets and maps are still in use since their updating process is not yet complete. Since some map sheets were common in Lumbini Zone mapping project and WNTMP, there are altogether 682 grid sheets (563 grid sheets of 1:25000 scale and 119 grid sheets of 1:50000 scale) covering whole Nepal in present topographic base map update series.

2. NEED FOR UPDATE

Updating of topographical maps is directly related to the extent of development activities in the given area. It means the more the developments in a given area, the more outdated are the topographic maps of that area. With the change in time, it is obvious that there have been changes in features that are included in these base maps. Therefore, all the users of topographic base maps from decision makers to researchers naturally expect the updated maps to fulfil their purpose. Moreover, the updated maps depict the changing scenario likes decreasing agricultural lands, densification of residential area, proportion of development in different regions, availability of infrastructures and so on. Hence, regular updating of these maps is undoubtedly, most essential at present to address all the activities that rely on using Topographic maps.

Survey Department started updating the topographical base maps in a rapid pace from fiscal year 2075/76 B.S. based on ZiYuan-3 Survey and Mapping (ZY-3) satellite images. These images are provided in free of cost by Land Satellite Remote Sensing Application Center(LASAC), China based on MOU (in 2018) between LASAC, Ministry of Natural Resources of P.R. China and Government of Nepal, Ministry of Agriculture, Land Management and Cooperatives, Survey Department to provide satellite image till 2023. The ZY-3 (Ziyuan-3, 'Resource-3') series represents China's first high resolution, stereoscopic mapping satellites for civilian use with 2.1 m panchromatic and 5.8 m multispectral spatial resolution (Wang, *et al.*, 2013). The images are, in general, in WGS84 UTM coordinate system.

Before this, some efforts were also made to update the maps in eastern region of terai. However, without the standard specifications for updating the maps digitally, final results were not achieved. In FY 2075/76 B.S, preparation of standard specification for topographical base map update and field team mobilization for data collection and verification were conducted simultaneously and the standard specification document namely **"Specifications for 1:25000 and 1:50000 Topographic Base Maps"** was later approved from Mapping Technical Subcommittee. With this, all the database has been prepared and corresponding maps have been compiled with reference to this standard specification.

3. OVERVIEW OF TOPOGRAPHIC BASE MAP UPDATE

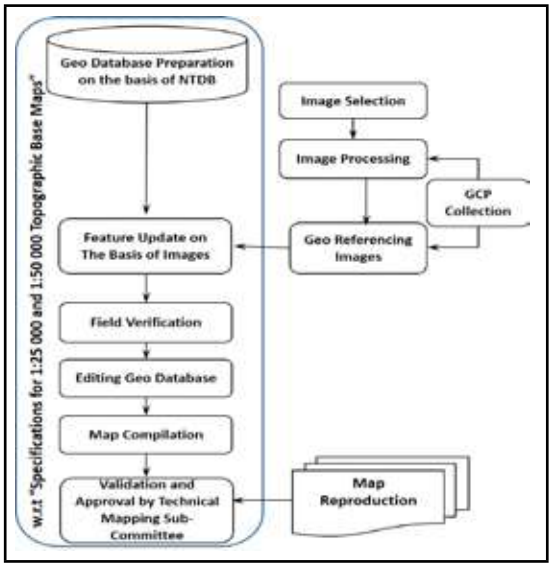

Figure 2: Overall workflow diagram for topographic base map update

For updating the existing topographical base maps, the department has been using ZY3 satellite images to detect changes, to include new features in the original database and/or to remove non-existing features supplemented by field verification and subsequent cartographic works in digital environment. The original digital databases (coverage file format) of topographic map sheets are acquired from the Geographic Information Infrastructure Division (GIID), Survey Department. A sheet wise file geodatabase for each topographic map sheet is then created based on the standard specification document. Thereafter, data from each coverage file is imported to

corresponding feature class of corresponding geodatabase for update process. The detailed methodology is explained below and its work flow diagram is shown in Figure 2.

3.1 Image processing

Latest satellite images covering the planned grid sheets area are selected with cloud coverage less than 5% as far as possible from the image database. This includes the corresponding raw panchromatic and multispectral image pairs. Thereafter, Ground Control Points (GCPs) are marked in the images considering the coverage of entire working areas. GPS survey is then carried out in the pre-marked areas in the field following standard procedure. The processed data is then used to transform from WGS 84 coordinate system to MUTM system.

In this stage, each panchromatic and multispectral images are orthorectified using processed GCPs (in WGS84 UTM) collected from Differential Global Positioning System (DGPS), Rational Polynomial Coefficient (RPC) geometry file of satellite image and corresponding Digital Elevation Model (DEM). Both orthorectified panchromatic and multi-spectral images are mosaicked for applicable scenes and then pansharpened to enhance visual image interpretation process. Thus obtained pansharpened image and processed GCP coordinates (in MUTM) are used to obtain the georeferenced image which are then used for feature update process.

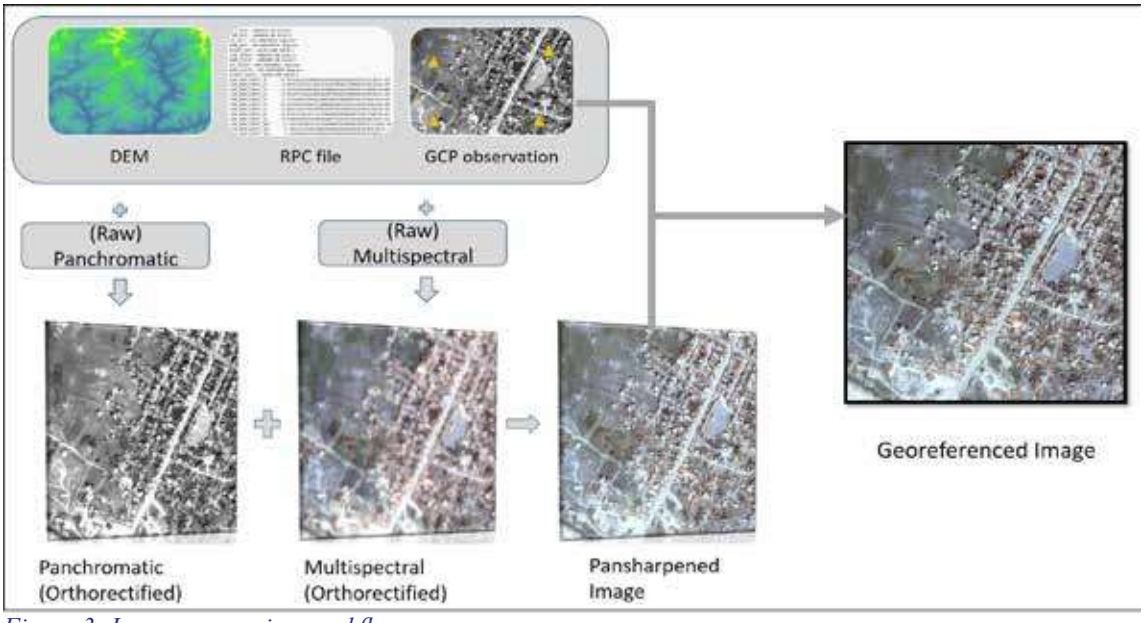

Figure 3: Image processing workflow

3.2 Feature update and field verification

In this phase, on top of georeferenced images, existing feature datasets of base map are displayed. With respect to the satellite image, the existing features are verified and then updated in GIS environment by using on-screen digitization technique. The major features that are updated using images are land cover, transportation network, hydrographic features and building points.

The updated data from the images and the existing database are then verified from field visit and necessary corrections are made. Furthermore, other details of point features such as government academic institutions, government hospitals, service center, health post, police stations/posts, major religious places, etc. are also collected from field visit.

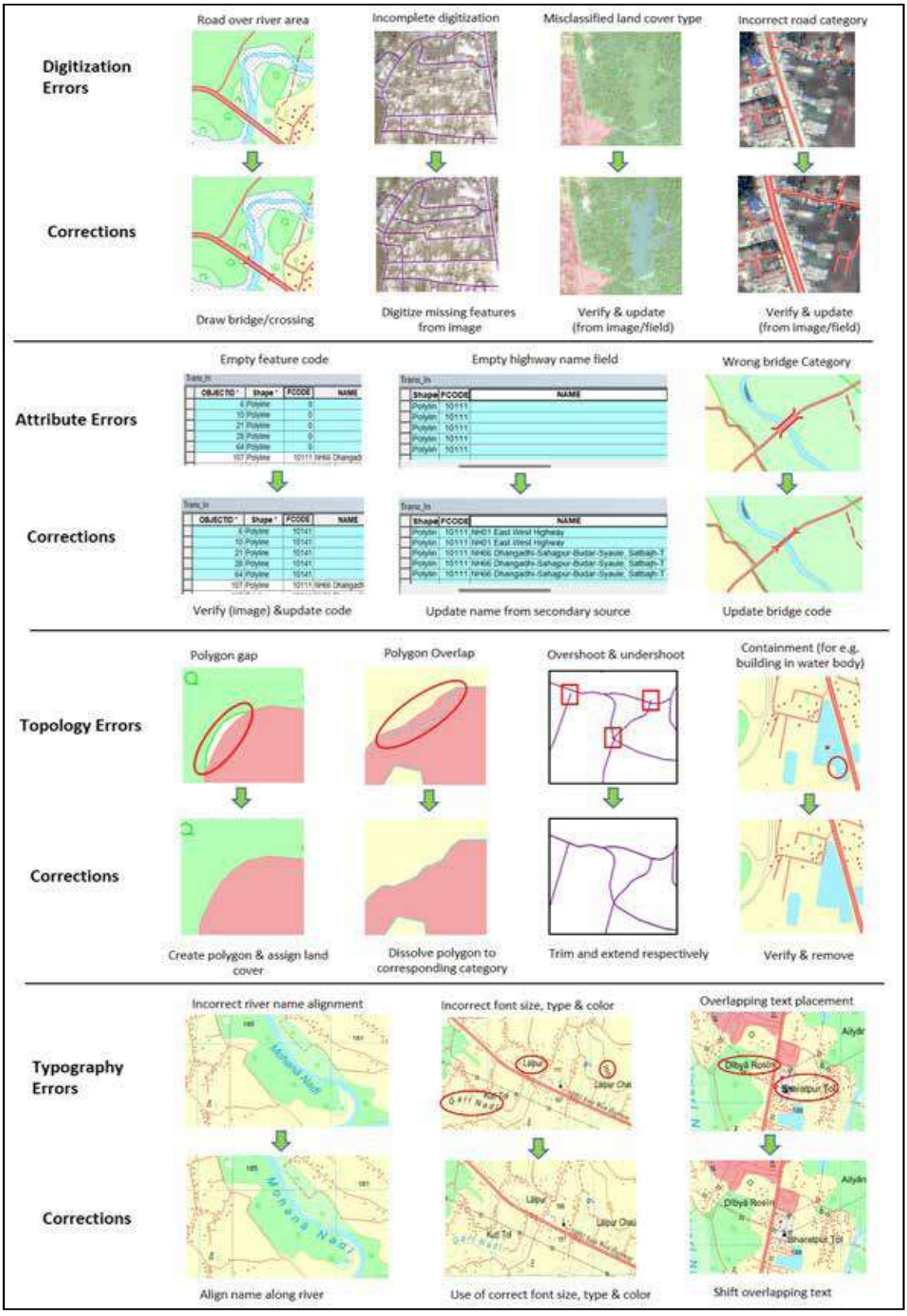

Figure 4: Sample of error types and their correction measure

Apart from these, the team collects additional features, names and other attributes as required. Along with these, for features like transportation (national highways), designated area boundaries, transmission lines and canals, secondary data are collected from authorized sources.

3.2 Field data compilation and finalization

Features are edited and updated after subsequent field verification and are incorporated in the sheet wise database. In case of new added features, corresponding feature code and/or attribute codes are also updated in attribute table with reference to standard specification. Once all the features are updated and verified, topology test is conducted to detect and correct digitization errors. This test ensures the spatial relationship among the features and helps to maintain the topological consistency in data. Besides, several other errors such as errors in database schema, attribute table, typography are identified and then corrected. Figure 4 shows some samples of errors that are mostly identified during data verification phase and their corresponding correction measures.

3.3 Map compilation in digital environment

The basic objective in the map compilation phase is to prepare a composite containing all the reference data, geographical features, text etc. that appear in the map in digital environment. The final edited database is used to compile the updated topographic map. Figure 5 and 6 respectively represent a sample of originally compiled topographic base map and a sample of updated base map compiled in digital environment. The final layout of the compiled map consists of following elements:

3.3.1. Map body

According to the map sheet layout system in Nepal, the map body (the area within the neat lines) represents the ground area of extent 7' 30" in longitude and 7' 30" in latitude in case of map at scale 1:25 000; and 15' 00" in longitude and 15' 00" in latitude in case of map at scale 1:50 000. The features are represented in the map with the help of different symbols viz. point, line and polygon along with the textual notations for required feature label.

a) Use of Symbols and Symbol Levels: All the features shown in topographical base maps are symbolized based on their feature and/or attribute code. Symbol and color description (CMYK values) with their dimension are also listed in standard specification document.
b) Features Hierarchy: For cartographic visualization, feature hierarchy is maintained in order to ensure that all features are visible in final compiled map.
c) Cartographic Generalization: Considering map scale, features are generalized. It includes features simplification, smoothing, aggregation, displacement, omission, exaggeration, enhancement and classification. While displacing the features in need, displacement priority rule is considered.

3.3.2. Map border

This section between the neat line and the map body frame, consists of two map elements; grid and graticule, and destination annotations (nearest destination of the roads).

3.3.3. Marginal information

Marginal information of each map sheet consists of sheet title, sheet number, legend, administrative index, map sheet history, index to sheets, location diagram, edition, map scale, copyright, contour and datum information and pronunciation guide.

3.4 Map and Database Approval and Map Reproduction

In this stage, the final products of topographic base map update i.e. maps and database are presented to Mapping Technical Subcommittee for final approval. Once approved, for low quantity production, the maps are directly

printed from the wide format color printer. While in case of mass production, the printing plates are produced directly from the EPS (Encapsulated PostScript) file through Computer to Plate (CTP) machine.

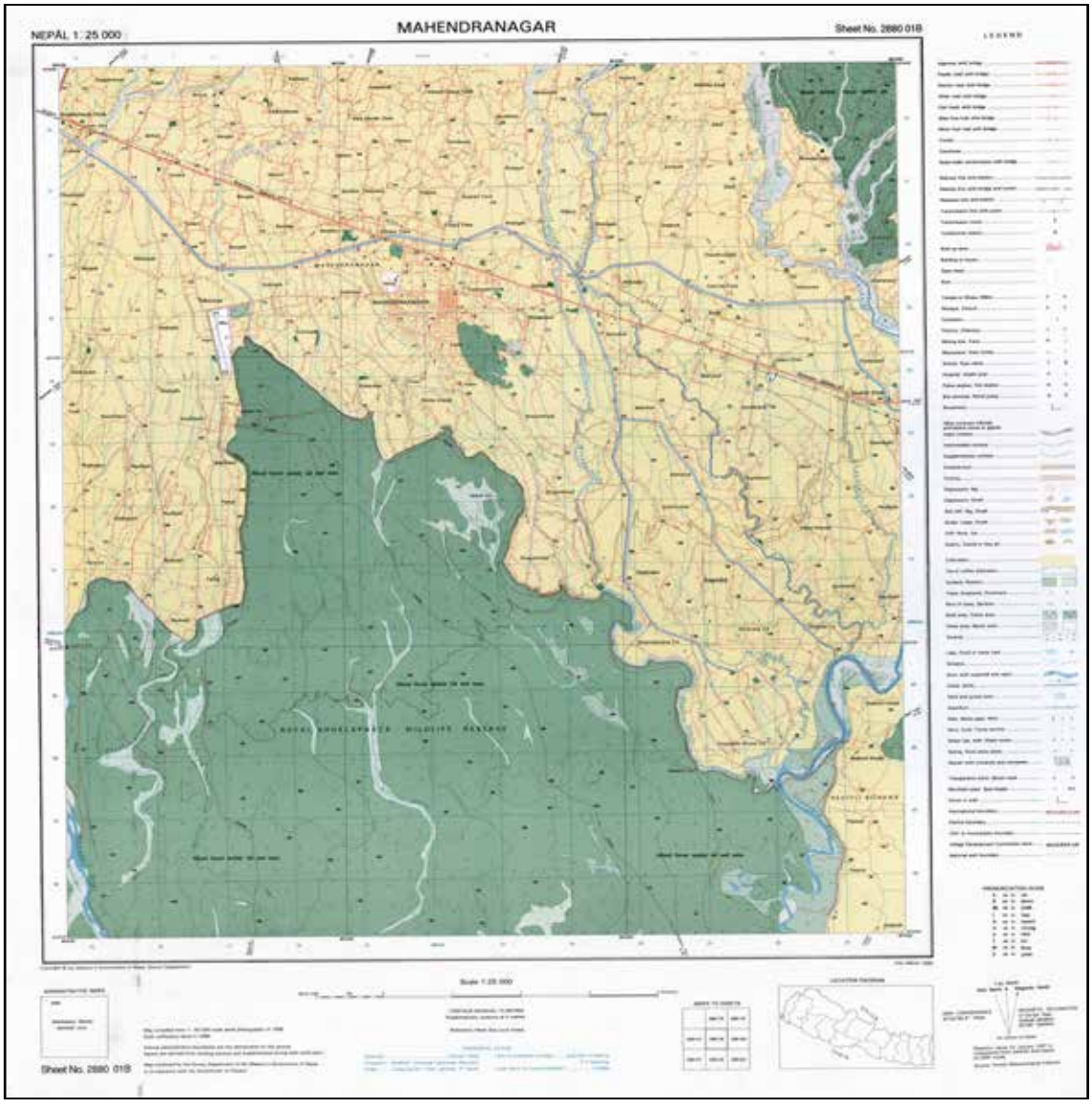

Figure 5: A sample of originally compiled topographic base map (Sheet No: 288001B, Mahendranagar) (Source: Topographic Survey and Land Use Management Division)

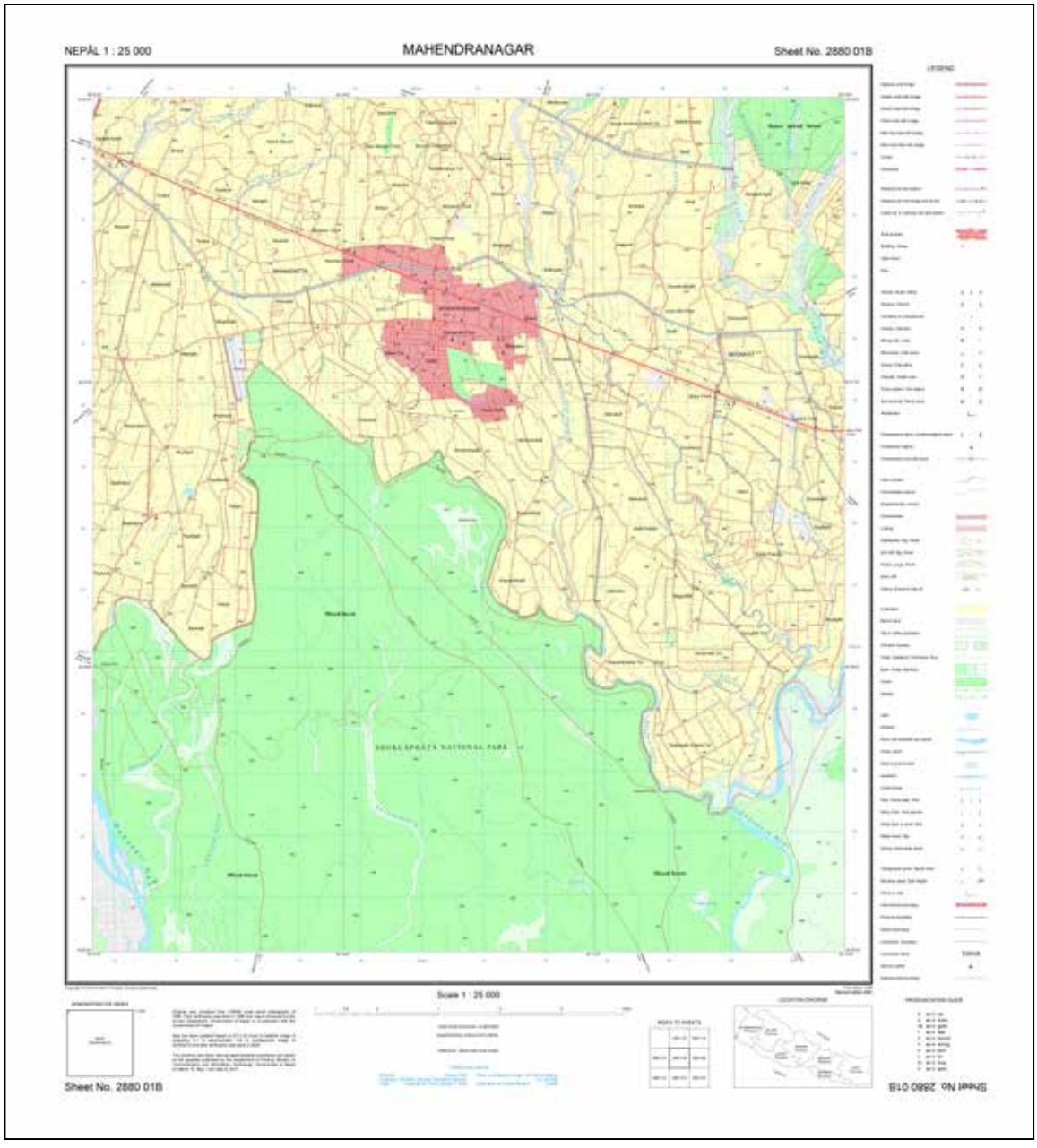

Figure 6: A sample of updated topographic base map compiled in digital environment (Sheet No: 288001B, Mahendranagar) (Data Source: Topographic Survey and Land Use Management Division)

4. ACCOMPLISHMENTS SO FAR

Survey Department started extensive topographic base map update work from fiscal year 2075/76 B.S. which covered almost all of the Terai region of whole Nepal. Then, map sheets covering most of the hilly region of Nepal were prepared by update work in fiscal year 2076/77 B.S. Proceeding update work, remaining map sheets were updated in the fiscal year 2077/78 B.S. and 2078/2079 B.S. Figure 5 shows timeline of topographic base map update series of 682 map sheets from fiscal year 2075/76 to fiscal year 2079/80.

At present, the updated topographic base maps are in the phase of approval by Mapping Technical Subcommittee and reproduction.

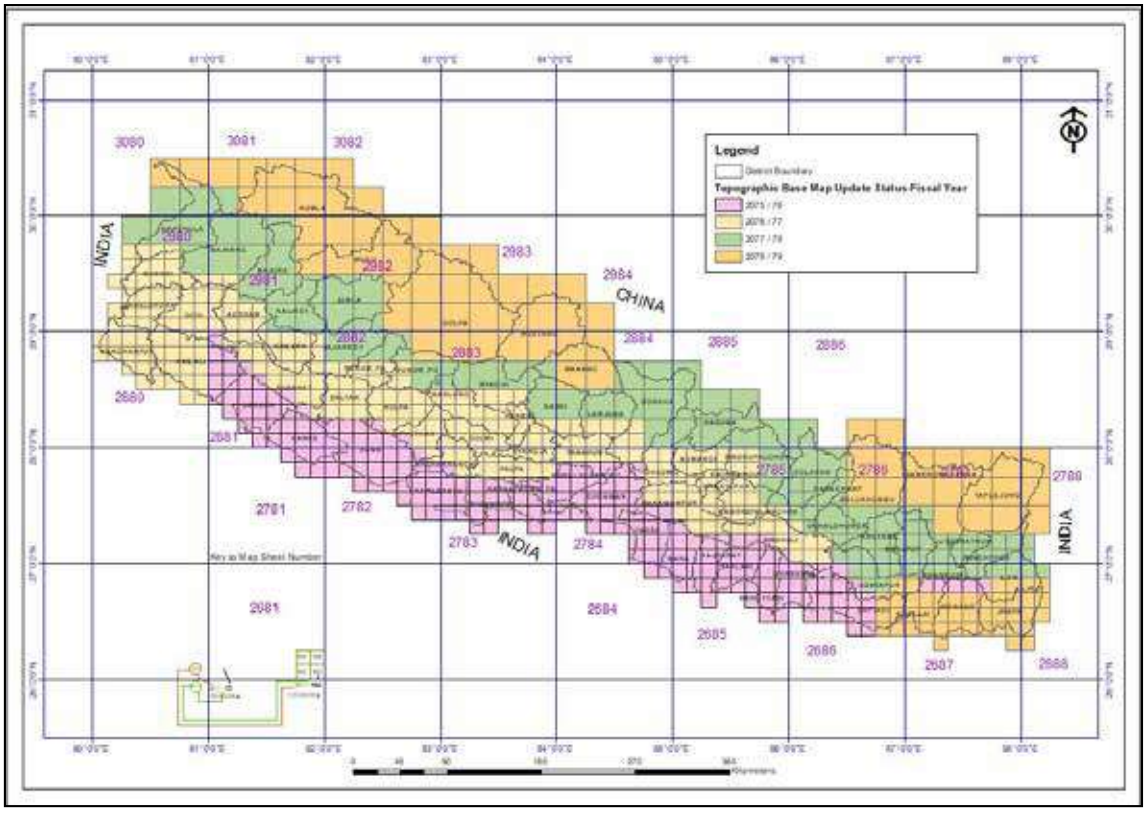

Figure 7: Topographic base map update from fiscal year 2075/76 to 2078/79 (Data Source: Topographic Survey and Land Use Management Division)

At the end of 2079 B.S, around 250 number of sheets (mostly western terai and mid-hill region) have been approved and are made available by the department.

5. CHALLENGES AND LIMITATIONS

Topographic base map update involves a series of desktop and field work with rigorous digitization and verification procedure as explained before and therefore takes time in finalizing both the database and maps. Level of image interpretation and feature update may differ upon human resource and their experience to some extent although they are trained beforehand. Since this is an update process and not a new mapping, it involves more manual work in digitization process which tends to generate errors. It is clear that the major errors/blunders are fixed through several error detection tools however, minor errors may still remain.

The updated features/details are based on used image acquisition date and corresponding field verification date regardless of map print date. During field verification process, features of topographically inaccessible areas of Nepal, are verified and updated from local level representatives. Digital database prepared is based on digital cartographic model rather than digital landscape model. In this case, features are generalized with respect to map scale and thus displacement of features can occur to some extent.

6. WAY FORWARD

Obviously, the first target of the Survey Department is to approve and publish the remaining topographic map series of whole Nepal in the coming days. This will provide a base to generate several thematic data and maps of whole Nepal as well. Furthermore, administrative maps of smaller scale like

district level maps can be compiled based on this updated topographic data with further field verification.

At present, the department has been publishing topographic base maps at the scale of 1:25000 and 1:50000. which covers a broader area and lesser detail and mostly useful for regional planning and infrastructure development. On the other hand, large scale topographic base maps not only provide with higher topographic details with better accuracy but also is applicable for infrastructural planning, disaster management and emergency responses, resource management, among others at city/ local level.

With the advancement of technology, availability of higher resolution images from LiDAR, UAV and other resources, and mapping tools and algorithms for automatic and semi-automatic feature extraction, there are opportunities for large scale topographic mapping. Together with this, availability of required infrastructures and resources are mandatory to conduct large scale mapping series

REFERENCES

Pradhananga, T. B. (2003). Topographical Survey Branch with remote sensing. *Journal of Geoinformatics, Nepal*, 47-52.

Shrestha, K. G. (2009). Updating of Topographic Maps in Nepal. *Journal on Geoinformatics, Nepal*, 52-56.

Shrestha, S. M. (2021). *Cartography and Georaphic Information System.* Kathmandu.

Wang, T., Zhang, G., Li, D., Tang, X., Jiang, Y., Pan, H., Fang, C. (2013). Geometric accuracy validation for ZY-3 satellite imagery. *IEEE Geoscience and Remote Sensing Letters 11.6*, 1168-1171.

Author's Information

Name	:	Er. Tina Baidar
Academic Qualification	:	MSc. In Geospatial Technologies
Organization	:	Survey Department
Current Designation	:	Survey Officer
Work Experience	:	8 years
Published paper/article	:	6

UAV Images for Agriculture Land Parcel Delineation through Edge Detection Algorithm: A Case Study of Hilly and Terai Regions

Arun Kumar Bhomi[1], Jiya Thapa[1], Mamta Kadel[1], Nischal Acharya[1], Prawal Parajuli[1], Sudeep Kuikel[1], and Uma Shankar Panday[1]
arunbhomi12345@gmail.com, thapajiya2018@gmail.com, mamtakadel88@gmail.com, nischalacharya642@gmail.com, prawalparajuli7@gmail.com, sudeep.kuikel@ku.edu.np, uspanday@ku.edu.np
[1]Kathmandu University, Dhulikhel, Nepal

KEYWORDS

Parcel Delineation, UAV, GIS, Edge Detection, Segmentation, Agriculture

ABSTRACT

The use of unmanned aerial vehicles (UAVs) for remote sensing applications has gained significant attention in recent years. One important aspect of UAV-based remote sensing is the accurate delineation of parcels, which is essential for a wide range of applications, including land use planning, agricultural monitoring, and cadastral map preparation among several others. The on-screen manual digitization method can delineate parcels with great precision. However, the method is labor-intensive, time-consuming, and expensive. Alternatively, it can be achieved by utilizing automated algorithms. In this study, an edge detection algorithm is employed to delineate agriculture parcels using UAV images in the ENVI platform. The algorithm uses a pre-programmed algorithm to automatically detect and delineate field boundaries. The delineated boundaries were cleaned and refined by smoothing the polygon and the line vectors. The obtained parcel boundaries and their geometric parameters were assessed against manually digitized parcel boundaries using the same UAV ortho-mosaic. The method was tested on two scenarios: i) Terai farms having flat topography and small dikes and ii) Hill farms having undulated terrain in a terraced farming structure and crowded parcels. The mean of the percentage change in area for the land parcel was found to be 2.43% and 4.69% respectively for Terai and Hilly regions. Similarly, the mean of the percentage change in the perimeter of the land parcels were 8.82% and 2.43% respectively for Terai and Hilly regions. The study demonstrated the feasibility of using UAV images for agriculture land parcel delineation and highlighted the potential of an in-built edge detection algorithm as a time-efficient and reliable alternative to manual digitization if refinement and proper selection of algorithm and parameters are done. Thus, automated algorithms can be utilized to reasonably delineate agriculture parcels from UAV images.

1. INTRODUCTION

An agricultural land parcel is a specific piece or plot of land that is used for agricultural purposes such as farming, agroforestry, etc. It is demarcated and identified with natural and man-made features like roads, streams, bunds,

walls, etc. Also, it can be defined as boundaries where a change in crop type, crop mixture, or farm management practice takes place, or where two similar cultivations are separated by a natural disruption in the landscape, like a bund or a ditch (Rydberg & Borgefors, 2001).

Due to human activities, natural calamities, and changes in seasonal vegetation in farmland, there is a frequent modification in agricultural land boundaries (Paul & Rashid, 2017). Farmland delineation is one of the first primary requirements for various parcel-based applications such as the estimation of agricultural subsidies, irrigation planning, fertilizers dose estimation, pesticide management, crop insurance, and establishment of agricultural policies and taxation (Ajayi & Oruma, 2022). Therefore, there is a high demand for accurate and up-to-date land parcel boundary information.

Parcel delineation is the process of identifying and demarcation of the boundaries of individual land parcels (Aung *et al.,* 2021). The delineation of land parcels on orthoimage is done on the basis of the shape and size of the parcels, color intensity, pattern, location, and presence of physical objects like roads, ditches, drainage, and spontaneous recognition (Ajayi & Oruma, 2022). It has wide use in downstream governmental policies of land allocation like cadastral mapping, agricultural planning, and taxation (Djordje, 2019). While ground-surveying methods are a decades-old practice, manual on-screen digitization using satellite, aerial or Unmanned Aerial Vehicle (UAV) images has been in practice in recent times.

Land parcel delineation using the ground survey method, such as with the use of a Total Station, involves physical inspection of various aspects of the land and measuring land boundaries' corners, followed by GIS (Geographic Information System) processing to delineate the parcel boundaries. Likewise, manual land parcel digitization records and converts land boundaries into a digital format using GIS software through an on-screen method. This can be used to manually identify and delineate the boundaries of individual land parcels utilizing satellite, aerial or UAV image mosaics. It allows for the creation of a comparatively accurate database and thus facilitates the preparation of detailed maps. However, these methods are labor-intensive, time-consuming, and expensive. Segmentation and edge detection algorithms, on the contrary, are computer programs that are designed to automatically identify and delineate the boundaries of fields based on certain criteria, such as the shape and size of the parcels, pixel intensity, and color (Khairee & Thakur, 2013).

The parcel size of Nepali farms is small with an average area of 0.24 hectares (CBS, 2006). Therefore, land parcel delineation using satellite imagery would be inappropriate in the Nepalese context. UAV, on the contrary, provides ultra-high-resolution images that could be utilized to obtain detailed information about farmland and land boundaries. It can precisely capture visible field boundaries of agricultural lands often marked by physical objects such as agricultural bund, water drainage, ditches, etc. Therefore, an inbuilt edge detection algorithm in Environment for Visualizing Images (ENVI) was used in this study to delineate agricultural land boundaries of a Terrain and a Hilly farm area using UAV images.

2. STUDY AREA

The case study areas were selected at agricultural farmlands in Lakshminiya Rural Municipality of Dhanusha District and Dhulikhel Municipality of Kavre District respectively representing Terai and Hilly farmlands. In addition, the two selected areas distinguish themselves in terms of agricultural bund and roads to indicate the farmland boundaries. Besides these, there are significant

changes in the size and shape of the farmlands. Furthermore, different seasonal crops are grown in the two study areas. While potatoes and paddy are primarily grown in Dhulikhel, paddy, wheat, and lentils are mainly grown in Lakshminiya. The data was collected in June 2022 at the pre-paddy plantation stage in Lakshminiya while the UAV images from Dhulikhel were acquired in October 2022 when paddy was harvested from some portion of the fields (even crop was harvested from a part of the same field while those from the remaining area of the field was yet to be harvested). The study areas are represented in the map shown in Figure 1.

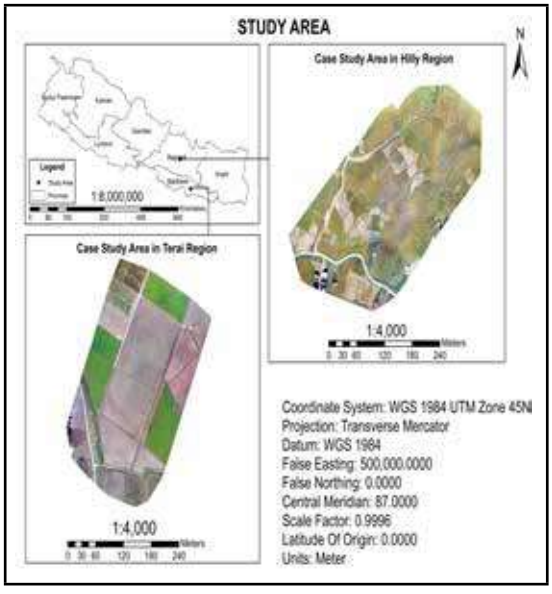

Figure 1: Study area map.

3. METHODOLOGY

Plans for Ground Control Points (GCPs) establishment and UAV flights to cover the entire study sites were prepared. GCPs were measured using Differential GPS in WGS84 Coordinates System and post-processing was done. UAV flights were conducted to capture ultra-high-resolution images of the areas. The images were processed with the input of GCPs coordinates to obtain orthophoto in centimeter-level accuracy. Land boundaries

Figure 2: Methodology adopted.

using edge detection algorithms followed by a smoothing and refinement process. The parcel boundaries were manually digitized for accuracy assessment. After post-processing of the boundaries delineation using edge detection, the results were assessed against the manually digitized parcel data. The details of the methods adopted are discussed in the following subsections and are summarized in Figure 2.

3.1. Data collection

The location of GCPs was planned in such a way that the points are sufficient to cover the study area and variation in elevation (in the case of hilly terrain). These points were measured using STONEX S8 PLUS DGPS in static mode with a cutoff angle of 15 degrees, a time interval between the signals of 15 seconds, and a PDOP (Position Dilution of Precision) threshold of 3. In total, 6 GCPs were measured for both hilly and Terai areas. The measured coordinates were processed with TBC (Trimble Business Centre) software to obtain the resulting coordinates.

A 30cm by 30cm black and white GCP Marker was placed at each of the GCP locations before the UAV flight was conducted. A DJI Mavic 2 Pro UAV was flown to acquire the digital

images of the areas. The images were captured with forward and side overlap of 80% and 70% respectively from a flying height of 70m above the ground. In total 160 images (acquired on 19th October 2022) and 215 images (acquired on 20th June 2022) were captured covering approximately 54,000 m^2 and 74,735 m^2 area on the ground from the Hilly and the Terai areas respectively.

3.2 Generation of ortho-photo

Pix4Dmapper software was used to process the UAV images. After the determination of the orientation and the position of camera stations, the coordinates of GCPs measured using DGPS survey were provided to re-optimize the orientation and the coordinates of camera stations, and thus the object space coordinates of the points in the images. Ultimately, an ortho-mosaic was prepared from the software.

3.3. Parcel delineation

3.3.1. Using edge detection algorithm

The original UAV ortho-image with a Ground Sampling Distance (GSD) of approximately 2 cm was resampled to lower resolutions with 5 cm and 10 cm GSD. The selected GSDs allowed the study of the impact of different GSDs on the results of automatic boundary extractions. In addition, extracting objects from a UAV ortho-image of lower spatial resolution smooths out the heterogeneity present in an individual field and is computationally less expensive.

ENVI Feature Extraction tool was used to delineate the parcel boundaries. The ENVI FX module uses two approaches: the edge method and the intensity method. The edge method works based on the gradient map calculated using the edge detection algorithm and modification of the gradient map defined by a scale level and a merge level parameter whereas the intensity method converts each pixel to a spectral intensity value by averaging it across the selected image bands. The intensity method is suitable for digital elevation models, images of gravitational potential and images of electromagnetic fields. The edge method is used for detecting features with distinct boundaries. Therefore, the Edge-Detection method was used for this case study.

The edge method consists of two parameters: Scale level and Merge level. The scale level is the relative threshold on the cumulative histogram from which the corresponding gradient magnitude can be determined. For example, the lowest 50 percent of gradient magnitude values are discarded from the gradient image at a scale level of 50. Increasing the scale level results in fewer segments and keeps objects with the most distinct boundaries. Likewise, merging aggregates over-segmented areas by using the ENVI FX default full Lambda schedule algorithms (Fetai *et al.,* 2019). The algorithm is meant to aggregate object outlines within larger, textured areas, such as trees and fields, based on a combination of spectral and spatial information. The merge level represents the threshold Lambda value. Merging occurs when the algorithm finds a pair of adjacent objects such that the merging cost is less than a defined threshold Lambda value. If the merge level is set to 20, it will merge adjacent objects with the lowest 20 percent of Lambda values. In this step, the selection of Texture Kernel Size (the size of a moving kernel centered over each pixel value) is optional. The ENVI FX default Texture Kernel Size is 3, and the maximum is 19. The final step was to export the object boundaries in the vector format.

The ENVI FX module was applied to the original as well as the down-sampled images. The detection of visible boundaries was based on the edge detection algorithm. The number of objects extracted varies accordingly with the scale and merge levels values of the algorithm used as well as the scale of the image. Thus, a combination of image scale (GSD), scale, and merge parameters of the used algorithm were

applied to get the optimal combination. When a large change was detected in the number of extracted objects, the incremental value was slightly adjusted. To obtain the optimal scale and merge levels values and the image GSD, all possible ranges of scale level, merge level and GSD combinations were tested for both study sites.

After the delineation of boundaries using the edge-based method, the results were post-processing. This step consists of dissolving boundaries smaller than a pre-set area followed by the smoothing of the field boundaries. All extracted objects that were smaller than the minimum object area from the reference data were dissolved in the larger boundaries containing the smaller ones. The total number of remaining objects after dissolving were then smoothened using the Generalize Tool in ArcMap based on the Maximum Allowable Offset parameter.

3.3.2. Onscreen digitization

A single operator manually digitized the parcel boundaries using the On-Screen method based on the UAV image of the original scale. The operator visually identified the field boundaries using the original scale UAV image-mosaic. The single operator completed the digitization for the sake of maintaining uniformity in digitizing the parcel boundaries. The agricultural land parcels were flat, more of a regular shape, and large enough with the most recognizable agricultural bund width in the Terai region while the agricultural fields in Hilly terrain were small, more of an irregular shape, and crowded. However, the boundaries of the parcels were distinctly separable, and the parcel boundaries were recognizable in both cases.

3.4 Accuracy assessment

Finally, the extracted boundaries from the ENVI FX-edge algorithm were assessed against the manual digitization of land parcels based on spontaneous recognition. The assessment was made on the basis of the percentage change in the area and the percentage change in the perimeter of the delineated land parcels. First, the difference in area and perimeter of each parcel was calculated. Keeping the area and the perimeter of the parcels using the manual method as a reference, the percentage change in the parameters was obtained. Finally, the mean and standard deviation of the percentage change in these parameters were calculated.

$$Percent\ Change\ in\ Area\ (\%\ \Delta A) = \frac{Area_{manual} - Area_{edge}}{Area_{manual}} \times 100$$

$$Percent\ Change\ in\ Perimeter\ (\%\ \Delta P) = \frac{Perimeter_{manual} - Perimeter_{edge}}{Perimeter_{manual}} \times 100$$

Where,

$Area_{manual}$ represents the area of the parcels obtained using manual digitization.

$Perimeter_{manual}$ represents the perimeter of the parcels obtained using manual digitization.

$Area_{edge}$ represents the area of the parcels obtained using the edge-based method.

$Perimeter_{edge}$ represents the perimeter of the parcels obtained using the edge-based method.

4. RESULTS

Resampling the UAV orthoimage to lower spatial resolution i.e., a larger value of GSD, resulted in the fewer and faster extractions of object boundaries. ENVI FX-edge detection algorithm was used for segmentation with the original scale as well as with the resampled Ortho-mosaic with 5cm and 10cm GSD.

Scale level and merge level parameters were selected in the range from 30 to 60 and 80 to 99.9 respectively. The optimal results were obtained with a scale level parameter of 50 and a merge level parameter of 99.9. While the ortho-mosaic with the original GSD of about 2 cm resulted in many tiny field boundaries, those with the larger GSD (smaller image scale)

reduced the number of such tiny boundaries (Figure 3). This improvement in the removal of tiny boundaries is because of the reduction of heterogeneity in image intensities due to spatial variation of crop characteristics within the individual fields.

(a)

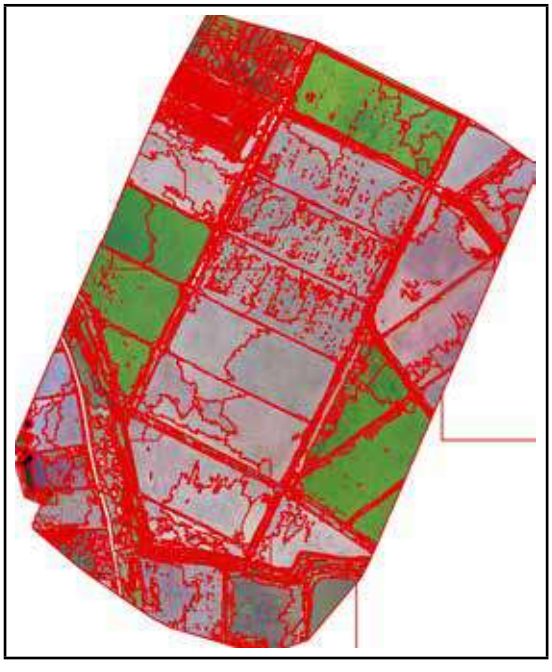

(b)

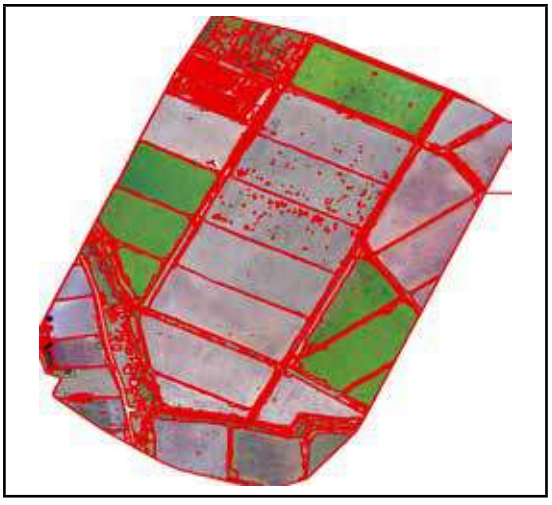

(c)

Figure 3: Extracted boundaries from the Terai region study area at original GSD of about 2 cm (a), at 5 cm GSD (b), and at 10cm GSD (c) with a scale level of 50 and merge level of 99.9. Many tiny boundaries were obtained at the original scale image which drastically reduced correspondingly at the image GSD of 5 cm and 10cm (c).

(a)

(b)

Figure 4: Extracted boundaries from the Hilly

region study area at 5 cm GSD and 10 cm GSD with a scale level of 50 and merge level of 99.9. Many tiny boundaries were obtained at the image GSD of 5 cm (a) which drastically reduced at the image GSD of 10 cm (b).

The dissolve operation was additionally performed to remove the objects under the minimum reference object area and dissolve them with the larger boundaries containing them. The boundaries smaller than 5 m2 were dissolved with the larger field boundaries containing them. Finally, the dissolved boundaries were smoothened using the Generalize tool of ArcMap with a Maximum Allowable Offset parameter of 0.5. A comparison of manually digitized boundaries, automatically segmented boundaries using the edge method, and smoothened boundaries after the edge method is shown in Figure 5.

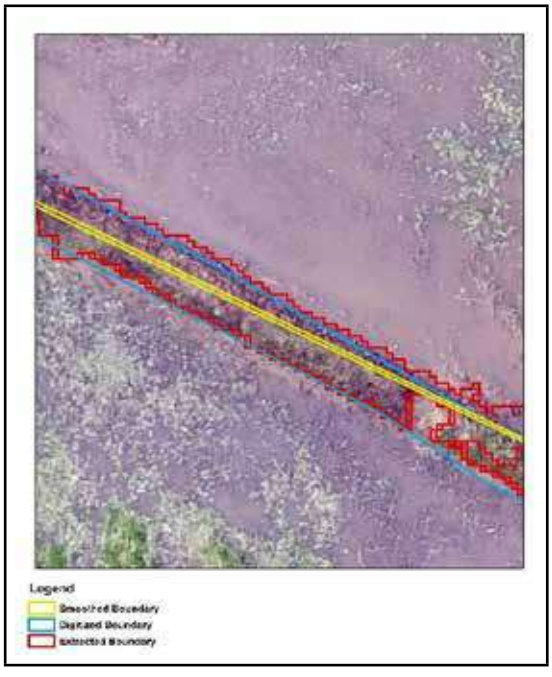

Figure 5: A comparison of manually digitized boundaries automatically detected boundaries from the edge method and smoothed boundaries after automatic detection.

For accuracy assessment, all the parcels in the Terai region were taken whereas only the non-harvested parcels were considered for the Hilly region. The reason for choosing such parcels in the Hilly region was the non-uniformity of the harvesting process which result in unnecessary segmentation of land boundaries. The accuracy assessment resulted in the mean and standard deviation of the percentage change in the area of 2.43% and 1.65% for the Terai region study case and 4.69% and 1.04% for the Hilly region study case respectively (Table 1). In addition, the mean and standard deviation of the percentage change in perimeter of 8.82% and 8.85% for the Terai region study case and 2.43% and 2.91% for the Hilly region study case respectively were obtained. These percentage changes in area and perimeter for agricultural application are acceptable for agriculture planning, resource estimation, and taxation purposes. Therefore, the utilization of UAV images together with edge detection algorithms can provide agriculture parcel boundaries with a reasonable accuracy faster, cheaper, and requires minimum human interaction. The final delineated boundary is shown in Figure 6.

Table 1: Statistical results.

Parameter	Statistics	Value	
		Terai Region Case	Hilly Region Case
Parcels	Count	20	10
Percentage Change in Area (%)	Maximum	8.33	5.373
	Minimum	4.96	1.851
	Mean	2.43	4.69
	Standard Deviation	1.65	1.04
Percentage Change in Perimeter (%)	Maximum	5.84	6.377
	Minimum	4.35	0.94
	Mean	8.82	2.43
	Standard Deviation	8.85	2.91

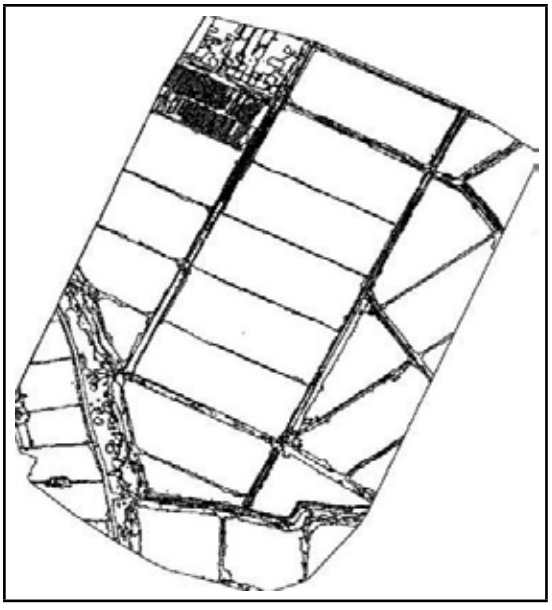

(a)

(b)

Figure 6: Results of an automated delineation method of the Terai region (a) and that of the Hilly region (b).

5. CONCLUSION AND RECOMMENDATIONS

In this study, the land parcels from Terrain and Hilly sites were delineated from ultra-high-resolution UAV images using the Edge Detection in-built algorithm in ENVI. The obtained results were assessed against the manually digitized parcel boundaries from the same image mosaic. The results showed that the ENVI-Edge Detection algorithm can reasonably delineate the visible parcel boundaries like ditches, wider land bunds, and foot trails at a larger value of GSD. Similarly, variations in segmented results were studied under different values of scale and merge parameters which show the large deviations in results in small changes in the algorithm parameters. From this study, it is concluded that Scale level and Merge level algorithmic parameters, and the image GSD are key controls for the parcel delineation. The comparison of automated and manual land delineation of parcels shows that agriculture parcel boundaries can be delineated from UAV images using the Edge detection algorithm with reasonable accuracy, time, and cost which demands minimum operator interaction. Therefore, this approach could be utilized routinely to delineate field boundaries after crop rotation to estimate irrigation, pesticide, and fertilizers planning and management.

ACKNOWLEDGMENT

The fieldwork for the Terai region case study was supported by funding from the University Grant Commission (UGC) Nepal under Ph.D. Fellowship program (UGC Award No. PhD-77/78-Engg-01).

REFERENCES

Aung, H. L., Uzkent, B., Burke, M., Lobell, D., & Ermon, S., (2021). *Farmland parcel delineation using spatio-temporal convolutional networks*.

Batić, D., (2019). *Deep learning for delineating farm boundaries.* Retrieved on August 2, 2022. https://datadragon.eu/2021/09/16/deep-learning-for-delineating-farm-boundaries/

CBS, (2006). *Land fragmentation. In agricultural census monograph: National Census of Agriculture 2001/02* (p. 12). Kathmandu, Nepal: Central Bureau of Statistics. Retrieved

from http://old.cbs.gov.np/agriculture/agriculture_monograph_preface_and_contents

Fetai, B., Oštir, K., Fras, M., & Lisec, A., (2019). *Extraction of visible boundaries for cadastral mapping based on UAV imagery*. Remote Sensing, 11(13). DOI: 10.3390/RS11131510.

Gbenga, A. & Emmanuel, O., (2022). *On the applicability of integrated UAV photogrammetry and automatic feature extraction for cadastral mapping*, 71(1):1–24.

Khaire, A. & Thakur, N. V., (2013). An overview of image segmentation algorithms. *International Journal of Image Processing and Vision Science*, 1, DOI: 10.47893/IJIPVS.2013.1028

Paul, B. K., & Rashid, H., (2017). Land use change and coastal management. *Climatic Hazards in Coastal Bangladesh*, 183–207. DOI: 10.1016/B978-0-12-805276-1.00006-5.

Rydberg, A., (2001). Integrated method for boundary delineation of agricultural fields in multispectral satellite images. *IEEE Transactions on Geoscience and Remote Sensing*, 39.

Author's Information

Name	:	Arun Kumar Bhomi
Academic Qualification	:	Undergraduate Student of Geomatics Engineering
Organization	:	Department of Geomatics Engineering, Kathmandu University
Current Designation	:	Student

CALENDAR OF INTERNATIONAL EVENTS

XXIVth ISPRS Congress, Imaging today, Foreseeing Tomorrow
Date:06-11 Jun 2022
Country: Nice, France
Website: http://www.isprs2020-nice.com/

COSPAR 2022, 44th Scientific Assembly of the Committee on Space Research (COSPAR) and Associated Events
Date: 16-24 Jul 2022
Country: Athens, Greece
Website: https://www.cospar-assembly.org/

12th Workshop on Pattern Recognition in Remote Sensing
Date: 21 August 2022
Country: Canada
Website: http://iapr-tc7.ipb.uni-bonn.de/prrs-2022/

FOSS4G 2022 Academic Track
Date: 22-28 August 2022
Country: Italy
Website: https://2022.foss4g.org/

SUNRISE (Seashore and UNderwater documentation of aRchaeological herItage palimpSests and Environment) SUMMER SCHOOL
Date: 3-9 September 2022
Country: Italy
Website: https://www.sunrisesummerschool.com/

XXVII FIG Congress
Date: 11-15 September 2022
Country: Poland
Website: https://www.fig.net/fig2022/

41st EARSel Symposium
Date: 13-16 September 2022
Country: Cyprus
Website: https://cyprus2022.earsel.org/index.php

58th Photogrammetric Week
Date: 13-16 September 2022
Country: Germany
Website: https://phowo.ifp.uni-stuttgart.de/

43rd Asian Conference on Remote Sensing
Date: 3-7 October 2022
Country: Mongolia
Website: http://www.acrs2022.mn/

The 7th International Conference on Smart City Applications
Date: 18-20 October 2022
Country: Portugal
Website: http://www.medi-ast.org/SCA22/

InterGEO Conference
Date: 18-20 October 2022
Country: Germany
Website: https://www.intergeo.de/

Smart Data, Smart Cities, 2022
Date: 19-21 October 2022
Country: Australia
Website: https://conference.unsw.edu.au

9th International Symposium on the History of Cartography
Date: 24-26 October 2022
Country: Germany
Website: https://history.icaci.org/berlin-2022/

ISPRS WG IV/7: Geoinformation week 2022
Date: 14-17 November 2022
Country: Malaysia
Website: https://www.geoinfo.utm.my/geoweek/

Pacific Islands GIS and Remote Sensing User Conference
Date: 28 November – 1 December 2022
Country: Suva Fiji
Website: http://www.pgrsc.org/

Geo Week
Date: 13-15 February 2023
Country: USA
Website: https://www.geo-week.com/

20th International Course on Engineering Surveying
Date: 11-15 April 2023
Country: Switzerland
Website: https://ingenieurvermessungskurs.com/

FIG Working Week 2023
Date: 28 May – 1 June 2023
Country: USA
Website: www.fig.net/fig2023

The 12th International Conference on Mobile Mapping Technology
Date: 24-26 May 2023
Country: Italy
Website: https://www.cirgeo.unipd.it/mmt/

Nepal Remote Sensing and Photogrammetric Society (NRSPS)

Executive Committee

Susheel Dangol, ***President***
susheeldangol@gmail.com

Er. Sanjeevan Shrestha, ***Vice President***
shr.sanjeevan@gmail.com

Er. Janak Parajuli, ***Secretary***
janak.parajuli1@gmail.com

Raj Kumar Thapa, ***Assistant Secretary***
thapark2013@gmail.com

Er. Tina Baidar, ***Treasurer***
tina.baidar13@gmail.com

Members
Dr. Chhabilal Chidi
chidichhabilal@gmail.com

Jagat Raj Poudel
jagatrajpoudel@hotmail.com

Roshani Sharma
anjarija@gmail.com

Girija Pokharel
girija.pokhrel12@gmail.com

E-mail: nrspsociety@gmail.com

Earth Observation

Editorial Board

Rabin K. Sharma, ***Advisor***
rabinks51@gmail.com

Sanjeevan Shrestha. ***Chief Editor***
shr.sanjeevan@gmail.com

Anu Bhalu Shrestha, ***Member***
shrestha.anu17@gmail.com

Tina Baidar, ***Member***
tina.baidar13@gmail.com

The society supported the "International workshop on Land use Planning and Land Administration: Integration and Decentralization" organized at Land Management Training Center in February 16-17, 2023 (Falgul 3-4, 2079). The then secretary of the society Mr. Susheel Dangol received certificate of appreciation during the event on behalf of the society.

The then president of NRSPS Rabin Kaji Sharma participated in a half day program to observe 6th Global Surveyor's Day in the capacity of president of NRSPS, organized by Nepal Institution of Chartered Surveyor and Survey Department on 20th March 2023 (6th Chaitra 2079).

The society also participated in the talk program organized by Nepal Institution of Chartered Surveyor and Survey Department on the issue of coordinate transformation organized at the Survey Department on February 24, 2023.

Eleventh issue of "Earth Observation" newsletter was also published in this year which can be downloaded from www.nrsps.org.np.

Nepal Surveyor's Association (NESA)

NESA CEC
Secretariate

Mr. Ambadatta Bhatta
Acting President

Mr. Saroj Chalise
General Secretary

Mr. Prakash Dulal
Secretary

Mr. Durga Phuyal
Secreatry

Mr. Sahadev Ghimire
Treasurer

Mr. Dadhiram Bhattarai
Co-treasurer

Mr. Hari Prasad Parajuli
Member

Ms. Jyoti Dhakal
Member

Other Officials

Mr. Ram Sworup Sinha
Vice President
Eastern Development Region

Mr. Tanka Prasad Dahal
Vice President
Central Development Region

Mr. Gopinath Dayalu
Vice President
Western Development Region

Mr. Ramkrishna Jaisi
Vice President
Mid-Western Development Region

Mr. Karansingh Rawal
Vice President
Far-Western Development Region

Other Members:
Mr. Premgopal Shrestha
Ms. Geeta Neupane
Mr. Laxmi Chaudhari
Mr. Kamal Bahadur Khatri
Mr. Bibhakta Shrestha
Mr. Sahadev Subedi
Mr. Balam Kumar Basnet
Mr. Nawal Kishor Raya
Mr. Santosh Kumar Jha
Mr. Khim Lal Gautam

Background

Utilizing the opportunity opened for establishing social and professional organizations in the country with the restoration of democracy in Nepal as a result of peoples movement in1990, Survey professionals working in different sectors decided to launch a common platform named Nepal Surveyors' Association (NESA) in 1991, as the first government registered Surveyors' Organization in Nepal.

Objectives

The foremost objective of the association is to institutionalize itself as a full fledged operational common platform of the survey professionals in Nepal and the rest go as follows

- To make the people and the government aware of handling the survey profession with better care and to protect adverse effects from it's mishandling.
- To upgrade the quality of service to the people suggesting the government line agencies to use modern technical tools developed in the field of surveying.
- To upgrade the quality of survey professionals by informing and providing them the opportunity of participation in different trainings, seminars, workshops and interaction with experts in the field of surveying and mapping within and outside the country
- To upgrade the quality of life of survey professionals seeking proper job opportunities and the job security in governmental and nongovernmental organizations
- To work for protecting the professional rights of surveyors in order to give and get equal opportunity to all professionals without discrimination so that one could promote his/her knowledge skill and quality of services.
- To advocate for the betterment of the quality of education and trainings in the field of surveying and mapping via seminars, interactions, workshops etc
- To wipe out the misconceptions and illimage of survey profession and to uplift the professional prestige in society by conducting awareness programs among the professionals and stakeholders
- To persuade the professional practitioners to obey professional ethics and code of conduct and to maintain high moral and integrity
- To advocate for the satification of Survey Council Act and Integrated Land Act for the better regulation of the profession and surveying and mapping activities in the country.

Organizational Structure

The Organization is nationwide expanded and it has the following structure: 14 Zonal Assemblies (ZA), 14 Zonal Executive Committees (ZEC), 5 Regional Assemblies (RA), 5 Regional Executive Committees (RAC), Central General Assembly (CGA) and a Central Executive committee (CEC).

Membership Criteria

Any survey professional obeying professional ethics and code of conduct, with at least one year survey training can be the member of the Association. There are three types of members namely Life Member, General Member and Honorary Member. At present there are 2031 members in total.

Nepal Geomatics Engineering Society (NGES)

contactgeomatics@gmail.com

About NGES

Nepal Geomatics Engineering Society(NGES) is a non-profit organization formed to function as an umbrella for all Geomatics Engineers of Nepal.Geomatics Engineering program for the first time was launched in 2005 AD by Purbanchal University, in 2007 AD by Kathmandu University and in 2012 AD by Tribhuvan University. Till date, there are more than 650 Geomatics graduates in Nepal working in different sectors.

Geomatics as a new global profession can be used as a special tool in planning, policy building and decision making. In order to explore and enhance the role of Geomatics engineering in nation building through cooperation among the geomatics graduates and professional practice, the geomatics pioneers of Nepal recognized the importance of a society and hence formed Nepal Geomatics Engineering Society in August 26, 2015.

As driven by the society's regulation, the executive committee is paying its full strength to develop cooperation among geomatics professionals through various professional and recreational activities.

Executive Committee

President
Er. Arun Bhandari
Vice-President
Er. Rabin Karki
Secretary
Er. Sunil Bogati
Joint-Secretary
Er. Thakur Lamichhane
Treasurer
Er. Binita Shahi
Executive Members
Er. Sujan Sapkota
Er. Ashmita Dhakal
Er. Bibek Chand
Er. Gobinda Upadhyaya
Er. Rabi Shrestha
Er. Saugat Pratap Singh Karki
Er. Ashish Chalise
Er. Naresh Bista

NGES organized a virtual talk program on "**Geospatial Technologies for Disaster Risk Reduction**" on 13 October, 2022 (**International DRR day**).

NGES organized "**Map Design Competition**" on 16 November 2022 on the occasion of **GIS Day.** The event is organized in Survey Department hall. More than 30 participants contested the competition.

Then president and Members of NGES participate in **UNWGIC** in China

NGES voluntarily supports Dhurmus Suntali Foundation in Construction Survey of **Gautam Buddha Cricket Stadium** in Chitwan.

10th National Science Day 2022, NGES Showcasing the latest advancements in the survey and geospatial sector.

Global Surveyors' Day - March 2, 2019 was a mega event for the professionals and academia of Geomatics in Nepal. The program on the initiation of NGES was jointly organized by NGES, NeSA, NSPRS and NICS. Two da long program included friendly footwall tournament, Map competition, Inspirational speech, Panel discussion on five different generations on Surveying and Mapping in Nepal (5Gs) and Networking Sessions. Minister of Land Management, Cooperatives and Poverty Alleviation – Hon. Padma Aryal was Chief Guest of the program.

Call for papers

The editorial board requests for papers related to geo-information science and earth observation for the publication in 23rd issue of the Journal on Geoinformatics, Nepal.
Last date of submission is 30th March 2024.
For more information, please contact editorial board

Survey Department

P.O. Box 9435, Kathmandu Nepal
Tel: +977 1 4106508, 4106957, Fax: +977 1 4106757
email: info@dos.gov.np

Instruction and Guidelines for Authors Regarding Manuscript Preparation

- Editorial Board reserves the right to accept, reject or edit the article in order to conform to the journal format.
- The contents and ideas of the article are solely of authors.
- The article must be submitted in Microsoft Word by email.
- Editorial Board has no obligation to print chart/ figure/table in multi colour, in JPEG/TIFF format, the figure/picture should be scanned in a high resolution.
- Authors are also requested to send us a written intimation that the same articles is not sent for publication in other magazine/journal.

Page size: A4

Format: Single line spacing with two columns.

Margin: upper 1", left 1.15", right 1", bottom 1".

Length of manuscript: The article should be limited upto 6 pages including figures and references.

Body text font: Times New Roman "11".

Title: The title should be centrally justified appearing near top of 1st page in Cambria, "20" point (Bold).

Authors Name: Authors name should be in Times New Roman "10" with Upper and lower casing, centrally justified. There should be a gap of one lines with 11 pt between the title and author's name.

Authors Email: Authors email should be in Times New Roman "10" centrally justified. There should not be gap between the name and email.

Keywords: Four to five keywords on paper theme

in Times New Roman "10" with two spacing under

the Authors email left justified.

Abstract: Single line spacing after keywords, limited to around 300 words in Italic, Times New Roman "10".

Major heading (Level 1) should be flushed with the left margin in Times New Roman "10" bold font and with Upper casings. Color Dark blue. Numbering 1

Minor heading (Level 2) should be flushed with the left margin in Times New Roman "11" Bold font and with Upper and Lower Casing. Color Dark blue. Numbering 1.1

Minor heading (Level 3) should be flushed with the left margin in Times New Roman "11" Bold font, Italic and with Upper and Lower Casing. Color Dark blue. Numbering 1.1.1

Minor heading (Level 4) should be flushed with the left margin in Times New Roman "10" Italic and with Upper and Lower Casing. Color Dark blue. Numbering 1.1.1.1

BulletPoint: Use only (•).

Placement of photographs/tables: Photographs or tables should be pasted in appropriate place of manuscript pages with caption in their positions in Times new Roman "10" with Upper and lower casing.

Equations: All equations should be in Times New Roman, "11" and italic with consecutive equation numbers placed flush right throughout the paper.

References: References should be listed in alphabetical order at the end of paper in following sequence and punctuation. Author's last name, Author's initials, (Year of publication). *Title of references article in italic,* name of book or journal, volume number, country or city, name of publisher etc.

Citation: All papers are to be cited like (Rajabifarad, 2012), (Dangol & Kwak, 2014), (Zebenbergen, *et. al*., 2018). Upto two authors, the last name should be cited for both and if more than two, then cite it as *et. al.*.

(Primary) Author's Information: The author should provide

Name, Academic Qualification, Organization, Current Designation, Work Experience (in years),

Published Papers/Article (Number) and scanned copy of author's passport size photo.

Note: "Author should send the picture of all the figures kept in paper as separate file."

Survey Officer Dipesh Suwal participated in "XXVII FIG Congress" organized from 11-15 September 2022 at Warsaw, Poland.

Survey Officer Jyoti Dhakal participated in "United Nations Subregion Workshop on the Implementation of the Degree of Urbanization Methodology in South-Ease Asian Countries" organized in Bangkok, Thailand from November 28- December 02 2022.

Survey Officer Greecma Pradhan participated in "Management and utilization of national control points for efficiency of survey" in Japan organized by JICA in collaboration with Infrastructure Development Institute Japan (IDI) and Geospatial information Authority of Japan (GSI)

Chief Survey Officer Ram Kumar Sapkota participated in "Planning and management of national mapping and surveying" in Japan organized by JICA in collaboration with Infrastructure Development Institute Japan (IDI) and Geospatial information Authority of Japan (GSI)

Participants of the orientation program for the team leaders of survey team from the survey office organized for western sector survey offices at Pokhara, Kaski.

Making Sense of Geo-spatial data for total solution in National and Local Development Activities

Available Maps and Data

- Geodetic Control data
- Aerial Photographs
- Topographic Base Maps
  - Terai and middle mountain at the scale of 1:25,000
  - High hills and Himalayas at the scale of 1:50,000
- Land Use Maps
- Political and Administrative Map of Nepal
- Digital Topographic Data at scales 1:25,000 & 1:50,000
- Cadastral Plans
- Orthophoto Maps
- Orthophoto Digital Data
- SOTER Data
- Topographic Digital Data at scales 1:100,000 1:250,000 1:500,000 1:1,000,000

Available Services

- Establishment of control points for various purposes of Surveying and Mapping
- Cadastral Surveying
- Surveying and mapping for development activities
- Topographic and large scale mapping
- Digital geo-spatial database support
- GIS Development

Price of some of the publications of Survey Department

- List of Geographical Names, Volume I to V – NRs 600/- per volume.
- The Population and Socio - Economic Atlas of Nepal, 2011 (HardCopy) NRs.2,500.00 (In Nepal), €200.00 (Outside Nepal)
- The Population and Socio - Economic Atlas of Nepal, 2011 (CDVersion) NRs.250/-

Contact Address:

SURVEY DEPARTMENT

Min Bhawan, Kathmandu, Nepal
Phone: +977-1 -4106508, Fax: +977-1 -4106757
E-mail: info@dos.gov.np
website: www.dos.gov.np

ISSN 2717-5022